UNIVERSITY OF GHANA

INTERGRATION OF GROUND MAGNETIC AND FREQUENCY DOMAIN ELECTROMAGNETIC DATA, A CASE STUDY FROM NKWANTA AND ASUOGYA IN THE WESTERN REGION.

BY

JUDE TEI ADDO

(10395192)

THIS THESIS IS SUBMITTED TO THE UNIVERSITY OF GHANA, LEGON IN PARTIAL FULFILMENT OF THE REQUIREMENT FOR THE AWARD OF M. PHIL GEOLOGY DEGREE

JULY, 2014

DECLARATION

This thesis is the result of research undertaken by Jude Tei Addo towards the award of Master of Philosophy Degree in Geology in the Department of Earth Science, University of Ghana.

…… ……

JUDE TEI ADDO DATE

(Student)

…… …….

DR. THOMAS K. ARMAH DATE

(Principal Supervisor)

…….. ……

DR. PAULINA AMPONSAH DATE

(Co-Supervisor)

ABSTRACT

Ground magnetics and electromagnetic datasets were processed to interpret the subsurface geology and structure of the southwest of Ghana within the Tarkwain and Volcanics in the central part of the Ashanti belt. The study was aimed at mapping lithology, delineating structural lineaments and their trends as well as the trend of mineralization in the study areas. The data processing steps involved enhancement filters such as reduction to the pole, analytical signal, the first horizontal and vertical derivative, reduced to equator and upward continuation all of which helped delineate zones of mineralization and their geological, structures and lithology control within the Ashanti belt. The electromagnetic datasets displaying the conductivity information within the study area proved valuable in delineating mineralization and structural trends of both study areas. The upward continuation filter serves as a great tool in delineating deeper source and determining the extent of mineralization. The objective of this work was aimed at delineating the structural and mineralization zones of the sturdy area. Both the magnetic and EM images were instrumental in showing the structural orientation in the study area. The orientation of Asuogya was delineated as NW-SE and that of Nkwanta was found as a N-S. This orientation also indicates zones of mineralization.

DEDICATION

I dedicate this work to my dear parent, Miss Elizabeth Kwashie.

To my siblings Charles Addo and David Karim. I am most grateful for your love and support and may God richly bless you.

ACKNOWLEDGEMENTS

I am grateful to our Lord Jesus Christ, for he has been so merciful to me and it is by His grace that I have gone through this programme successfully. He deserves all the glory.

I am grateful to my supervisors Dr. Thomas K Armah and Dr.Paulina Amponsah for their immense supervision, constructive criticisms and support in making this thesis work one of a success. God richly bless you.

I am also deeply indebted to Professor Prosper Nude, Professor Dampari, Professor Asiedu, Professor Atta Peters, Dr. Tetteh of the Earth science Department.

I am most grateful to my wife, children, and my siblings whose emphatic encouragement and prayers has made this work possible. Finally, I thank the Almighty God for all I have received and all that is yet to come.

TABLE OF CONTENTS

LIST OF FIGURES

LIST OF TABLES

APPENDIX

CHAPTER ONE

INTRODUCTION

1.1 OVERVIEW OF GEOPHYSICAL METHODS

An integrated survey utilizes multiple geophysical methods and for that reason can enhance the potential for comprehensive site characterization compared with singular method surveys. Integrated surveys can be especially effective if survey methods target more than one physical property. Associated with this characterization approach, joint modelling of differing geophysical datasets can mathematically improve resolution of resultant images. In addition, the synergy and resolution improvement achieved by utilizing multidisciplinary geoscience methods (i.e., geological, hydrogeological, and geophysical) in site characterization need to be recognized (Sandberg, 1993).

Magnetic survey makes use of the natural source of magnetic field which is also known as a potential field. Any field with a potential in free space that satisfies Laplace's equation is termed a potential field, although in geophysics, the term potential fields primarily refers to magnetic and gravity data. There are a number of methods of measuring these fields, including vector, scalar, and gradient based methods (Blakely, 1995).

The exploration and localization of targets with only magnetic signature, depends on the depth of the target and on the material the hidden body is made of, since a nonmagnetic body is completely transparent to detection by this kind of investigation. This limitation can be removed if other techniques such as active electromagnetic, based on different physical properties of the inspected matter, are used.

1.2 OVERVIEW OF MAGNETIC METHOD

The aim of a magnetic survey is to investigate subsurface geology on the basis of anomalies in the Earth's magnetic field resulting from the magnetic properties of the underlying rocks. Although most rock-forming minerals are effectively non-magnetic, certain rock types contain sufficient magnetic minerals to produce significant magnetic anomalies. Similarly, man-made ferrous objects also generate magnetic anomalies. Magnetic surveying thus has a broad range of applications, from small scale engineering or archaeological surveys to detect buried metallic objects, to large-scale surveys carried out for mineral exploration and investigation of regional geological structure. Magnetic surveys can be performed on land, at sea and in the air. Magnetic field measurements can be used to detect ores that contain magnetic minerals such as magnetite, because magnetite has a high magnetic susceptibility compared with most rocks (Kearey, 2002).

Magnetic intensity measurements are taken along survey traverses (normally on a regular grid) and are used to identify mineralization that is related to magnetic materials (normally magnetite and/or pyrrhotite). Magnetic data are also used as a mapping tool to distinguish rock types, identify faults, bedding, structure and alteration zones. Line and station intervals are usually determined by the size and depth of the exploration targets.

A small bar magnet is said to have north and south poles, but it is more accurate to say it has a "north-seeking" pole and a "south-seeking" pole. By these expressions, we mean that if such a magnet is used as a compass, one end will "seek," or point to, the geographic North Pole of Earth and the other end will "seek," or point to, the geographic South Pole of Earth. We conclude that the geographic North Pole of Earth

corresponds to a magnetic south pole, and the geographic South Pole of Earth corresponds to a magnetic north pole. In fact, the configuration of Earth's magnetic field, very much resembles what would be observed if a huge bar magnet were buried deep in the Earth's interior.

If a compass needle is suspended in bearings that allow it to rotate in the vertical plane as well as in the horizontal plane, the needle is horizontal with respect to Earth's surface only near the equator. As the device is moved northward, the needle rotates so that it points more and more toward the surface of Earth. The angle between the direction of the magnetic field and the horizontal is called the dip angle. Finally, at a point just north of Hudson Bay in Canada, the north pole of the needle points directly downward, with a dip angle of 90°. This site, first found in 1832, is considered to be the location of the south magnetic pole of Earth. It is approximately 1300 miles from Earth's geographic North Pole and varies with time. Similarly, Earth's magnetic north pole is about 1 200 miles from its geographic South Pole. This means that compass needles point only approximately north. The difference between true north, defined as the geographic North Pole, and north indicated by a compass varies from point to point on Earth, a difference referred to as magnetic declination. For example, along a line through South Carolina and the Great Lakes a compass indicates true north, whereas in Washington state it aligns 25° east of true north.

Evidence for the direction of the earth's magnetic field in the geological past may be found in the remnant magnetisation of rocks collected from lake-floors, lava flows, sea-floor spreading and other sources. Earth does have large deposits of iron ore deep beneath its surface, but the high temperatures in the core prevent the iron from retaining any permanent magnetization (Lowrie, 2007). The source of Earth's

magnetic field is electric current in the liquid part of its core. This current, which is not well understood, may be driven by an interaction between the planet's rotation and convection in the hot liquid iron core. The circulation patterns within the core are not fixed and change slowly with time. This is reflected in a slow, progressive, temporal change in all the geomagnetic elements known as secular variation (Kearey, 2002).

The Earth's magnetic field also varies because of changes in the strength and direction of currents circulating in the ionosphere. In the normal solar quiet (Sq) pattern, the background field is almost constant during the night but decreases between dawn and about 11 a.m., increases again until about 4 p.m. and then slowly declines to the overnight value. Peak to trough amplitudes in mid-latitudes are of the order of a few tens of nanoTesla. Since upper atmosphere ionization is caused by solar radiation, diurnal curves tend to be directly related to local solar time. Short-term auroral effects are special cases of the irregular disturbances known as magnetic storms. These are produced by sunspot and solar flare activity and, despite the name, are not meteorological, often occurring on clear, cloudless days. Within about 5^{o} of the magnetic equator the diurnal variation is strongly influenced by the equatorial electrojet, a band of high conductivity in the ionosphere about 600 km (5^{o} of latitude) wide. The amplitudes of the diurnal curves in the affected regions may be well in excess of 100 nT and may differ by 10 to 20 nT at points only a few tens of kilometres apart. Many of the magnetic phenomena observed in Polar Regions can be explained by an auroral electrojet subject to severe short-period fluctuations. In both equatorial and polar regions it is particularly important that background variations be monitored continuously (Milsom, 2003).

A body placed in a magnetic field (H) acquires a magnetization (M) which, if small, is proportional to the field: M = kH. The susceptibility, k, is very small for most natural materials, and may be either negative (diamagnetism) or positive (paramagnetism). The fields produced by dia- and paramagnetic materials are usually considered to be too small to affect survey magnetometers, but modern high-sensitivity magnetometers are creating exceptions to this rule. Most observed magnetic anomalies are due to the small number of ferro- or ferri-magnetic substances in which the molecular magnets are held parallel by intermolecular exchange forces. Below the Curie temperature, these forces are strong enough to overcome the effects of thermal agitation (Milsom, 2003). Magnetite, pyrrhotite and maghemite, all of which have Curie temperatures of about 600 ^{o}C, are the only important naturally occurring magnetic minerals and, of the three, magnetite is by far the most common. Hematite, the most abundant iron mineral, has a very small susceptibility and many iron ore deposits do not produce significant magnetic anomalies (Milsom, 2003).

The susceptibility of a rock usually depends on its magnetite content. Sediments and acid igneous rocks have small susceptibilities whereas basalts, dolerites, gabbros and serpentinites are usually strongly magnetic (Milsom, 2003).

Weathering generally reduces susceptibility because magnetite is oxidized to hematite, but some laterites are magnetic because of the presence of maghemite and remanently magnetized hematite. In gold exploration, the magnetic survey is of particular importance because it may map areas of structural complexity, carbonatization, and silicification. Sedimentary rocks generally have a very small magnetic susceptibility compared with igneous or metamorphic rocks, which tend to have a much higher magnetite (a common magnetic mineral) content. Most magnetic

surveys are designed to map the geologic structure on or inside the basement rocks (the crystalline rocks that lie beneath the sedimentary layers) or to detect magnetic minerals directly (Gunn, 1997).

The purpose of magnetic surveying is to identify and describe regions of the Earth's crust that have unusual (anomalous) magnetizations. In the realm of applied geophysics the anomalous magnetizations might be associated with local mineralization that is potentially of commercial interest, or they could be due to subsurface structures that have a bearing on the location of oil deposits. In global geophysics, magnetic surveying over oceanic ridges provided vital clues that led to the theory of plate tectonics and revealed the polarity history of the Earth's magnetic field since the Early Jurassic. Magnetic surveying consists of (1) measuring the terrestrial magnetic field at predetermined points, (2) correcting the measurements for known changes, and (3) comparing the resultant value of the field with the expected value at each measurement station (Telford, 1990). The expected value of the field at any place is taken to be that of the International Geomagnetic Reference Field (IGRF). The difference between the observed and expected values is a magnetic anomaly. The magnetic anomaly can be calculated by subtracting the International Geomagnetic Reference Field (IGRF) from the observed field (F observed – F IGRF) (Reeves, 1997).

Ground magnetic measurements are usually made with portable instruments at regular intervals along more or less straight and parallel (traverse) lines which cover the survey area. Often the interval between measurement locations (stations) along the lines is less than the spacing between lines. The instrument used to measure magnetic fields is called a magnetometer. Early torsion magnetometers used compass needles

mounted on horizontal axes (dip needles) to measure vertical fields. These were in use until about 1960, when they began to be replaced by fluxgate, proton precession and alkali vapour magnetometers or optically pumped magnetometers. Instruments of all these types are now marketed with built-in data loggers and can often be set to record automatically at fixed time intervals at base stations. All three can be used singly or in tandem as gradiometers, although care must then be taken with precession instruments to ensure that the polarizing field from one sensor does not affect the measurement at the other. The systems operate on broadly similar principles. The proton precession instrument utilises proton rich fluids surrounded by an electric coil. A momentary current is applied through the coil, which produces a corresponding magnetic field that temporarily polarises the protons. When the current is removed, the protons realign or process into the orientation of the Earth's magnetic field. The precession generates a small electrical current in the surrounding coil, at a frequency directly proportional to the local magnetic field intensity. The sensitivity of the proton precession instruments is in the order of 0.01-1 nT (Milsom, 2003).

In the flux gate magnetometer method, a high susceptibility alloy rod (fluxgate) is used which responds parabolically to an applied magnetic field strength. The fluxgate is excited with a sinusoidally varying magnetic field using a coil around it and measures one directional component of the magnetic field usually the vertical component. The sensitivity of fluxgate instruments is in the order of 1 nT (Milsom, 2003).

In the alkaline vapour magnetometer instruments, alkali atoms in ground states are excited to the states related to the external magnetic field using optical methods, and the decrease in the intensity of the light is measured. Sensitivities of these instruments

are in the order of 0.01nT. Gradiometers measure the magnetic field gradient rather than total field strength, which allows the removal of background noise. As is known, magnetometers can be successfully used to detect ferromagnetic targets because they can measure the superposition of the earth's magnetic field and the induced magnetic field in the targets that depends on their volume magnetic susceptibility. In this way, local variation in the geomagnetic field can be used to identify and to locate the presence of buried ferromagnetic bodies (Kearey, 2002).

The surveying of magnetic anomalies can be carried out on land, at sea and in the air. In a simple land survey an operator might use a portable magnetometer to measure the field at the surface of the Earth at selected points that form a traverse or grid over a suspected geological structure. This method is slow but it yields a detailed pattern of the magnetic field anomaly over the structure, because the measurements are made close to the source of the anomaly.

Diurnal correction: To make accurate anomaly maps, temporal changes in the earth's field during the period of the survey must be considered. Normal changes during a day, sometimes called diurnal drift, are a few tens of nT but changes of hundreds or thousands of nT may occur over a few hours during magnetic storms. During severe magnetic storms, which occur infrequently, magnetic surveys should not be carried out (Kearey, 2002).

The correction for diurnal drift can be made by repeat measurements of a base station at frequent intervals. The measurements at field stations are then corrected for temporal variations by assuming a linear change of the field between repeat base station readings. Continuously recording magnetometers can also be used at fixed base sites to monitor the temporal changes. If time is accurately recorded at both base

site and field location, the field data can be corrected by subtraction of the variations at the base site. The base-station memory magnetometer, when used, is set up every day prior to collection of the magnetic data (Lowrie, 2007). The base station ideally is placed at least 100 m from any large metal objects or travelled roads and at least 500 m from any power lines when feasible. The base station location must be very well described in the field book as others may have to locate it based on the written description. Some procedures require that several field-type stations be occupied at the start and end of each day's work. This procedure indicates that the instrument is operating consistently. As the base may vary by 10-25 nT or more from day to day, this correction ensures that another person using the same base station and the same asserted value will get the same readings at a field point to within the accuracy of the instrument. This procedure is always a good technique but is often neglected by persons interested in only very large anomalies (> 500 nT, etc.) (Milsom, 2003).

A magnetic anomaly originates in the magnetization contrast (ΔM) between rocks with different magnetic properties. However, the shape of the anomaly depends not only on the shape and depth of the source object but also on its orientation to the profile and to the inducing magnetic field, which itself varies in intensity and direction with geographical location. In oceanic magnetic surveying the magnetization contrast results from differences in the remanent magnetizations of crustal rocks, for which the Königsberger ratio is much greater than unity (i.e, $Qn>>1$). Commercial geophysical prospecting is carried out largely in continental crustal rocks, for which the Königsberger ratio is much less than unity (i.e., $Qn<<1$) and the magnetization may be assumed to be induced by the present geomagnetic field. The magnetization contrast is then due to susceptibility contrast in the crustal rocks (Renolds, 1997).

Magnetic exploration may directly detect some iron ore deposits (magnetite or banded iron formation), and magnetic methods often are useful for deducing subsurface lithology and structure that may indirectly aid identification of mineralized rock, patterns of effluent flow, and extent of permissive terranes and (or) favorable tracts for deposits beneath surficial cover. Geo-environmental applications may also include identification of magnetic minerals associated with ore or waste rock from which hazardous materials may be released. Such associations permit the indirect identification of hazardous materials such as those present in many nickel-copper or serpentine hosted asbestos deposits (Hoover, 1992).

Individual magnetic anomalies - magnetic signatures different from the background- consist of a high and a low (dipole) compared to the average field. In the Southern Hemisphere the high is located to the north and the low to the south of the magnetic body. The position and size of the anomaly depend on the position and size of the magnetic body. A change in latitude will also affect the positioning of anomalies over the magnetic body. This allows the geoscientists to interpret the position of the body which has caused the anomalous reading. Often however the reading is complicated because of the position of the body in relation to other rocks, its size, and what happens to the body at depth (Nicolas, 2009).

Data are usually displayed in the form of a contour map of the magnetic field, but interpretation is often made on profiles. From these maps and profiles geoscientists can locate magnetic bodies (even if they are not outcropping at the surface), interpret the nature of geological boundaries at depth, find faults etc. Like all contoured maps, when the lines are close together they represent a steep gradient or change in values. When lines are widely spaced they represent shallow gradient or slow change in

value. A modern technique is to plot the magnetic data as a colour image (red = high, blue = low and all the shades in between representing the values in between). This gives an image which is easy to read (Nicolas, 2009).

Advantages of using the magnetic method for mineral exploration are the relatively low costs of conducting the survey, and the relative ease of completing a survey in a short time. Little, if any, site preparation is necessary. Surveying requirements are not as stringent as for other methods, and may be completed with a transit or Brunton-type pocket transit and non-metallic measuring tape. Very often, a magnetic investigation is a very cost effective method for the initial assessment of the survey site (Kearey, 2002).

There are certain limitations in the magnetic method. One limitation is the problem of "cultural noise" in certain areas. Man-made structures that are constructed using ferrous material, such as steel, have a detrimental effect on the quality of the data. Features to be avoided include steel structures, power lines, metal fences, steel reinforced concrete, surface metal, pipelines and underground utilities. When these features cannot be avoided, their locations should be noted in a field notebook and on the site map.

Gupta and Fitzpatrict (1971) noted that magnetic effects due to the terrain can be as much as 1000 gammas in areas of moderate relief, where the bedrock contains a few percent of magnetite. Mineralogical studies and susceptibility measurements on drilled core indicated the presence of pyrrhotite associated with sulfide mineralization including gold only at the target. This revealed a good correlation between susceptibility and gold grade on the bases of susceptibility measurements and geochemical analysis on drilled core.

1.3 OVERVIEW OF ELECTROMAGNETIC METHOD

The EM ground method was developed during the 1920s in Scandinavia, the United States, and Canada, regions where the detection of conductive base-metal deposits was facilitated by their large contrast with the resistive host rock and generally thin overburden. The airborne version was introduced some 30 years later. Until the early 1960s, practically all EM equipment transmitted and received continuously on one frequency at a time. Such a continuous wave system is said to be operating in the frequency domain (FEM or FDEM). Although several attempts were made, dating back to the 1930s, to transmit transient pulses and detect the ground response during off-time (Statham, 1936), the first successful applications of this type did not appear until 1962. These were the airborne Input (Barringer, 1962), the MPP0-1 ground transient system in the USSR, and the EMP pulse ground equipment of Newmont Exploration (Dolan, 1970). Since the early 1970s, there has been a dramatic increase in the development of such time-domain systems (TEM or TDEM).

Electromagnetic (EM) methods are used to map variations in electrical properties. The main physical property involved in these methods is inductive electrical conductivity (in siemens/m and for convenience generally expressed as millisiemens/m) of subsurface deposits, which is a measure of how easily electrical current can pass through a material. Conductivity is a complex function of several variables including the conductivity of solid materials, conductivity of pore fluids, porosity, arrangement of pores and degree of saturation (Lane, 2000).

Subsurface materials exhibit a very large range of electrical conductivity values. Fresh rock is generally a poor conductor of electricity, but layers of graphite and certain metallic minerals containing iron, copper or nickel are very good conductors. These

latter substances conduct electricity by allowing the migration of electrons and are hence termed "electronic conductors". Moreover fluids that conduct electricity through the migration of ions are termed ionic conductors (Lane, 2000).

The most significant advances have been to EM systems that image conductivity as a function of depth. Improvements in acquisition systems and data processing (eg. bandwidth of recorded information, signal to noise ratio and methods to convert recorded information into subsurface conductivity) have combined to enhance the quality of the information about the subsurface and to simplify interpretation.

EM systems are classified in various ways by different authors according to the instrumentation, geometry of the transmitter-ground-receiver elements and the nature of the transmitted and recorded signal. The most common of these EM technique are the frequency domain electromagnetic (FDEM) which uses either one or more frequencies in taking measurements and the time domain electromagnetic (TDEM) which takes measurement as a function of time.

A pure frequency domain (FD) EM system transmits a magnetic field signal at a single frequency with sinusoidal variation in amplitude. The recorded response can either be described by its total amplitude and phase with respect to the transmitter signal or by the amplitudes of components in-phase ("real") and 90° out of phase ("quadrature") or the tilt angle system with respect to the transmitter signal. These ere explained systematically below.

(1) Amplitude and phase. The amplitude of the secondary field can be measured and is usually expressed as a percentage of the theoretical primary field at the receiver. Phase shift, the time delay in the received field by a fraction of the period, can also be measured and displayed.

(2) In phase and out-of-phase components. The second method of presentation is to electronically separate the received field into two components. The first component is in phase with the transmitted field while the second component is exactly 90 degree out-of-phase with the transmitted field. The in-phase component is sometimes called the real component. The in-phase component, while generally not responsive to changes in bulk conductivity, is especially responsive to discrete, highly-conductive bodies such as metal objects, and the out-of-phase component is sometimes called the "quadrature" or "imaginary" component. The out-of-phase (or quadrature-phase) component, using certain simplifying assumptions, can be converted to a measure of apparent ground conductivity.

(3) Tilt angle systems. The simpler frequency domain EM systems are tilt angle systems which have no reference link between the transmitter and receiver coils. The receiver simply measures the total field irrespective of phase, and the receiver coil is tilted to find the direction of maximum or minimum magnetic field strength. At any point the secondary magnetic field may be in a direction different from the primary field. With tilt angle systems, therefore, the objective is to measure deviations from the normal infield direction and to interpret these in terms of geological conductors.

EM conductivity method induces the flow of current in the ground without actual electrical contact. An alternating current in a primary (input) coil produces an alternating magnetic field that induces the flow of eddy currents in the ground. These eddy currents, in turn, generate their own magnetic field which is called the secondary magnetic field. This secondary magnetic field produces current flow in a receiver coil located at the other end of the instrument. The receiver coil divides this signal into two components, the in-phase and quadrature parts, differing in phase by 90 degrees.

The quadrature-part of the signal is used to arrive at a measure of apparent ground conductivity (in mS/m). The in-phase component may be used for detecting large metal objects and to compute the magnetic susceptibility of near-surface soils (Dalan, 1992).

The response parameter of a conductor is defined as the product of conductivity-thickness (σt), permeability (μ), angular frequency ($\omega = 2\pi f$), and the square of some mean dimension of the target (a^2). The response parameter is a dimensionless quantity. In MKS units, a poor conductor will have a response parameter of less than about 1, whereas an excellent conductor will have a response value greater than 1,000. In frequency domain EM, depth and size of the conductor primarily affect the amplitude of the secondary field. The quality of the conductor (higher conductivity means higher quality) mainly affects the ratio of in-phase to out-of-phase amplitudes (AR/AI), a good conductor having a higher ratio and a poorer conductor having a lower ratio (Robert, 1990).

A single or multi-turn loop is generally used as the transmitter element of EM systems. A time varying current passing through the loop is used to create a time varying magnetic field. Wire coils are most commonly used as the receiver element of EM systems, but Superconducting Quantum Interference Device (SQUID) magnetometers have also been used. A voltage is induced in the receiver coils proportional to the time rate of change of the magnetic field directed along the axis of the coil. Two or three coils may be used to measure the response along perpendicular axes. The horizontal component of the response along the survey line is referred to as the X component. The horizontal component of the response perpendicular to the survey line is referred to as the Y component. The vertical component of the response

is referred to as the Z component. An X component transmitter loop teamed with a trailing X component receiver coil is referred to as a horizontal "coaxial" configuration. A Z component transmitter loop teamed with a trailing Z component receiver coil is referred to as a vertical axis "coplanar" configuration (Lane, 2000).

Two major coil configuration are used in EM survey namely the Sligram and the Turam. The Slingram system is limited in size of transmitter (TX) coil. This system has their transmitter and receiver connected by a cable and their separation kept constant as they are moved together along the traverse. The magnetic field through the receiver has two sources which are the primary field of the transmitter and the secondary field produced by the target.

The Turam system is more powerful than the Slingram. It uses a very large stationary transmitter coil or wire laid out on the ground, and only the receiver is moved. The transmitter is 1-2 km long, loop over 10 km long. The receiver consist of either one coil or two coils kept at a fixed distance between 10-15 km apart (Reynolds, 1997). Ground EM measurements are acquired at points along line traverses or at individual spot locations using either FD or TD instruments.

A range of simple-to-operate, compact instruments are available to map average conductivity to depths of less than a metre to several metres. The most popular FD ground EM instruments are the Geonics suite of instruments (eg. EM31, EM34 and EM38). These instruments take measurements using a single transmitter frequency and apply an approximate transformation to convert the output to apparent conductivity. A Max Min I1 unit manufactured by Apex Parametrics Limited of Uxbridge, Ontario was used for this survey. Both in and out of phase readings were

taken at 25 meters station intervals on the grid lines. The frequencies read were 222 Hz 888 Hz and 3555 Hz while the coil separations of 100m and 150m were used.

The Max-Min I1 instrument can operate at eight frequencies out of which the following frequencies were used (3555 HZ, 888 HZ, 222 HZ), and is capable of coil separations from 12.5 meters to 400 meters and reliable data from depths of up to 60O m (1969ft). Although it can be used in the vertical loop mode as well as minimum coupled, it is most often used in the Maximum Coupled, Co-Planer mode which is in effect a Horizontal Loop Electromagnetic Survey. The instrument records the "In-Phase" and "Out-of-Phase" components of the anomalous resultant field from a conductor as a percentage of the primary field strength. Both components are used in the interpretation of the results. Generally, the larger the ratio of peak negative responses between In-Phase and Out-of-Phase, the higher the conductivity of the anomaly. A ratio of 1:1 is considered a medium conductor.

The purpose of reading more than one frequency is to obtain more information about the conductor itself as well as the conductivity of the overburden etc. As a result the signal from these frequencies can attenuate very quickly, possibly not penetrating to the bedrock at all. The lower frequencies having a longer wavelength tend to penetrate deeper and generally only respond to anomalies with a higher order of conductance. Thus as with most geophysical techniques it is a trade off as to depth of penetration versus conductance threshold detectable.

The use of multi frequency surveys helps to alleviate this problem at a minimal extra cost. Moving source (horizontal-loop) method known also as Slingram and Ronka EM was used, this system, like so many others, was developed in Sweden and has been popular in North America since about 1958. Both transmitter and receiver are moved,

a fixed spacing of 100 to 1,200 ft (30 to 360 m) between them being maintained by a cable. The transmitter is low power (1 to 10 W) and the transmitter coil is about the same size as the receiver. In some sets the coils are wound on insulating frames - 1 m in diameter; in others, ferrite-core coils are employed. The coils are coplanar and almost always oriented to detect the vertical component, although this is not a necessary requirement. In at least one model, the connecting cable is replaced by a radio link; but the cable serves the additional purpose, on reasonably level ground, of maintaining correct spacing, which is quite critical (Telford, 1976).

The depth at which the signal may penetrate the subsurface could be either the depth of penetration or the skin depth. The depth of penetration (Ze) of the electromagnetic waves is the maximum depth at which a conductor may still produce a recognizable EM anomaly and the skin depth is the depth at which the amplitude of a plane wave has decreased to 1/e or 37% relative to its initial amplitude (Ao) (Reynolds, 1997).

Interpretation of electromagnetic surveys follows basic steps. The first step is to attempt to determine from the shape of the anomaly a simple model geometry which can be thought to approximate the cause of the anomaly. The second step is to measure characteristics of the anomaly such as in-phase and out-of-phase amplitudes, and to plot these at the scale of the appropriate nomograms. Nomograms are diagrams on which the measured parameters, e.g., in-phase and out-of-phase components, are plotted for varying model conductivity and one or more geometrical factors. From the nomogram and the shape of the anomaly, estimates generally can be made for: quality of the conductor, depth to top of the conductor, conductor thickness, dip, strike, and strike length (Robert, 1990).

Field interpretation of magnetic data allows areas needing infill or checking to be identified and then revisited immediately and at little cost. Good interpretation requires profiles, which preserve all the detail of the original readings, and contour maps, which allow trends and patterns to be identified. Fortunately, the now almost ubiquitous laptop PC has reduced the work involved in contouring (provided the necessary programs have been loaded).

Published reports on the use of FDEM profiling in groundwater exploration using the Slingram method have been given by Palacky et al, (1981) and for measurements at low induction numbers by McNeill (1980a and b). The technique is usually used to measure lateral conductivity variations along line profiles either as single lines or grids of data. Further recent improvements in FDEM has seen the integration of GPS technology with the FDEM instruments which has led to a dramatic increase in the rate at which electromagnetic surveys can be accomplished. A number of manufacturers offer FDEM equipment that vary in physical size, ease of operation and survey depth from which a wide range of choice can be made.

From February 13 to 17, 1984 Norontex Exploration Ltd. of Dryden Ontario carried out a detailed geophysical exploration on claims nos. 569634 and 569635 of Moran Resources Corporations Sturgeon Lake property using a max-min 11 instrument. The survey was a follow up to earlier airborne geophysics which indicated a VLF conductor and a good HEM anomaly along the southeast shore of UcEdwards Lake in conjunction with gold mineralization in a sulphide/quartz vein structure (Rain, 1984).

A useful example of FDEM for groundwater studies has been given by Godio (1998) in a mountainous area in north-eastern Italy. Here a frequency domain survey using

20 m and 40 m coil separations gave information on the electrical resistivity for locating a number of water wells.

Taylor et al. (1988) also used electromagnetics to locate shallow water wells in highly fractured aquifers. Other writers have also demonstrated a combination of FDEM and vertical electrical soundings to locate zones of enhanced groundwater yield from fractures in arid areas.

1.4 PROBLEM STATEMENT

Integration of regional geophysical datasets and detailed field observations provide new insight into the paleoproterozoic structural evolution of southwestern Ghana (Perrouty et al., 2012). The major vein gold deposits, with the exception of the Bibiani Mine, are all located near the Birimian/Tarkwaian boundary along the northwestern margin of the Ashanti belt (Eisenlohr, 1992). As a result, the structural control at the northwest margin of these deposits, has long been recognized and studied by many writers such us Cooper (1934) and Leube et, al, (1990). The subsurface geology has less been performed by integrated geological and ground geophysical data set. In spite of immense geological observation on the Ashanti belt, only little attempt has been made so far at the southern part of south western Ghana of the Birimian and Tarkwain rocks using geophysical methods to understand the detailed relationship between structural mineralization control observed on the ground and extended to the subsurface.

The purpose of this survey is aimed at processing integrated ground geophysical magnetic and electromagnetic data to study the subsurface features with respect to their intensity of mineralization in the study areas. An attempt would be made to

display a three dimensional grid to assist in showing the structural trend. This will also help in locating the presence of ore minerals possessing contrasting magnetic and conductivity properties, which reveal themselves by causing disturbances or anomalies in the conductivity and the magnetic intensity of the subsurface geology.

1.5 OBJECTIVE OF THE RESEARCH

The main objective of the research is to carry out structural interpretation based on the trend, structural control and intensity of mineralization of the study area using ground geophysical data set namely magnetic and electromagnetic data set.

Specific objective are:

To delineate the subsurface (shallow and deep seated) magnetic sources.

To map the spatial distribution patterns of zones of heavy mineral concentrations.

To map zones of conductivity distribution.

1.6 LITHOSTRATIGRAPHY IN GHANA

Ghana can be subdivided into four distinct major lithostratigraphic or lithotectonic complexes which are as follows:

(1) Paleoproterozoic supracrustal and intrusive rocks which are made up of the Birimian Supergroup, Tarkwaian group, Tamnean plutonic suite and Eburnian plutonic suite and all of which were formed between the ages of 2195 and 2072 million years.

(2) Neoproterozoic to early Cambrian, lithologically diverse platform sediments known as the voltain supergroup which consist of the Kwahu-morango (bombouaka) group of ages between 1000 Ma to 950 Ma which lies at the base of the platform. This

was followed after a hiatus of 300 Ma by Oti-Panjari group which was deposited after 630 Ma and on top of this is the late Neoproterozoic to early Cambrian Obosum group.

(3) Rocks of the Pan african Dahomiyide Orogenic belt which include listed according to increasing degree of deformation and metamorphism, the Buem structural unit, the Togo structural unit as well as the gneisses of the Dahomeyan supergroup with peak metamorphism of approximately 600 Ma and some interleaved Eburnean protoliths and finally

(4) Isolated and spatially restricted sedimentary basin of Ordovician to Cretaceous age, mostly related to the opening of the Atlantic or proto-Atlantic ocean and classified as the Secondian group, Accraian group, Amisian group and apollonian group.

1.5.1 Geological location of study area

The study areas fall within two towns namely Asuogya and Nkwanta which are located near Tarkwa in the Wassa West district of the Western region of Ghana as shown in (Figure 1). Lithostratigraphically, the study area falls within the Birimian Supergroup and the Tarkwain group in the central part of the south of the Ashanti belt. The Asuogya lithology is made up of the Tarkwaian undifferentiated detrital sediment in the Ashante belt and the Sericite schist, quartz-sericite schist locally with garnet or staurolite of the protoliths or intrusive of Birimian Supergroup. The Nkwanta lithology is made up of Basaltic flow or Subvolcanic rock and minor interbedded volcaniclastics of the volcanic belt of Birimian Supergroup.

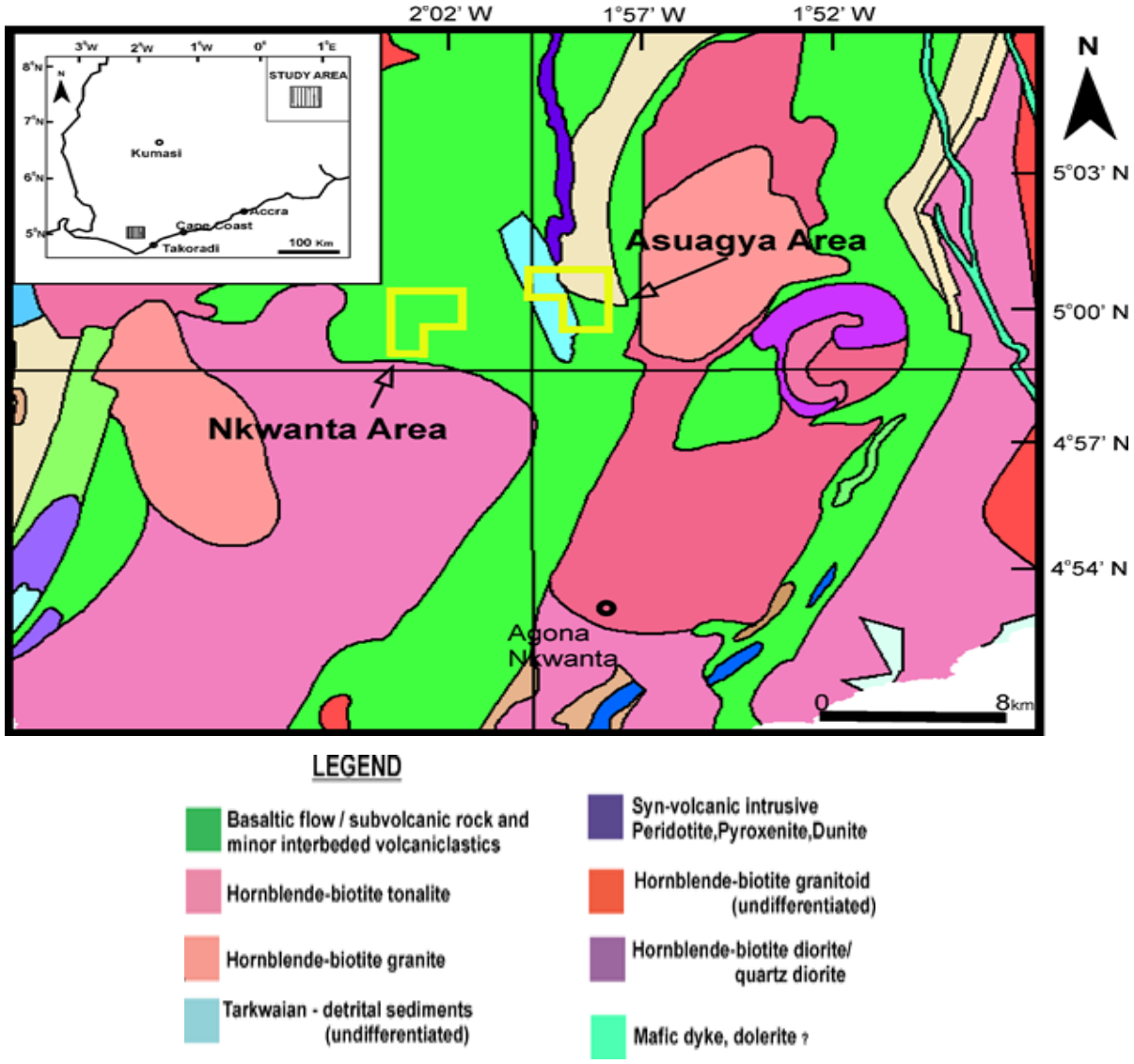

Figure 1: Geological map of the study area

1.5.2 Location and Size:

The Wassa West District which is one of the Districts in the Western Region of Ghana is located between Latitude $4^{o}00'00''$N and $5^{o}00'40''$N and Longitudes $10^{o}00'$ $45''$, W and $20^{o}00'10''$'W. Bounded to the north of the district is the Wassa Amenfi District, the south by the Ahanta West District, the West by the Nzema East District and the East by Mpohor Wassa East District. The District has a total land area of 2354 sq. km.

1.5.3 Topology and Drainage

The topography is generally undulating with summit averaging 153 meters (500ft). There is a good network of rivers and streams. Notable are rivers Tano and Ankobra. The rivers could be a source of water for irrigation purposes especially for vegetable farmers in the dry season. The volume of these rivers reduces considerably during the dry season. Most of the streams dry out completely in the dry season when they are needed. Thus, many enclaves (towns) in the district suffer acute water shortage during the dry season.

1.5.4 Climate and Vegetation

There are three main vegetation zones: semi deciduous forest, the south-west rainforest and the transitional forest, all of which are suitable for the cultivation of both food and cash crops. The forests of the district are part of the only surviving forests of Ghana.

1.5.5 Soil

The Wasa West District is located on the Birimian rock system; the district lies within the Kumasi Basin and partly within the Sefwi Gold belt, however major part of the district is positioned in the transitional zone of Sefwi and the Axim-Konongo gold belts.

The Asankrangwa-Manso-Nkwanta belt features as a prominent fault which has gold potential. The rock type also provides mineralization for Bauxite, Manganese, and Iron-ore deposits. Alluvial gold deposits occur in the Tano River basin within the district.

CHAPTER TWO

LITERATURE REVIEW

2.1. THE WEST AFRICAN CRATON

West Africa, an area roughly the size of Europe, features a wide variety of geological terranes with a complicated geological history. Although the broad geological framework was established by pioneer workers much earlier in this century, it has only been in the last few decades that more detailed regional studies have helped to unravel details of the geological history and establish a general chronology of events based on fairly extensive radiometric age-dating. Figure 2.1 outlines the major geological 'provinces' of West Africa and the following sections of this chapter very briefly describe the major features of the region. Wright et al. (1985), Petters (1991), and Dallmeyer et al. (1989) have summarized much of the regional information in several excellent texts. The BRGM report on the 'West African Gold Deposits' (Milesi et. al., 1989) also provides a very good review of the regional geology, as well as considerable detail on various types of gold deposits in the region.

In broad terms, the region features a West African Craton of older Precambrian rocks surrounded by younger Precambrian and Phanerozoic units. The southern part of this craton is now generally referred to as the Man Shield. Some French geoscientists continue to use the term Leo Shield for much of the same area and restrict the use of Man Shield to the Archean portion of the craton. However, this has not received wide acceptance and this report will utilize the term Man Shield in it broad context. The oldest Precambrian rocks are Archean in age (>2500 Ma) and appear to be limited to a

core zone along the coastal region extending from western Côte d'Ivoire through Liberia, Sierra Leone and into southern Guinea.

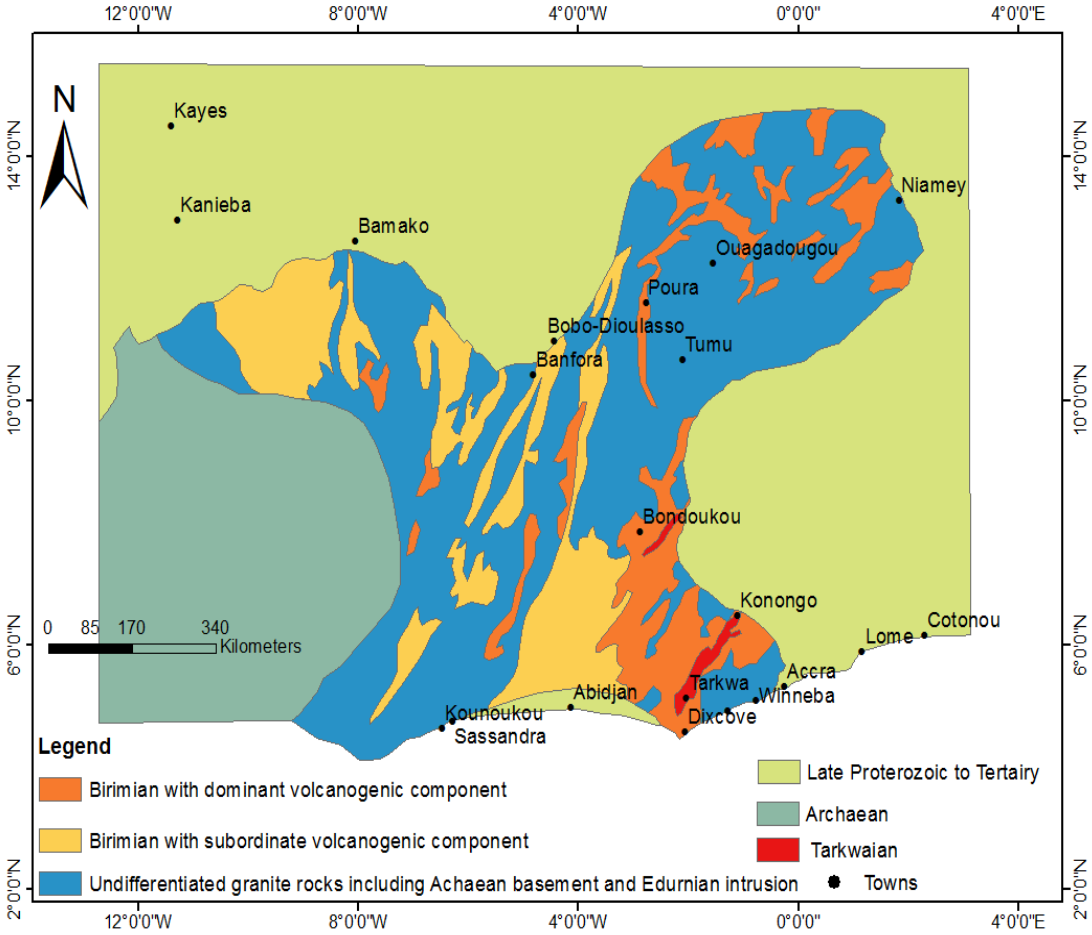

Figure 2.1: Generalised distribution of Birimian supracrustal belts in West Africa (Wright et al., 1985).

2.1.1 The Eburnean Orogeny in Ghana

The accretion of the Birimian Supergroup onto the Man Shield during the Late Paleoproterozoic is referred to as the Eburnean Orogeny (Attoh et al., 1997). It involves the accretion of volcanic arcs, deformation and intrusion of granitoids. Granitic intrusives present in both Tarkwaian and Birimian rocks either pre-date (i.e. Dixcove granites) or coincide with (i.e. Cape Coast granites) or immediately postdate

(i.e. Bongo granites) the Eburnean tectonothermal event and resulted locally in high-grade contact metamorphic aureoles in the surrounding Birimian and Tarkwaian strata. The exact timing and duration of the Eburnean Orogeny is not entirely clear at present. Milesi et al., (1992) do, however, suggest that compressional deformation commenced at ~2.1 Ga with an early phase of low-angle thrusting and folding. This phase of deformation is well represented. This phase is thought to precede the deposition of the Tarkwaian siliciclastics. Two later phases of deformation (sinistral and dextral strike-slip faulting) occurred after deposition of the Tarkwaian (Milesi et al., 1992).

Rocks of the Birimian Supergroup were affected by upper greenschist facies regional metamorphism (Eisenlohr and Hirdes, 1992; Davis et al., 1994; Kleinschrot et al., 1994, Hirdes et al., 1996). According to Kleinschrot et al. (1994), pressure and temperature (P-T) conditions reached upper greenschist facies (maximum of 500^0C and 5 kbar). In contrast, John et al., (1999) suggest that regional metamorphism was as high as amphibolite facies (500 - 650^0C and 5 - 6 kbar) and that the greenschist facies metamorphism only represents a retrograde event associated with large-scale aqueous fluid infiltration.

Large-scale aqueous fluid infiltration took place into Birimian strata along major late tectonic shear zones and smaller associated faults. One such shear zone is the NE-SW trending Obuasi shear zone to the west of the Nsuta manganese mine. It is a major strike-slip shear with dominant sinistral movement (Oberthur et al., 1994). Hydrothermal Gold mineralization associated with the Obuasi shear zone is post peak metamorphic and was dated at 2058±6 Ma (Oberthur et al., 1998). This constrains the age and duration of the Eburnean tectonothermal event between 2.17 and 2.06 Ga, a

period of 110 Ma, comparable to typical time periods envisaged for one half of a plate tectonic Wilson cycle.

2.2 THE BIRIMIAN IN GHANA

The Birimian comprises an assemblage of sedimentary/volcaniclastic rocks (Lower Birimian) which separate a series of subparallel, roughly equal-spaced northeast trending volcanic belts (Upper Birimian). Rocks of the Tarkwaian are dominated by coarse clastic sediments that are mostly located within the volcanic belts (Fig. 2.2). Metaluminous, relatively Na-rich, granitoids that may be pene-contemporaneous with volcanism are emplaced in the volcanic belts. This contrasts with peraluminous granitoids that intruded the Birimian volcaniclastic/sedimentary assemblage toward the end of deformation (Eisenlohr and Hirdes in prep.). The two granitoid types are referred to as Dixcove and Cape Coast-type granitoids respectively. Sm/Nd isotopic studies show that both the Birimian and, with a few minor exceptions, the granitoids represent juvenile crustal additions with Sm/Nd model ages of ca. 2.0 to 2.3 Ga (Taylor et al. 1988). Typical lithologies of the lower Birimian include tuffaceous shale, siltstone, greywacke and chemical (Mn-rich) sediments that are largely confined to the basin margins. Upper Birimian rocks include an assemblage of tholeiitic basalts with some interflow sediments. Traditionally, Upper Birimian rocks were considered to overlie Lower Birimian rocks (Junner 1935). However, in a recent reinterpretation of the stratigraphy Leube et al. (1990) recognise the two assemblages as coeval with the sedimentary/volcaniclastic units representing the distal facies, or basins, between sequences of evenly-spaced volcanic belts. The Tarkwaian consists of coarse clastic sediments and is usually regarded as the detritus of Birimian rocks that were uplifted and eroded following the Eburnean tectonothermal event (cf. Leube et

al. 1990). This interpretation is not universally accepted and the Tarkwaian is considered to be the youngest unit in the Birimian by some workers (Bessoles 1977; Hastings 1982; Eisenlohr, 1992).

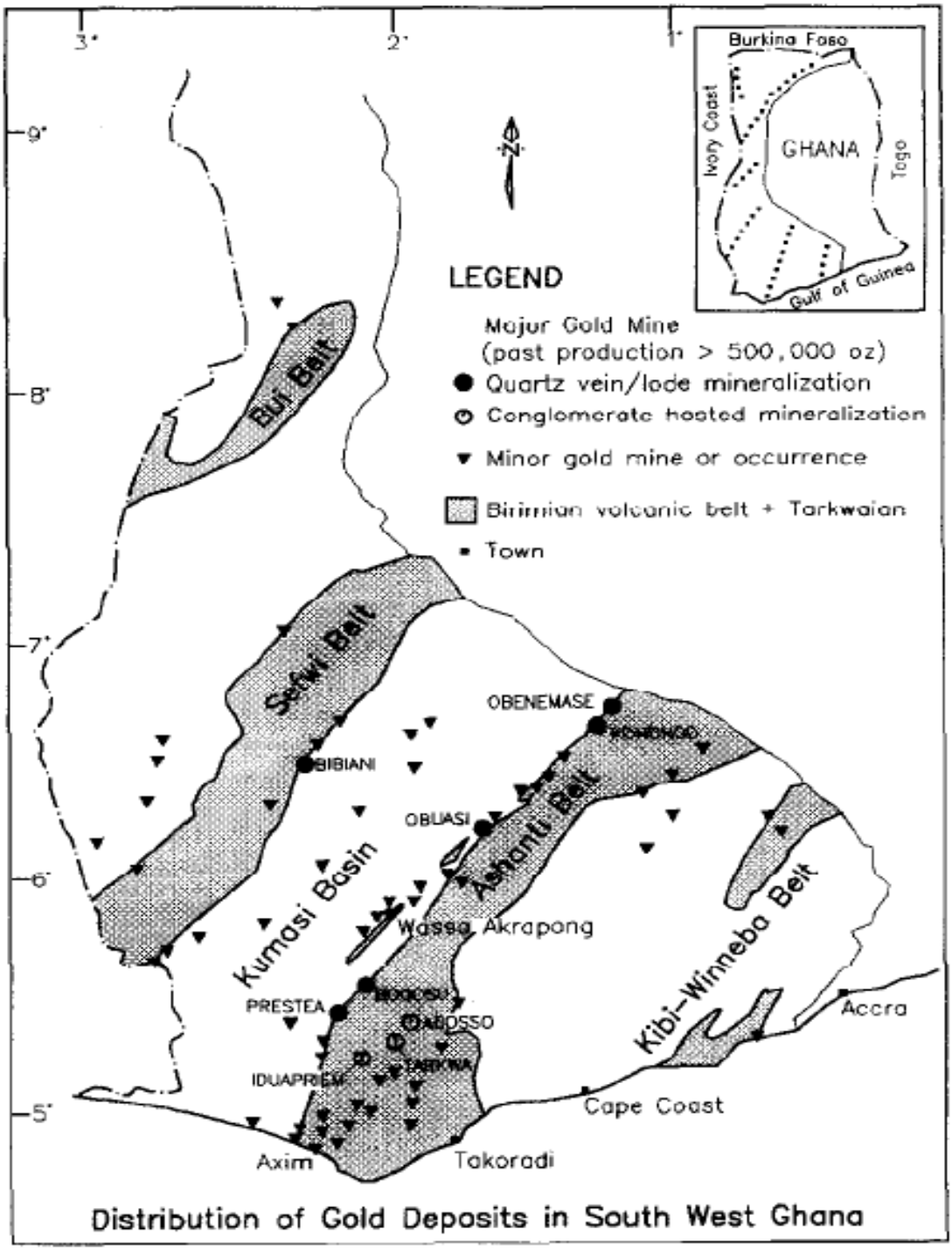

Figure 2.2: Geological sketch map of southwest Ghana (Taylor et al., 1992; Leube et al., 1990). Inset shows location of all volcanic belts as dotted lines.

2.2.1 Volcanic rocks of the Birimian

The most striking feature of the geology of Ghana is the parallel disposition of evenly spaced belts of folded Birimian metalavas (Fig.2.2). Gravity data by Hastings (1983) indicate their northeasterly continuation below flat-lying Voltaian sediments of late Precambrian to possibly early Paleozoic age into neighbouring countries, thus reaching lengths of several hundred kilometres. Belt width is 15-40 km. Distances between individual belts are approximately 90 km. Only the Lawra belt in the extreme northwest of Ghana shows N-S trend. Terranes between individual belts consist of isoclinally folded metasedimentary rocks and granitoids in varying proportions. In southern Ghana erosion has affected Birimian rocks to a comparatively small extent. In northern Ghana and Burkina Faso the level of erosion is deeper due to uplift of the West African shield towards the north. Granitoids dominate and volcanicbelts become narrow (i.e. deeper levels are exposed on the present surface). The bulk of the Birimian metalavas in Ghana are basaltic in composition. Volcaniclastic sediments occur interbedded within the basaltic flows of all volcanic belts. The proportion of metalavas to metapyroclastics varies between belts. The highest pyroclastics/lava ratios are encountered in the Ashanti belt, the lowest in the Sefwi belt. The variable pyroclastics/lava ratios could in part be a function of erosion level. The metamorphic grade of the volcanic rocks varies between pumpellyite-prehnite facies and almandine-amphibolite subfacies; however, metamorphism of most rocks is confined to the chlorite zone of the greenschist facies. Amphibolite- facies assemblages occur sporadically but especially around the margins of granitoid bodies. Similarly, Granitoid pebbles in Tarkwaian rocks imply a pre-Tarkwaian age of contact metamorphism (Leube, 1990).

2.2.2 Metasedimentary rocks of the Birimian.

Birimian metasedimentary rocks of Ghana are divided into: (1) volcaniclastic rocks; (2) turbidite-related wackes; (3) argillitic rocks; and (4) chemical sediments. Boundaries between these subdivisions are gradational (Leube, 1990).

2.2.3 The Volcaniclastic rocks.

The presence of bipyramidal quartz, idiomorphic plagioclase crystals, chloritized glass fragments, and the absence of rounded heavy minerals suggests that the sediments comprise chiefly sand- to silt-sized, partly reworked pyroclastics. Volcanogenic epiclastic rocks are also present and are mixed with the pyroclastics in varying proportions. Lapilli-sized pyroclastic rocks rarely occur in the Birimian of Ghana. Volcaniclastic sediments are present as minor constituents within the volcanic belts but make up the bulk of the basin sediments (Leube, 1990).

2.2.4 Turbidite-related wackes

Evidence of submarine slumping of the sediments is readily detectable in fresh exposures and drill cores. Pyroclastic and epiclastic sediments that were transported down slopes at basin edges by turbidity currents produced wackes displaying graded-bedding. Major components of wackes are chert (partly graphitic), graphitic schist, quartz, and to a lesser degree lava. Granitic fragments are absent. Source areas producing such a pebble lithology are likely to be the Birimian volcanic belts including chemical sediments at their flanks rather than older sialic crust of Liberian age, as proposed by Breakey and Breakey (1977).

2.2.5 Argillites

Argillites are widespread within the Birimian basins of Ghana. Interbedding of fragmental and argillitic sediments is very common. The argillite/volcaniclastic rock proportions depend on the distance from one of the volcanic belts. Evidence for slumping and intraformational brecciation is present in many argillites. Breakey and Breakey's (1977) suggestion that argillitic sediments represent the 'normal' background sedimentation of basinal muds and silts within the depository is supported. Windblown ashes, ash -sized tephra discharged directly into the water during the initial build-up of a volcanic island, as well as the finest-grained particles of volcaniclastic turbidites, constitute sources of this fine-grained background sedimentation. Periodic influxes of fragmental rocks (fall-out products of subaerial eruptions, pyroclastic flows and surges, epiclastic sediments, and/ or volcaniclastic turbidites) produced the sand-sized intercalations so frequently present in Birimian argillitic piles. Phyllites and volcaniclastic rocks show comparable chemical compositions, pointing to a common origin for both rock types. Argillitic sedimentary rocks of the Birimian occur as two types: phyllites and carbonaceous schists. Argillites in transition zones between belt volcanics and basin sediments seem to be especially rich in carbonaceous matter (Leube, 1990).

Penecontemporaneous deposition of the tholeiitic flows and the various sedimentary rocks is indicated by a transition from volcanic rocks into sedimentary rocks along strike, and interbedding between the two rock types. This implies that existing schematized chronostratigraphic concepts (Junner, 1935; Papon, 1973; Hottin and Quedraogo, 1975), which are largely based on very localized observations, should be replaced by a lithofacies approach taking into account the dynamic evolution of any depositional environment in time and space. TDM model ages for eight samples of

various Birimian basin sediments range from 2.01 Ga up to 2.31 Ga, and so differ very little from any of the analysed Birimian volcanic rocks. Although this range appears comparatively large it shows that the sediments are not of Archean provenance but of Birimian (early Proterozoic) age. It may thus be concluded that the input of detritus into the Birimian sedimentary basins derived from ancient crustal sources has been insignificant; rather a derivation of detritus from contemporaneous igneous activity in the volcanic belts is confirmed by isotopic data (Leube, 1990).

2.2.6 Chemical Sediments.

A chemical facies (chert, Mn-rich rock, CaFe-Mg carbonates, carbon-rich rock, and sulphide-rich rock) predominantly occurs at the transition zone between belt volcanics and basin sediments, i.e. in the volcanic/volcaniclastic and volcaniclastic/argillite facies; however, it is discontinuously developed, as is the wacke facies. The areal distribution of the different facies shows some symmetry. This is especially apparent in the case of the wacke facies, which occurs proximal to the western margin of the Ashanti belt, and near the eastern edge of the Sefwi belt. The symmetry also becomes evident from the areal distribution pattern of the chemical facies defined by Mn and Au occurrences along the belt boundaries mentioned (Fig. 2.2), as well as an increase in argillitic sediments going northwestwards from the Ashanti belt and southeastwards from the Sefwi belt. A further indicator of facies changes towards the basin centres could be the higher contents of organic carbon as compared with juvenile, magmatogenic carbon in the few investigated samples of carbonaceous schists deposited in distal, low-energy environments (Leube, 1990).

2.3 INTRUSIVE ROCKS

Four main types of granitoids are recognised in the Birimian of Ghana. They include Winneba, Cape Coast, Dixcove and Bongo granitoids (Junner 1940; Kesse, 1985). The latter three have been recently termed "Basin", "Belt" and "K-rich" granitoids. (Leube et al., 1990; Hirdes et al., 1993). The Cape Coast and Dixcove type granitoids are widespread in Ghana, the Winneba type is limited to small areas near Winneba, and the Bongo type crops out in the Bole-Navrongo Belt and in the Banso area.

2.3.1 Basin or Cape Coast type Granitoids

The first group (sedimentary basin granitoids) refers to large granitoid batholiths emplaced within basin sediments. The Cape Coast granites occur only within the Birimian sedimentary basins. Some of them are two mica granites. This group also includes gneisses, and these are especially well developed in the metasedimentary belts. They are typically biotite-bearing. It has been suggested that the Cape Coast granitoids, which appear migmatitic in some localities, might represent an older continental basement on which the Birimian supracrustals were deposited. However, there is no geochronologic support for this theory. Contacts between these granitoids and the metasediments are irregular; rafts of metasediments and relict structures from metasediments rise into the granitoids, and tendrils of granite vein the metasediments (Taylor, 1992).

2.3.2 Dixcove type Granitoids

Dixcove-type granitoids are metaluminous and typically dioritic to granodioritic in composition. They intrude Birimian volcanic rocks. They are typically hornblende-bearing and are commonly associated with gold mineralisation where they occur as small plutons within the volcanic belts. The granitoids are massive in outcrop, do not

have a compositional banding or foliation, and are thus generally considered post-deformation. Dixcove-type granitoids have never been shown to intrude or crosscut Cape Coast granitoids, However, some workers (Murray, 1960) have recognised Dixcove granitoid clasts in Cape Coast granitoids (Leube, 1990).

2.3.3 Winneba Granitoid

The Winneba-type granitoid is restricted to a single locality (the area of Winneba town) where it occurs within basin sediments. Layton (1958) described it as a porphyroblastic microcline-biotite adamellite cut by biotite granite. It is the only rock suite so far encountered in Ghana which shows evidence for an Archean sialic precursor (Sm/Nd model age of about 2.6 Ga (Taylor et al., 1988). Most samples are granodiorite; some are granites (s.s.). Foliation is common.

2.3.4 Bongo granitoids

The type locality for this granitoid is located in northern Ghana where the granites intrude Tarkwaian sediments that overlie the Bole-Navrongo Volcanic Belt. This granitoid is peraluminous and lacks foliation (Leube, 1990). The granitoid's Rb-Sr whole-rock isochron age is 1,968 ± 49 Ma (Hirdes, 1992). Despite their belt setting, they show consistently high K-values. Petrographically, they are characterized by pink porphyroblastic alkali feldspar 5-25 mm in length in a finer grained matrix. Hornblende appears as scattered subhedral crystals showing distinct cleavage.

2.4 STRUCTURE OF THE ASHANTI BELT

In the centre of the Ashanti belt, structures in the Tarkwaian rocks are characterised by a series of open, northeast plunging antiforms and synforms. Towards the strongly tectonised northwest margin these pass into a zone of overturned strata and reverse

faulting where the Tarkwaian is locally overthrust by Birimian rocks. Along this narrow zone, which stretches northeast from Axim to north of Konongo, high angle (65^{o}-75^{o}), northwest dipping thrust faults have been described from subsurface exposures (Cooper, 1934; Junner, 1932) and foliation/bedding relationships in the Prestea and Obuasi Gold mines suggest their location in overturned fold limbs (Eisenlohr, 1992). An intermittent outlier of Birimian volcanic rocks extends along the northwest margin of the belt and appears to represent the northwest limb of an overturned syncline which gradually tightens to the northeast. At the north of Obuom, this outlier merges with the belt margin to form a series of thrusts. Oblique thrusting of the Birimian onto the Tarkwaian is also indicated by the orientation of mesoscopic fabrics in these rocks along the northwest margin of the belt (Eisenlohr and Hirdes, 1992). The truncation of folds by thrusts along the northwest margin of the Ashanti Belt indicates that folding occurred prior to thrusting. In contrast, thrusting is not documented along the southeast belt margin where the Tarkwaian and Birimian appear to form a folded sequence. A sedimentological study of the southern part of the Ashanti Belt indicates that the Tarkwaian was deposited in a half-graben with a faulted western and flexured eastern margin (Strogen, 1988), which, along with other evidence, suggests both syn- and post-Tarkwaian activity along the northwest margin (Eisenlohr and Hirdes, 1992).

2.5 MAGNETICS

2.5.1 Background of the Earth Magnetic field

The magnetic field of the Earth is a vector, that is, it has both magnitude and direction. The magnitude, or intensity F (the field strength), of the field is measured in the same units as other B (magnetic field) fields, namely in tesla. However, a tesla is an extremely strong magnetic field, such as one would observe between the poles of a powerful electromagnet. The Earth's magnetic field is much weaker; its maximum intensity is reached near to the magnetic poles, where it amounts to about 6×10^{-5}T. Modern instruments for measuring magnetic fields (called magnetometers) have a sensitivity of about 10^{-9}T; this unit is called a nanotesla (nT) and has been adopted in geophysics as the practical unit for expressing the intensity of geomagnetic field intensity. There is a practical reason for adopting this unit. Most geomagnetic surveys carried out until the 1970s used the now abandoned c.g.s. system of units, in which the B-field was measured in gauss, equivalent to 10^{-4} T. The practical unit of geophysical exploration was then 10^{-5} gauss, called a gamma (γ). Thus, the former unit (γ) is conveniently equal to 10^{-9} T, which is the new unit (nT). The magnetic vector can be expressed as Cartesian components parallel to any three orthogonal axes. The geomagnetic elements are taken to be components parallel to the geographic north and east directions and the vertically downward direction (Lowrie, 1981).

As far as exploration geophysics is concerned, the geomagnetic field of the Earth is composed of three parts: 1. The main field, which varies relatively slowly and is of internal origin. 2. A small field (compared to the main field), which varies rather rapidly and originates outside the Earth. 3. Spatial variations of the main field, which

are usually smaller than the main field, are nearly constant in time and place, and are caused by local magnetic anomalies in the near-surface crust of the Earth. These variations are the targets in magnetic prospecting (Telford, 1990).

Main Field- This is the largest component of the magnetic field and is believed to be caused by electrical currents in the Earth's fluid outer core. For exploration work, this field acts as the inducing magnetic field. The Earth's main magnetic field originates in electric currents circulating in the liquid outer core, but can be largely modelled by a dipole source at the Earth's centre. The magnetic source is thought to be a self-excited dynamo in which highly conductive fluid moves in a complex manner caused by convection. The magnetic poles drift to the west at the rate of 19–24 km per year. As a result of the shifting poles there is a change in the direction of the field, referred to as a secular variation. This is a periodic variation with a period of 960 years. In addition there are annual and diurnal, or daily, variations. Distortions in the dipole field extending over regions thousands of kilometres across can be thought of as caused by a relatively small number of subsidiary dipoles at the core–mantle boundary.

External Magnetic Field - This is a relatively small portion of the observed magnetic field that is generated from magnetic sources external to the earth. This field is believed to be produced by interactions of the Earth's ionosphere with the solar wind. Hence, some temporal variations associated with the external magnetic field are correlated to solar activity. Most of the remaining small portion of the geomagnetic field appears to be associated with electric currents in the ionized layers of the upper atmosphere.

Time variations of this portion are much more rapid than for the main "permanent" field. Some effects are: 1. A cycle of 11 years duration that correlates with sunspot

activity. 2. Solar diurnal variations with a period of 24 h and a range of 30 nT that vary with latitude and season, and are probably controlled by action of the solar wind on ionospheric currents. 3. Lunar variations with a 25 h period and an amplitude 2 nT that vary cyclically throughout the month and seem to be associated with a Moon-ionosphere interaction. 4. Magnetic storms that are transient disturbances with amplitudes up to 1,000 nT at most latitudes and even larger in polar regions, where they are associated with aurora. Although erratic, they often occur at 27 day intervals and correlate with sunspot activity. At the height of a magnetic storm (which may last for several days), long-range radio reception is affected and magnetic prospecting may be impractical (Telford et al., 1990).

Crustal Field- This is the portion of the magnetic field associated with the magnetism of crustal rocks. This portion of the field contains magnetism caused by both inductions from the Earth's main magnetic field and from remnant magnetization. The Earth's crustal magnetic field is more complicated than a simple bar magnet dipole field, and much less intense than the main dipole field by nearly a factor of 100. Whenever molten lava solidifies on Earth’s surface, some of the ferro-magnetic elements in the lava (e.g. iron, nickel etc.) align themselves with the local dipole field. Once the lava cools below the Curie Point (about 800 F), the ferromagnetic atoms can no longer move freely, and so their magnetic orientation is frozen in. The process is not 100% effective, so the magnetization of this crustal magma is very weak, but it can be easily detectable with suitable equipment. In fact, prospectors for various commercially important ores and minerals use sensitive magnetometers to scan the surface for magnetic enhancements over the much stronger dipole field.

2.5.2 The geomagnetic field

The dipolar nature of the geomagnetic field necessitates taking some care in specifying the field's direction. The field is oriented vertically downward at the north magnetic pole, is horizontal (and pointing north) at the magnetic equator and points vertically upwards at the south magnetic pole. The magnetic poles have been observed to have moved considerably over historical times and detectable movement occurs even from year to year. However, it is thought that, on average over geological time, the dipole field which best fits the observed geomagnetic field has been coaxial with the geographic poles of rotation. Instantaneously, however - at times such as the present - the virtual magnetic poles may differ from the geographic poles by as much as 10 to 20 degrees.

The definition of the main geomagnetic field at any point on the earth's surface as a vector quantity requires three scalar values, normally expressed either as three orthogonal components (Figure 2.3) (vertical, horizontal-north and horizontal-east components) or the scalar magnitude of the total field vector and its orientation in dip and azimuth. With the exception of a few specialised surveys, magnetic surveys have always measured only the scalar magnitude of F (geomagnetic field), making the latter system more convenient for present purposes.

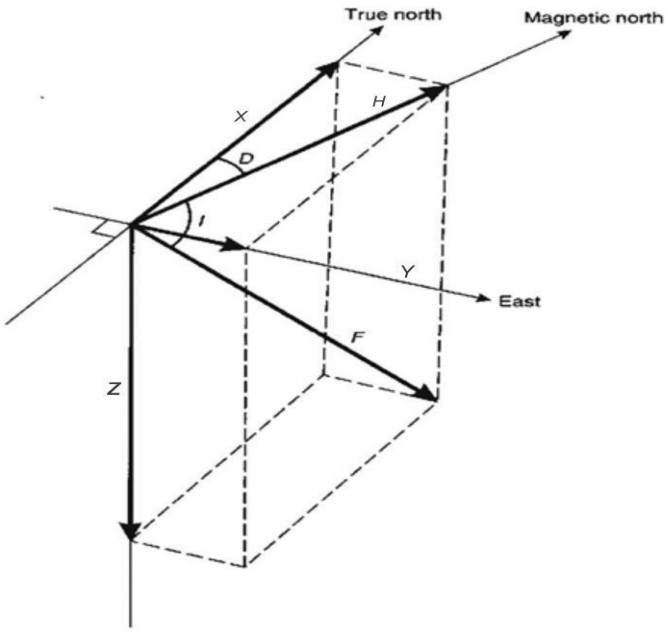

Figure 2.3 Elements of Earth‘s Magnetic Field; Z: Vertical component H: Horizontal component.

The angle the total field vector makes above or below the horizontal plane is known as the magnetic inclination, I, which is conventionally positive north of the magnetic equator and negative to the south of it. ($-90° \leq I \leq +90°$). The angle between the vertical plane containing F and true (geographic) north is known as the magnetic declination, D, which is reckoned positive to the east and negative to the west. The value of D is commonly displayed on topographic maps to alert the user of the difference between magnetic north, as registered by a compass, and true north. D is less than 15° in most places on the Earth, though it reaches values as large as 180° along lines joining the magnetic and geographic poles (Reeves, 2005).

Simple dipole theory predicts the magnetic inclination, I, to be related to geographic latitude, φ, as follows: $\tan I = 2 \tan \varphi$. Hence when, for example, $\varphi = 30°$, $I \cong 49°$ Actual measurements of I show some deviations from this simple prediction.

Similarly, the variations observed in F are not as simple as the dipole theory predicts. F varies from less than 22000 nT in southern Brazil to over 70 000 nT in Antarctica south of New Zealand. It is clear that in the cases of F, I and D there is variation with longitude as well as latitude. Since mapping of local variations in F attributable to crustal geology is the purpose of magnetic surveys, it is the definition of the 'normal' or global variation in F that must be subtracted from observed *f* to leave the (time invariable) magnetic anomaly that concerns us here. As often in geophysics, the need to define the normal before being able to isolate the 'anomaly' is clear (Reeves, 2005).

2.5.3 Temporal variations

The variations in F (geomagnetic field) with time over time-scales ranging from seconds to millions of years have a profound effect on how magnetic surveys are carried out, on the subtraction of the main field from the measured field to leave the anomaly, and in the interpretation of the resulting anomalies. These variations are described briefly, starting with variations of short time-span (some of which may be expected to occur within the duration of a typical survey) and ending with those of significance over geological time. The record of F from a magnetometer left recording for several weeks is shown in Figure 2.4.

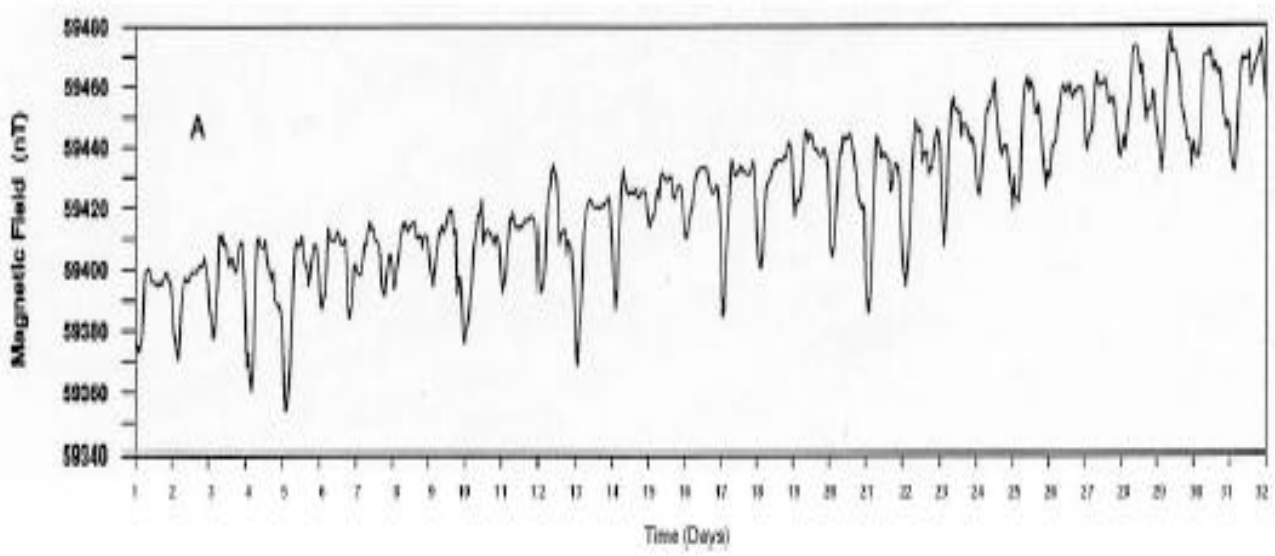

Figure 2.4 Variations in F at a fixed point recorded over a number of weeks. Each tick-mark on the time axis is one day.

2.5.4 Secular variation

Variations on a much longer time-scale - hundreds of years – are well documented from historical data and the accurate magnetic observatory records of more recent decades. The main manifestation of secular variation globally is changes in size and position of the departures from a simple dipolar field over years and decades. The effects of these changes at a given locality are predictable with a fair degree of accuracy for periods of five to ten years into the future, but such predictions need to be updated as more recent magnetic observatory and earth satellite recordings become available.

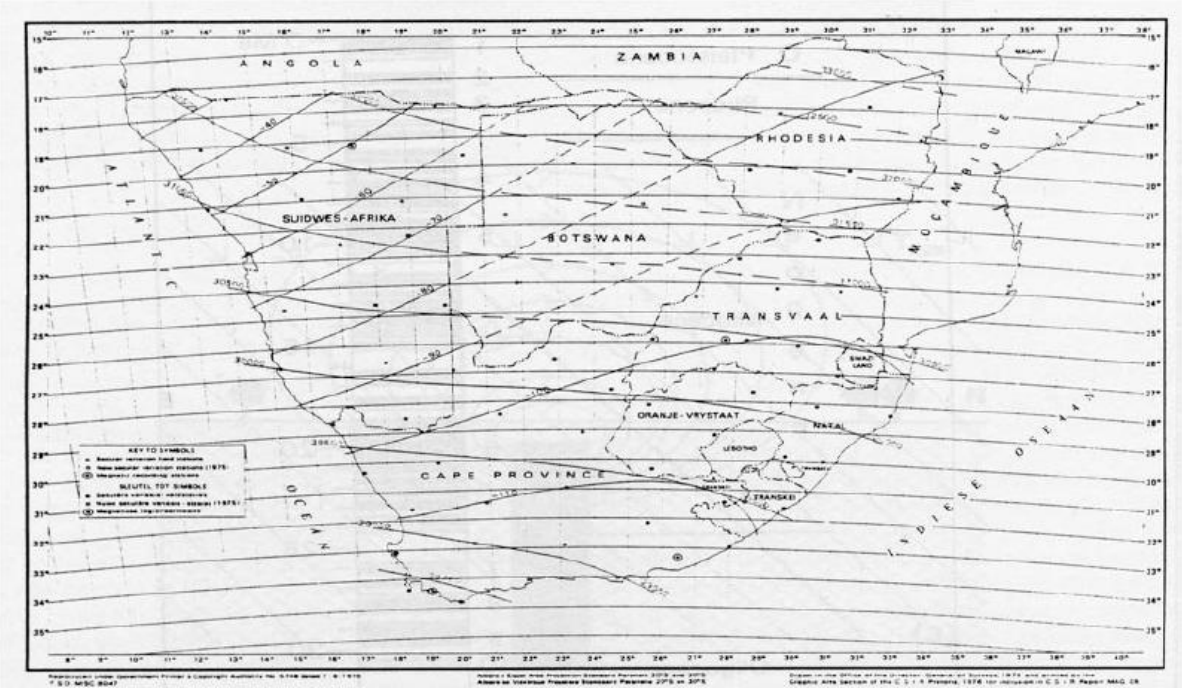

Figure 2.5 The variations in F from a series of observations at repeat station (dots) in 1970 and 1975.

The variations of F with position are shown as heavy lines, while thinner lines show the expected change in F with time in the years ahead. From the point of view of magnetic anomaly mapping, secular variations become important when surveys of adjacent or overlapping areas carried out several years apart are to be compared or merged together. Figure 2.5 shows values of F in southern Africa from observations made at 'magnetic repeat stations' (points on the ground visited to remeasure the main elements of the geomagnetic field at five-yearly intervals) for the epoch 1975. Thinner contours show the rate of change in F determined from observations made in 1970 and 1965. At a location such as Union's End (24.7 deg S, 20.0 deg E) the value of F at 1975 is seen to be about 30550 nT with an annual rate of change of about 83 nT. On the basis of these values, magnetic values in the vicinity of Union's End at 1990 (for example) would be expected to be about 30550 - (83 x 15) = 29305 nT – a change of 1245 nT (Reeves, 2005).

2.5.5 Diurnal variation

The Earth's magnetic field also varies because of changes in the strength and direction of current circulating in the ionosphere. In the normal solar quiet (Sq) pattern, the background field is almost constant during the night but decreases between dawn and about 11 a.m., increases again until about 4 p.m. and then slowly declines to the overnight value (Figure 2.6). Peak to-trough amplitudes in mid-latitudes are of the order of a few tens of nanoTesla. Since upper atmosphere ionization is caused by solar radiation, diurnal curves tend to be directly related to local solar time but amplitude differences of more than 20% due to differences in crustal conductivity may be more important than time dependency for points up to a few hundred kilometers apart. Short period, horizontally polarized and roughly sinusoidal micropulsations are significant only in surveys that are to be contoured at less than 5 nT. Within about 5^{o} of the magnetic equator the diurnal variation is strongly influenced by the equatorial electrojet, a band of high conductivity in the ionosphere about 600 km (5^{o} of latitude) wide. The amplitudes of the diurnal curves in the affected regions may be well in excess of 100 nT and may differ by 10 to 20 nT at points only a few tens of kilometres apart. Many of the magnetic phenomena observed in Polar Regions can be explained by an auroral electrojet subject to severe short-period fluctuations. In both equatorial and polar regions it is particularly important that background variations be monitored continuously (Milsom, 2003).

.

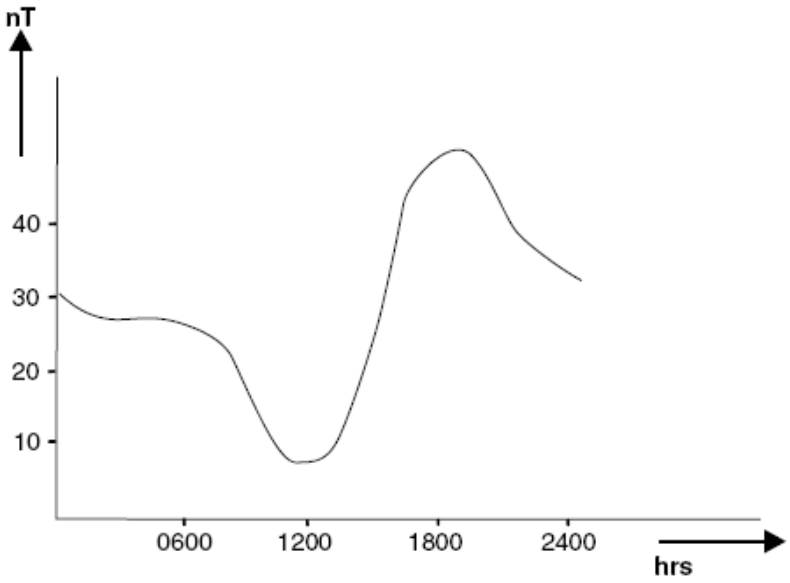

Figure 2.6 Typical 'quiet day' magnetic field variation at mid-latitudes.

2.5.6 Magnetic storms

Short-term auroral effects are special cases of the irregular disturbances (Ds and Dst) known as magnetic storms. These are produced by sunspot and solar flare activity and, despite the name, are not meteorological, often occurring on clear, cloudless days. There is usually a sudden onset, during which the field may change by hundreds of nT, followed by a slower, erratic return to normality. Time scales vary widely but the effects can persist for hours and sometimes days. Micropulsations are generally at their strongest in the days immediately following a storm, when components with periods of a few tens of seconds can have amplitudes of as much as 5 nT. Ionospheric prediction services in many countries give advance warning of the general probability of storms but not of their detailed patterns, and the field changes in both time and space are too rapid for corrections to be applied. Survey work must stop until a storm is over. Magnetic data are severely affected by quite small irregularities and for contract purposes technical magnetic storms may be defined, sometimes as departures from linearity in the diurnal curve of as little as 2 nT in an hour. Similar criteria may

have to be applied in archaeological surveys when only a single sensor is being used (rather than a two-sensor gradiometer) (Milsom, 2003).

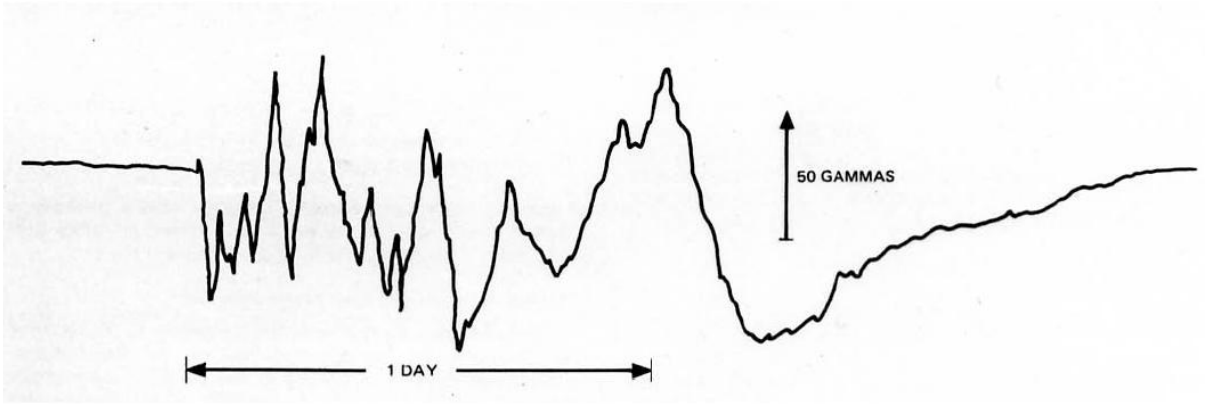

Figure 2.7: A typical magnetic storm, as observed at a time of high solar activity.
The onset of the storm is sudden and violent variations in F may be seen over several tens of hours. Return to 'normal field conditions may take several days (Reeves, 2005).

2.5.7 Elevation and terrain corrections

The vertical gradient of the geomagnetic field is only some $0.03nTm^{-1}$ at the poles and $-0.015nTm^{-1}$ at the equator, so an elevation correction is not usually applied. The influence of topography can be significant in ground magnetic surveys but is not completely predictable as it depends upon the magnetic properties of the topographic features. Therefore, in magnetic surveying terrain corrections are rarely applied. Having applied diurnal and geomagnetic corrections, all remaining magnetic field variations should be caused solely by spatial variations in the magnetic properties of the subsurface and are referred to as magnetic anomalies (Kearey, 2002**)**.

2.5.8 The International Geomagnetic Reference Field (IGRF)

The variations of the Earth's main field with latitude, longitude and time are described by experimentally determined International Geomagnetic Reference Field (IGRF) equations, defined by 120 spherical harmonic coefficients, to order N=10, supplemented by a predictive secular variation model to order N = 8. The shortest wavelength present is about 4000 km. IGRFs provides reasonable representations of the actual regional fields in well-surveyed areas, where they can be used to calculate regional corrections, but discrepancies of as much as 250 nT can occur in areas from which little information was available at the time of formulation. Because the long-term secular changes are not predictable except by extrapolation from past observations, the IGRF is updated every five years on the basis of observations at fixed observatories and is also revised retrospectively to give a definitive model (DGRF). IGRF corrections are vital when airborne or marine surveys carried out months or years apart are being compared or combined but are less important in ground surveys, where base stations can be reoccupied (Milsom, 2003).

2.5.9 Local Magnetic Anomalies

Local changes in the main field result from variations in the magnetic mineral content of near-surface rocks The sources of local magnetic anomalies cannot be very deep, because temperatures below 40 km should be above the Curie point, the temperature (=550°C) at which rocks lose their magnetic properties. Thus, local anomalies must be associated with features in the upper crust, Magnetic anomalies are caused by magnetic minerals (mainly magnetite and pyrrhotite) contained in the rocks. Magnetically important minerals are surprisingly few in number (Telford, 1990).

2.5.10 Magnetic Susceptibility

As a result of the presence of the earth's magnetic field, rocks containing magnetic minerals show induced magnetizations. From equation (2-1) the constant of proportionality between the inducing field and the magnetization is known as the magnetic susceptibility (k). The intensity of magnetization (I) is related to the inducing magnetic field (H) through a constant of proportionality (k). The magnetic susceptibility (k) is a measure of the ease by which the material can be magnetized. It is a dimensionless quantity. Magnetic susceptibility can take on positive or negative values. Positive values imply that the induced magnetic field (I) is in the same direction as the inducing field (H).

Negative values imply that the induced magnetic field is in the opposite direction as the inducing field. Magnetic susceptibility is the proportionality constant between H and I. For free space or a vacuum this constant is zero.

$I = kH$……Equation 2-1

$I = k H\cos\theta$……Equation 2-2

In the case of a homogenous external field H that define an angle θ with respect to the normal to the surface of a material capable of being magnetized, the intensity of magnetization (I) per unit area is shown in equation (2-2) or for a field normal to the surface I= KH. The magnetization contrast of the material is primarily the result of induced magnetization (Dobrin et al., 1988).

The magnetic susceptibilities of paramagnetic and diamagnetic materials are generally extremely small. Although susceptibility is unitless, its values differ depending on the unit system used to quantify H and I. The international system of units (SI), based on

the meter, kilogram, second, and ampere (mksa), was used. Based on the magnetic susceptibility, the solid materials can be classified into diamagnetic, paramagnetic, and ferromagnetic. In diamagnetic, k has low and negative values. Paramagnetic materials have low and positive k values. Ferromagnetism is a cooperative phenomenon observed in metals like iron, nickel, and cobalt. Ferromagnetic behaviour is characterized by high positive susceptibilities and strong magnetic properties. The intensity of magnetization of rocks can be determined in two different ways: by measuring the magnetic field produced either by a rock sample or by measuring the effect of the sample on the inductance of an electromagnetic circuit. The susceptibility of a rock usually depends on its magnetite content. Sediments and acid igneous rocks have small susceptibilities whereas basalts, dolerites, gabbros and serpentinites are usually strongly magnetic. Weathering generally reduces susceptibility because magnetite is oxidized to hematite, but some laterites are magnetic because of the presence of maghemite and remanently magnetized hematite. The susceptibilities, in rationalized SI units, of some common rocks and minerals are given in Table 2-1 below (Milsom, 2003).

2.5.11 Magnetism of Rocks and Minerals

Most common rock-forming minerals exhibit a very low magnetic susceptibility and rocks owe their magnetic character to the generally small proportion of magnetic minerals that they contain. There are only two geochemical groups which provide such minerals. The iron–titanium–oxygen group possesses a solid solution series of magnetic minerals from magnetite (Fe_3O_4) to ulvöspinel (Fe_2TiO_4). The other common iron oxide, haematite (Fe_2O_3), is antiferromagnetic and thus does not give rise to magnetic anomalies unless a parasitic antiferromagnetism is developed. The

iron–sulphur group provides the magnetic mineral pyrrhotite (FeS1+*x*, 0 <*x* <0.15) whose magnetic susceptibility is dependent upon the actual composition. By far the most common magnetic mineral is magnetite, which has a Curie temperature of 578°C. Although the size, shape and dispersion of the magnetite grains within a rock affect its magnetic character, it is reasonable to classify the magnetic behaviour of rocks according to their overall magnetite content (Kearey, 2002**)**

Basic igneous rocks are usually highly magnetic due to their relatively high magnetite content. The proportion of magnetite in igneous rocks tends to decrease with increasing acidity so that acid igneous rocks, although variable in their magnetic behaviour, are usually less magnetic than basic rocks. Metamorphic rocks are also variable in their magnetic character. If the partial pressure of oxygen is relatively low, magnetite becomes resorbed and the iron and oxygen are incorporated into other mineral phases as the grade of metamorphism increases. Relatively high oxygen partial pressure can, however, result in the formation of magnetite as an accessory mineral in metamorphic reactions. In general the magnetite content and, hence, the susceptibility of rocks is extremely variable and there can be considerable overlap between different lithologies. It is not usually possible to identify with certainty the causative lithology of any anomaly from magnetic information alone. However, sedimentary rocks are effectively non-magnetic unless they contain a significant amount of magnetite in the heavy mineral fraction. Where magnetic anomalies are observed over sediment covered areas the anomalies are generally caused by an underlying igneous or metamorphic basement, or by intrusions into the sediments. Common causes of magnetic anomalies include dykes, faulted, folded or truncated sills and lava flows, massive basic intrusions, metamorphic basement rocks and magnetite ore bodies. Magnetic anomalies range in amplitude from a few tens of nT

over deep metamorphic basement to several hundred nT over basic intrusions and may reach an amplitude of several thousand nT over magnetite ores (Kearey, 2002).

Table 2.1: Magnetic susceptibilities of common rocks and ores

Common rocks	**Susceptibilities**
Slate	0–0.002
Dolerite	0.01–0.15
Greenstone	0.0005–0.001
Basalt	0.001–0.1
Granulite	0.0001–0.05
Rhyolite	0.00025–0.01
Salt	0.0–0.001
Gabbro	0.001–0.1
Limestone	0.00001–0.0001
Ores	
Hematite	0.001–0.0001
Magnetite	0.1–20.0
Chromite	0.0075–1.5
Pyrrhotite	0.001–1.0
Pyrite	0.0001–0.005

2.5.12 Interpretation of the Magnetic Data

The magnetic anomaly of a finite body invariably contains positive and negative elements arising from the dipolar nature of magnetism. The poles of the magnets are negative on the surface of the body where the magnetization vector enters the body and positive where it leaves the body. The magnetic anomaly of a body of regular shape is calculated by determining the pole distribution over the surface of the body from the intensity of magnetization vector and a direction normal to the end face (Sharma, 1997).

The computation and analysis of magnetic depth solutions is the most important component of any high-resolution aeromagnetic survey interpretation. Also important is the direction of magnetization and horizontal location of the source boundaries. Together these determine the shape of anomaly caused by the source body. These methods are usually very complex (Sharma, 1997).

In general, most amplitude variations seen on magnetic anomaly maps results from variation in basement rock type and direction of magnetization, and not from basement topography. There are many methods used to interpret magnetic data. In the detection of structural trends or geological provinces, structures may be indicated by linear magnetic anomalies or alignment of anomalies and the different magnetic terrains have different magnetic signatures (Blakely, 1995).

Detection and analysis of specific anomaly sources for units with uniform susceptibility, k, and uniform polarization, equation (2-3), can relate magnetic potential to gravity potential resulting from a body of similar shape and size, i.e., magnetic potential (and hence magnetic field) can be found from the gravitational potential for the body (sphere, cylinder, polygon, etc.), using Poisson's equation (Blakely, 1995):

$$U_{mag} = \frac{1}{G\rho}\frac{dU_{grav}}{di}; \qquad \text{Equation 2-3}$$

where I = magnetization (polarization) = kĤ

i = direction of magnetization

p = density (used in getting U_{grav})

G = universal gravitational constant

For a detailed study, forward modelling is often useful. Model (3-D or 2.5-D) parameters such as depth size and location of buried bodies, intensity and direction of magnetization or density of each body, are estimated using the results of the background research. The 3-D modelling program is used to automatically refine the model parameters, minimizing the error between the theoretical and observed data. The 2.5-D modelling program can be used to interactively investigate complex modelling situations. The forward modelling procedures help define the basement topography and structure and delineate any intra-sedimentary magnetic features (from Sander Geophysics Limited).

2.5.13 Ground magnetic Survey

Magnetic surveying on the ground now almost exclusively uses the portable proton-precession magnetometer. The main application is in detailed surveys for minerals, but ground magnetics are also employed in the follow up of geochemical reconnaissance in base-metal search. Station spacing is usually 15 to 60 m; occasionally it is as small as 1m. Most ground surveys now measure the total field, but vertical-component fluxgate instruments are also used. Sometimes gradiometer measurements are made (Telford et. al., 1990).

Ground magnetic surveys are usually performed over relatively small areas on a previously defined target. Readings should not be taken in the vicinity of metallic objects such as railway lines, cars, roads, fencing, houses, etc, which might perturb the local magnetic field since most ground magnetometers have a sensitivity of about 1 nT. Base station readings are not necessary for monitoring instrumental drift as fluxgate and proton magnetometers do not drift, but are important in monitoring diurnal variations. Since modern magnetic instruments require no precise levelling, a magnetic survey on land invariably proceeds much more rapidly than a gravity survey (Kearey et al., 2002).

2.6 ELECTROMAGNETIC METHOD

2.6.1 Background

Electromagnetic (EM) methods utilizing controlled sources have traditionally been used in near-surface geophysical investigations such as mineral and hydrocarbon exploration as well as in geological mapping and structural studies. Recently, the EM methods have become popular in environmental, archeological, and engineering investigations.

In EM methods, the dominant petrophysical parameter is the electrical conductivity (or its reciprocal, the resistivity), which represents the ability of electric charges to move inside a matter. Certain geological targets, such as graphite bearing schist zones and massive sulphide ore bodies, can produce a strong anomalous EM response, because their conductivity is considerably higher than the conductivity of the host rocks The aim of geophysical interpretation is to invert the measured EM data into knowledge about the spatial distribution of conductivity inside the earth, and to use

that information in geological interpretation. Unfortunately, the inverse problem does not have a unique solution, because conductivity is a complex, continuous function and the data is collected using finite sampling. Therefore, direct inversion of EM data is not possible in practice.

For EM geophysical survey technique, the most favourable targets are metallic ores and underground pipes and cables, although this method has been used in delineating faults, shears, and thin conducting veins. A major advantage of EM methods over the electrical resistivity methods is that they do not require conductive ground connections.

2.6.2 Types of EM

There are two basic types of EM methods-Frequency Domain (FD) and Time Domain (TD). FDEM measures the electrical response of the subsurface at several frequencies (different separation distances between the transmitter and receiver can also be used) to obtain information about variations of conductivity (or its reciprocal, resistivity) with depth. TDEM achieves the same results by measuring the electrical response of the subsurface to a pulsed wave at several time intervals after transmission, longer time intervals measure greater depths. Both methods have overlapping applicabilities. EM systems are classified in various ways by different authors according to the instrumentation, geometry of the transmitter-ground-receiver elements and the nature of the transmitted and recorded signal (Zhdanov and Keller, 1994).

2.6.3 Frequency Domain

Frequency domain systems were development around the early 1950's. The first such systems measured only the quadrature component of the secondary EM field because it was not yet possible to record the secondary field and the primary field

simultaneously due to the large difference in signal amplitude. Barringer Research developed the first frequency domain system that measured both the in-phase and quadrature components of the secondary field. The benefit of the in-phase measurement is the fact that the amplitude of the measurement increases for increasing conductance, even for very conductive targets (Grant and West, 1965).

A pure frequency domain (FD) EM system transmits a magnetic field signal at a single frequency with sinusoidal variation in amplitude. The recorded response can either be described by its total amplitude and phase with respect to the transmitter signal or by the amplitudes of components in-phase ("real") and 90° out of phase ("quadrature") with respect to the transmitter signal.

2.6.4 Time Domain

A pure time domain (TD) EM system transmits a magnetic field signal with a sharp step. The time decay of currents induced in the subsurface is sampled at a number of delay times ("windows") following the step change in magnetic field. "Early" and "late" are qualifiers applied to windows in reference to the elapsed time following the change in the magnetic field. The window measurements contain information equivalent to that which would be obtained with a number of FD systems covering a range of frequencies. The equivalent range of frequencies is referred to as the "bandwidth" of the system. In practice, EM systems are often a combination of these two end members, and it is important to note both the bandwidth and signal to noise characteristics of the system being employed at each of these equivalent frequencies (Sidorov and Tickshaecy, 1969).

2.6.5 Frequency-domain electromagnetic induction measurement

The FDEM induction method for measuring ground resistivity, or more correctly, conductivity, is well known, and some extensive discussions of this technique can be found in the references given in the studies by McNeill (1980a, 1980b).

The FDEM induction method is based on the response of an induced alternating current in the ground. Consider a transmitter coil Tx energized with an alternating current at an audio frequency placed on the Earth (assumed to be uniform), and a receiver coil Rx located a short distance *s* away. The time-varying magnetic field arising from the alternating current in the transmitter coil can induce very small currents in the Earth. These currents generate a secondary magnetic field Hs, which is sensed by the receiver coil, together with the primary field, Hp. In general, this secondary magnetic field is a complicated function of the inter-coil spacing *s*, the operating frequency f, and the ground conductivity σ. Under certain constraints, which are technically defined as "operation at low values of induction number", the secondary magnetic field is a very simple function of these variables (McNeill, 1980a, 1980b). The ratio of the secondary to the primary magnetic field is linearly proportional to the terrain conductivity, a relationship that makes it possible to construct a direct-reading, linear-terrain conductivity meter by simply measuring this ratio. Given Hs/Hp, the apparent conductivity indicated by the instrument is defined by the equation (2-4) below. The MKS units of conductivity are the mho (Siemens) per m, or more conveniently, the millimho per m (McNeill, 1980).

The amplitude of these fields Hp and Hs is a function of frequency, ground conductivity, and other factors.

$$\frac{\mathrm{Hs}}{\mathrm{Hp}} = \frac{i\omega\mu_o s^2\sigma}{4} \qquad \text{Equation 2-4}$$

Where

Hs = secondary magnetic field at the receiver coil

Hp = primary magnetic field at the receiver coil

$\omega = 2\pi f$

f = frequency (Hz)

μ_o = permeability of vacuum

σ = ground conductivity (mho/m)

s = intercoil spacing (m), and

$i = \sqrt{-1}$.

In physical terms, if a conductive medium is present within the ground, the magnetic component of the incident EM waves induces eddy currents (alternating currents) within the conductor. These eddy currents then generate their own secondary EM field, which can be detected by the receiver, together with the primary field that travels through the air; consequently, the overall response of the receiver is the combined effects of both the primary and the secondary fields. The degree to which these components differ reveals important information about the geometry, size and electrical properties of any sub-surface conductors (Reynolds, 1997).

2.6.6 Ground Electromagnetic Conductivity

Electromagnetic conductivity surveys can be collected on the ground or from aircraft. The primary electromagnetic field travels from the transmitter coil to the receiver coil via paths both above and below the surface. The electrical conductivity in either approach is a function of the electrical properties of the soil and rock matrix, percentage of fluid saturation, and the conductivity of pore fluids. In general, the electrical current flows ionically through moist or saturated pore spaces in the soil and

rock, and electronically through the mineral grains themselves. Therefore, the bulk conductivity of the geologic units is generally higher or lower than the minerals from which they are composed (Stewart, 1981).

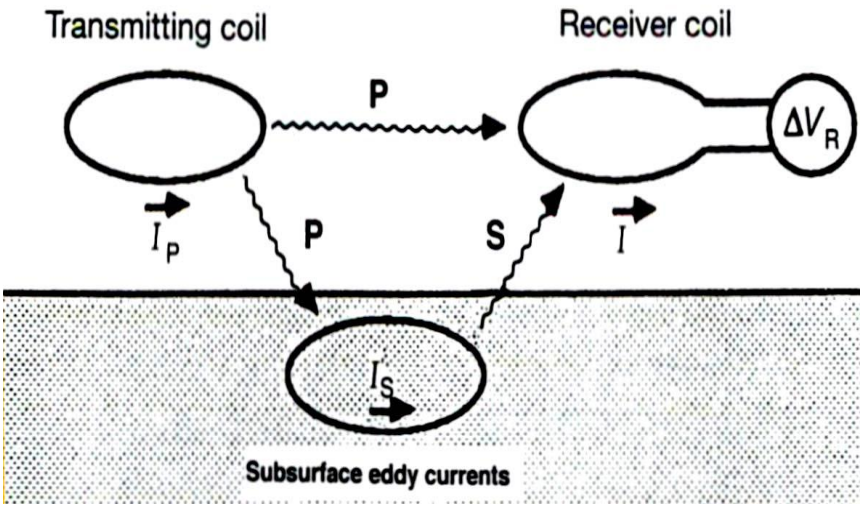

Figure 2.8: A generalized sketch of an electromagnetic induction prospecting system.

The transmitting coil, energized with an alternating current (Ip) in figure 2.8, produces a primary field, which induces eddy currents (Is) in the subsurface conductor. The receiver coil measures the resultant (R) of the primary field (P) and the secondary field (S) induced by subsurface eddy currents (Sharma, 1997).

Four field vectors, described by electromagnetic field theory, are represented by Max-well's equations (2-5, 2-6, 2-7 and 2-8). Their names, together with their SI units are: E the electric field intensity (V/m), H the magnetizing field intensity (A/m), B the magnetic induction, or flux density (Wb/m or tesla), and D the electric displacement (c/m) (Sharma, 1997):

$$\text{Curl } E = -\partial B/\partial t \qquad \text{Equation 2-5}$$

$$\text{Curl } H = J + \partial D/\partial t \qquad \text{Equation 2-6}$$

$divB = 0$ Equation 2-7

$divD = \rho c$ Equation 2-8

2.6.7 Propagation of electromagnetic field

Equations for the propagation of electric and magnetic field vectors in an isotropic, homogeneous medium with physical properties μ, σ, ε;

$\nabla^2 E = i\omega\mu\sigma E - \varepsilon\mu\omega^2 E$ Equation 2-9

and

$\nabla^2 H = i\omega\mu\sigma H - \varepsilon\mu\omega^2 H$ Equation 2-10

In the above equations (2-9 and 2-10) the terms involving ωμσ are related to conduction currents, whereas the terms involving $\varepsilon\mu\omega^2$ are related to the displacement currents. Consider the propagation parameter or the complex wave number which is indicated by k.

$k^{2=} \varepsilon\mu\omega^2 - i\omega\mu\sigma$ Equation 2-11

Two important situations arise: HIGH FREQUENCY and LOW FREQUENCY

At high frequency: $f>10^7$ Hz or $1/\rho = \sigma = 0$, then $\varepsilon\mu\omega^2 >> \omega\mu\sigma$

This stands for propagation or radar regime:

$$\nabla^2 E = \mathcal{E}\mu\frac{\partial^2 E}{\partial t^2} = \varepsilon\mu\omega^2$$ Equation 2-12

At low frequency: $f<10^5$ Hz, then $\varepsilon\mu\omega^2 << \omega\mu\sigma$

This gives the induction or diffusion regime:

$$\nabla^2 E = \mu\sigma \frac{\partial E}{\partial t} = \omega\mu\sigma$$ Equation 2-13

Equation (2-12) indicates that at high frequency propagating waves persist which is good for the detection of shallow features. The low frequency of equation (2-13) indicates that the signal travels deep which is good for detecting deeper sources.

2.6.8 Depth of penetration of EM waves

The wave attenuates so fast that it only propagates about a wavelength into the earth. Because the amplitude diminishes so rapidly and the waves travel so slowly, we generally talk about the EM wave "diffusing" into the earth. The depth of penetration of an electromagnetic field depends upon its frequency and the electrical conductivity of the medium through which it is propagating. Electromagnetic fields are attenuated during their passage through the ground, their amplitude decreasing exponentially with depth. The depth of penetration d can be defined as the depth at which the amplitude of the field A_d is decreased by a factor e^{-1} compared with its surface amplitude A where d is in metres, the conductivity σ of the ground is in Sm^{-1} and the frequency f of the field is in Hz (Spies, 1989);

$$A_d = A_o e^{-1}$$ Equation 2-14

In this case

$$d = \frac{500}{\sqrt{\sigma f}}$$ Equation 2-15

Where d = δ = skin depth

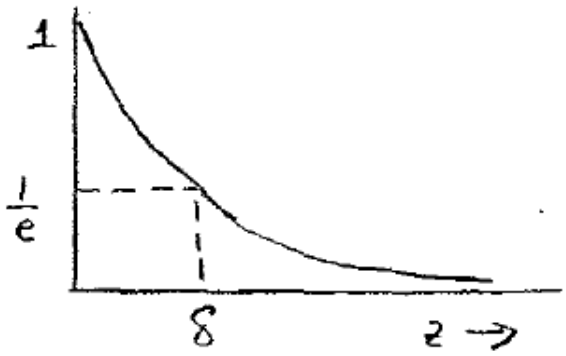

$$H = H_0 e^{-(1-i)z/\delta}$$
$$|H| = H_0 e^{-z/\delta}$$

Figure 2.9 Skin Depth: This is the depth by which the amplitude has decayed to 1/e or 37% of its surface value. For a uniform half space of conductivity σ the skin depth δ is;

$$\delta = \sqrt{\frac{2}{\mu_0 \omega \sigma}} \simeq 500\sqrt{\frac{1}{\sigma f}} = 500\sqrt{\frac{\rho}{f}};\quad in\ meters \qquad \text{Equation 2-16}$$

A maximum depth of investigation is provided by the skin depth rule, however for controlled source surveys we also need to take into account the source and receiver geometry. This generally reduces the depth of penetration. A rule of thumb for loop-loop systems is that the depth of penetration is about twice the separation of the source and receiver, but this is very approximate and is easily violated. Also, a necessary condition for this to happen is that the source/receiver separation s <<δ (coil separation is less than the skin depth).

The justification for the above statement is based upon the following. Consider a homogenous halfspace on the surface of which is located a horizontal coplanar coil (HCP) system. The time varying fields in the transmitting coils will induce eddy currents in the earth. For a homogeneous earth, these currents flow in horizontal planes. This is true even for the vertically oriented coils.

2.6.9 Relative response function

It is possible to calculate the contribution to the secondary field as measured from the surface from any thin layer of thickness *dz* at some depth z. Let Φv(z) denote this contribution from the vertical magnetic dipole source and receiver. A plot of this function is shown below:

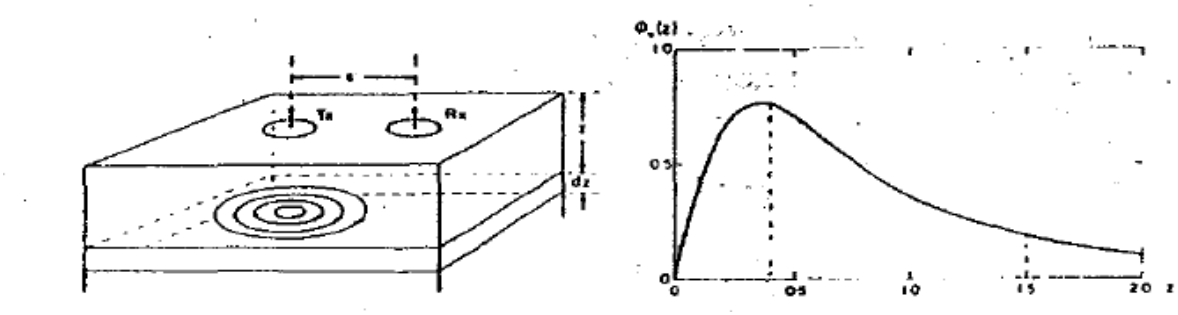

Figure 2.10: Relative response versus depth for vertical dipoles.

Φv(z) is the relative contribution to H_s from material in a thin layer dz located at (normalized depth z). Note that the vertical magnetic dipole has zero sensitivity at the surface, has a maximum at about $z = 0.4$ and is substantially diminished at $z = 2.0$. It is this type of diagram which says that the maximum depth of investigation is limited to about twice the coil separation. This rule of thumb however is valid only when the coil separation is much less than the skin depth.

The functions Φv(z) shows how conductivity at different depths contributes to the apparent conductivity measured by the instrument. This function is called the relative response. The relative response curve of Figure (2.10) above is useful for carrying out computations for the vertical dipoles. The subscript 'v' indicates that the TX and RX dipole axes are pointing in a vertical direction (McNeill, 1980). The response function curve of figure 2.10 is useful for carrying out the computation of equation 2-17:

$$\Phi_v(z) = \frac{4z}{(4z^2+1)^{\frac{3}{2}}};$$ Equation 2-17

Note that z is depth in the Earth normalized by the TX-RX distance. z = d/s.

The response function from the horizontal magnetic is very different. Let $\Phi_H(z)$ denote the relative contribution that arises from a horizontal magnetic dipole source and receiver. It has a maximum at the surface, so it is sensitive to the conductivity there, and it decreases monotonically with depth. The response function curve of Figure 2.11 below is useful for carrying out the computation of equation 2-18:

$$\Phi_H(z) = 2 - \frac{4z}{(4z^2+1)^{\frac{3}{2}}};$$ Equation 2-18

.

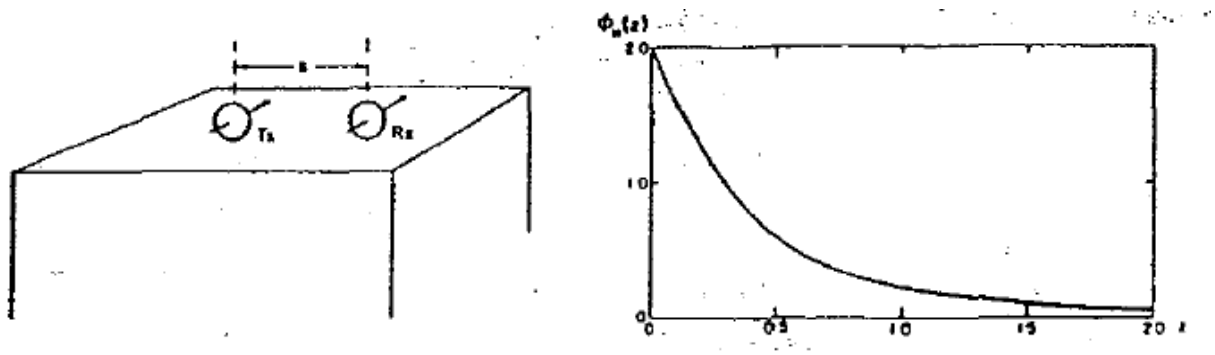

Figure 2.11: Relative response versus depth for horizontal dipoles

We therefore notice how two coil configurations couple differently with the ground and have different sensitivities with respect to the conductivity structure. Figure 2.12 below represent combined curves for the vertical and horizontal response functions.

2.6.10 Cumulative Response Functions

We often have a multi-layer earth (e.g. a thin resistive layer overlying a more conductive stratum, or vice versa) and we would like to estimate the thickness of the layer and the two conductivities. Cumulative response curves Figure (2.12) and Figure 2.13 below are useful for carrying out computations to define equations 2-19 and 2-20 for the vertical and horizontal dipole configuration.

$$R_v(z) = \int_z^{\infty} \emptyset_v\,(z)dz \;=\; R_v(z) = \frac{1}{(4z^2+1)^{\frac{1}{2}}}; \qquad \text{Equation 2-19}$$

$$R_H(z) = \int_z^{\infty} \emptyset_H\,(z)dz; \;=\; R_H(z) = (4z^2 = 1)^{\frac{1}{2}} - 2z; \qquad \text{Equation 2-20}$$

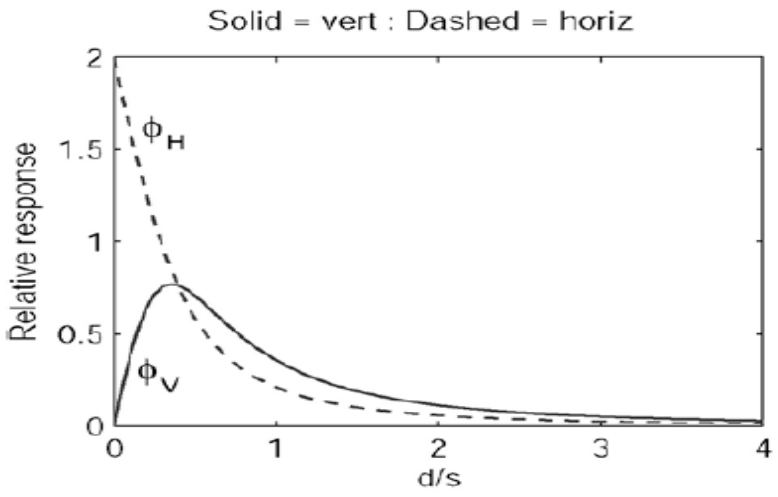

Figure 2.12: Comparison of relative responses for vertical (ϕv) and horizontal (ϕ_H) dipoles.

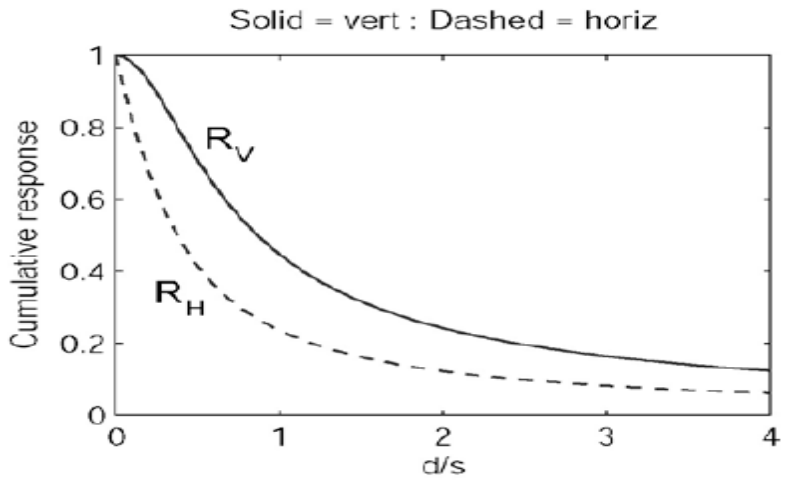

Figure 2.13: Cumulative response versus depth for vertical (RV) and horizontal (RH) dipoles (McNeill, 1980).

A depth of investigation might be defined as that depth below which only 25% of the signal arises. According to this rule the depth of investigation for the vertical dipole is about twice the intercoil spacing (2×s) while the depth for the horizontal dipole is only half that amount. At low induction number, the depth of penetration is controlled by the TX-RX separation. The skin depth is generally much larger than the TX-RX separation (McNeill, 1980).

At the Buried Body or target there is a time varying magnetic field impinging upon the conductor. This sets up an electric force which causes currents to flow. The strength of the currents is governed by Ohm's law: Ĵ = σË where Ĵ is current density in A/.$m^{2,}$ σ = conductance and E = electric field. The currents in the body produce their own magnetic field (This is known as Ampere's Law or BiotSavart Law). These currents do vary with time and their magnetic field can be measured at the receiver end. We refer to this field as the secondary magnetic field. The receiver measures the sum of the primary and secondary fields or it measures the associated voltages that are induced in a coil caused by the time varying magnetic flux.

2.6.11 The horizontal loop electromagnetic method (HLEM)

This method is popularly known also by the commercial names Slingram or Ronka. With this method, the receiver and transmitter are coupled by a fixed cable about 30 to100 m in length, and kept at a constant separation while the pair is moved along a traverse of a suspected conductor (Fig 2.14a). The cable supplies a direct signal that exactly cancels the primary signal at the receiver, leaving only the secondary field of the conductor (Reynolds, 1997). This is separated into in-phase and quadrature components, which are expressed as percentages of the primary field and plotted against the position of the mid-point of the pair of coils (Fig. 2.14b). The in-phase and quadrature signals are zero far from the conductor and at the places where either the transmitter or receiver passes over the conductor. This enables the outline of a buried conductor to be charted. The signal rises to a positive peak on either side or falls to a negative peak over the middle of the conductor.

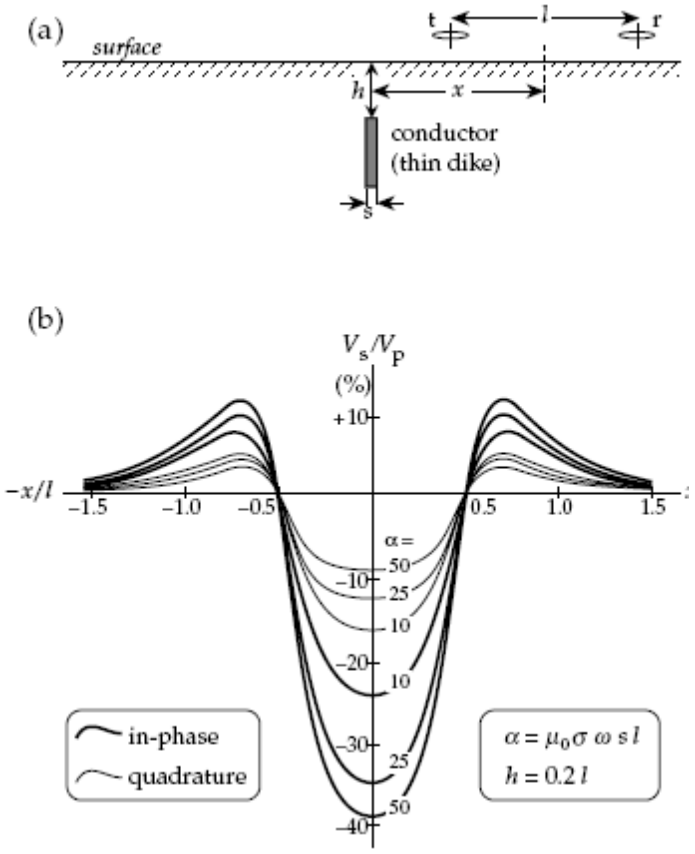

Figure 2.14(a) Geometry of an HLEM profile across a thin vertical dike.
Figure 2.14(b) In-phase and quadrature profiles over a dike at depth h/l = 0.2 for some values of the dimensionless response parameter a.

The peak-to-peak responses of the in-phase and quadrature components depend on the quality of the conductor, which is expressed by a response parameter such as in figure 2.14(b). A suitable function is the dimensionless parameter $\alpha = \omega\mu\sigma sl$, which contains the conductivity σ and width *s* of the conductor as well as the coil spacing *l* and frequency ω of the EM system. The systematic variation of the response curves with the value of *a* allows interpretation of the quality of the conductor. A simple way of doing this is with the aid of model response curves. The variation of in-phase and quadrature signals over a conducting orebody can be modelled experimentally on a smaller scale in the laboratory. The smaller values of s and l are compensated by larger values of σ and ω to give the same response parameter *a*. The model response

curves for different *a* are then directly applicable to the interpretation of real conductors measured in the field (Lowrie, 2007).

In electromagnetic conductivity measurements on the ground in the horizontal loop (vertical dipole) currents in the transmitter coil Tx produce an alternating current at an audio frequency and in the earth, which is considered as uniform. (McNeill, 1980).

2.6.12 In-Phase and Quadrature Phase Response.

What is generally measured is the ratio of the secondary field to primary field for a particular component of the field. (Remember that data could be magnetic fields measured with a magnetometer or voltages measured with a coil.) The data is the ratio of the secondary field to the primary field. Let the primary field be

Hpcos(wt). If secondary field is Hscos(wt+ Ψ) then Hscos(wt+Ψ) = Hs {cos(wt)cosΨ - sin(wt)sinΨ} = {HscosΨ}cos(wt) - {HssinΨ}sin(wt)

The first term has the same phase as the primary field and is referred to as the "in-phase" response. This is also sometimes referred to as the "real" part of the response. That terminology arises when derivations are made in terms of complex quantities. The in-phase (Hscos(Ψ)/Hp) is achieved by dividing the first term of the outcome of Hscos(wt +Ψ) after expansion by the primary field. The second term is the "out-of-phase" part or quadrature phase. The out-of–phase (Hssin(Ψ)/Hp) is achieved by dividing the second term of the outcome of HsSin(wt+Ψ) after the expansion by the primary field. Insight regarding the expected value of the In-phase and Out-of-phase components can be obtained by examining the response of a single loop of wire (of resistance R and inductance L).

The ratio of the secondary to the primary field is indicated as Hsecondary/Hprimary if the receiver measures the magnetic field or (V_S/V_p), if the receiver is a coil which

measures their respective voltages. This is given by the function (equation 2-21) below where the constants involve the mutual inductance of the loops and a plot of the function in brackets as displayed in Figure 2.15 provides considerable insight into electromagnetic data and is probably one of the most important plots in electromagnetic induction as shown below (McNeill, 1980):

$$\frac{\text{Hsecondary}}{\text{Hprimary}} \propto -\{\text{constants}\}\left(\frac{\alpha^2+i\alpha}{1+\alpha^2}\right) \qquad \text{Equation 2-21}$$

Where the response parameter α or $Q = \omega L/R$ where $\omega = 2\pi f$ and L= inductance and R = resistance

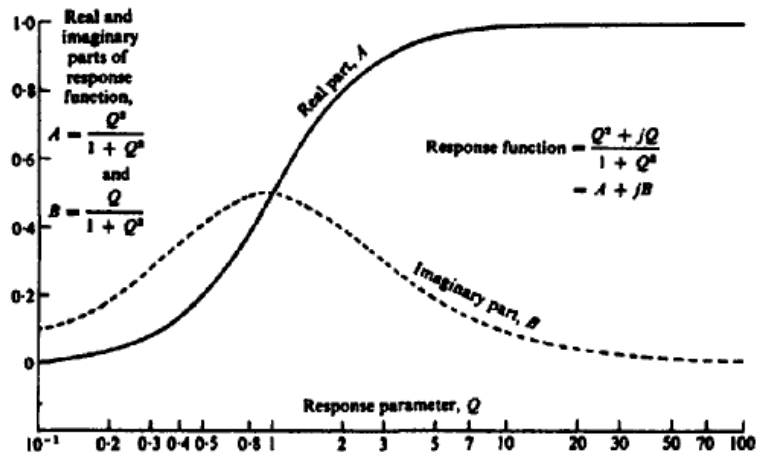

Figure 2.15 Response function of .a conductor in an ac field. (Grant and West, 1965).

The above (Figure 2.15) shows on the left side a poor conductor and on the right hand side a good conductor. This fact is based on the ratio of the in-phase (AR) to the out-phase (Ai) which is low on the left side and high on the right side.

When the value of *Q* is quite small the phase angle of this function is *π/2;* when *Q*= 1, it is 3π/4 after which it increases to *π* for a very good conductor, that is, the secondary

signal is opposed to the primary. In the range $0 \leq Q \leq 1$ the imaginary or quadrature component is larger than the real component, whereas from $1 \leq Q \leq \infty$ the reverse is true. Thus the ratio of in-phase to quadrature components is somewhat diagnostic of the conductor. It is also clear that if one measures only the imaginary component in an EM system, a very good conductor will give a very poor response (Telford et al., 1990).

Table 2.2: The strength of EM responses in relation to the conductance estimates

Strength	**Conductance (S)**	**In phase response**	**Quadrature response**	**Possible cause**
Poor	<1	Weak	moderate	-overburden response
Moderate	1-10	moderate	strong	-pyrite
Good	10-1000	strong	Strong to moderate	-clay rich overburden -graphite -salt-water-sediment -pyrrhotite-sulphide
Excellent	>1000	Very strong	weak	-pyrrhotite-sulphide -graphite -Salt-water

2.6.13 Interpretation of the Electromagnetic Conductivity Data

The observed electromagnetic response can be compared with the theoretical response. Theoretical computations of this type are very complex and limited to simple geometric shapes such as spheres, cylinders, thin sheets, and horizontal layers. Master curves are available for simple interpretation of moving source-receiver data where it can be assumed that the conductor has a simple geometric form (Sharma, 1997).

The transmitter frequency and the intercoil spacing determine the depth of penetration. Thus, the differences between conductivity values at different intercoil spacing or frequencies can be used to give some idea of the variation of conductivity with depth (Stewart, 1981). Shallow conductivity anomalies affect the values at shorter intercoil spacing and higher frequencies. Moreover, the deeper conductivity anomalies affect the values at longer intercoil spacing and are best-seen using lower frequencies.

CHAPTER THREE

METHODOLOGY

3.1 BACKGROUND

Magnetic and EM data can be acquired in two configurations: 1) a rectangular grid pattern, or 2) along a traverse. Grid data consists of readings taken at the nodes of a rectangular grid; traverse data is acquired at fixed intervals along a line. Each configuration has its advantages and disadvantages, which are dependent upon variables such as the site conditions, size and orientation of the target, and financial resources. In both traverse and grid configurations, the station spacing, or distance between readings, is important. “Single-point” or erroneous anomalies are more easily recognized on surveys that utilize small station spacing. If large areas of buried target or large sources are the targets, the station spacing can be large, sometimes as much as 20 to 25 metres. If the target is small, smaller station spacing is needed. In such instances, a station spacing of 5 to 10 metres is suggested. The survey configuration should be selected on a site-specific basis. The ground FDEM survey were conducted for two sets of data with transmitter (Tx) receiver (Rx) separation of 100 and 150m and readings taken at 25 m along a set of parallel traverses oriented E-W, a direction that is perpendicular to the general strike of the lithological units in the study area which approximately extends in an N-S direction. The magnetic measurements were made using traverse line separation of 100 m and readings taken at 25 m intervals. For the magnetic measurement a base station was placed at a reference point, selected far from artificial magnetic disturbances within the surveyed area. The ground raw magnetic survey measurements were subjected to essential corrections, including

diurnal. Diurnal corrections were made to remove the temporal variation of the earth's main field.

Data processing was performed using a computer software (geosoft) which is based on Fast Fourier Transform The FDEM method uses the process of induction where a time varying magnetic field is injected into the ground which in turn induces alternating current (eddy current) in the target of interest which also generate a secondary magnetic field which is measured by the receiver. The receiver measures both the in-phase and out-phase component of the signal as a function of the primary signal.

There are three basic modes of operation for most geophysical methods: (1) sounding, (2) Profiling and (3) sounding-profiling. In sounding, the transmitter-receiver separation is changed, or the frequency is changed, and the results are interpreted in terms of a layered earth. Because the earth usually is not layered in mineral prospecting, sounding has little application (Gerald, 2010). In profiling, the transmitter or receiver, or both, are moved along the earth to detect anomalies. The most useful method is a combination of sounding and profiling which delineates both lateral and vertical variations.

3.2 ACQUISITION OF DATA

The main data set used in this study is a secondary ground geophysical survey data acquired in 10th May, 2010. Different areas were surveyed by using integrated geophysical techniques which are magnetics and FDEM. With the frequency domain the horizontal loop configuration was used in taking measurement to give a deeper depth response since it gives a higher sensitivity at z = 0.4 compared to the vertical loop whose sensitivity is maximum at the surface and diminishes with depth. Coordinates were recorded in the WGS84 (World Geodetic System) datum in the

UTM (Universal Transverse Mercator) zone 30N. The GPS (Global Positioning System) was used for navigation. Both survey lines were oriented perpendicular to the geological strike (or at least to the structures of most interest) for maximum information to be extracted.

The total magnetic-field intensity measurements were carried out using a portable proton-precession magnetometer which is ScintrexEnvimag and which has a sensitivity of 0.1 nT and a measuring range from 25,000 to 100,000 nT. The output from the magnetometer was sampled at 0.2 s to a resolution of 0.01 nT. The sensor was kept at a constant height above the ground. The MaxMin-11(eight-frequencies) was used for the electromagnetic data collection. Out of the eight frequencies of the above mentioned instrument, three were used in the HLEM mode for both surveys. Even though all the other frequencies could have been used, these three were chosen for the sake of time. The frequencies were evenly chosen such that they will give a better representation of the entire range of frequencies. Both magnetic and electromagnetic measurements were made at regular intervals of 25 m. It would have been better to sample at shorter distances but this will take a lot of time and effort. Station spacing is also a function of the size of the target with smaller targets having smaller ranges and larger target having larger spacing. A trade off between cost and the required detail determines the traverse line spacing – smaller line spacing equates to higher cost but also higher resolution. The distribution and shape of the magnetic sources to be mapped is important. Since narrow features have narrow anomalies they may not be resolved if the line spacing is too coarse. Conversely, deeper sources have broader anomalies (though more subtle), accordingly it is not always necessary to use a fine line spacing if the sources are deep. Also increasing the intercoil separation increases the coil to target distance hence deeper depth are investigated using 150 m

separation than using 100 m. From the processed grid it could be deduced that the survey produced high resolution ground geophysical information for mineral exploration purposes.

3.2.1 Data Processing

The processing of ground data for this research involved the application of enhancement technique, the application of a gridding routine, and removal of the Earth‘s background magnetic field. Diurnal corrections were made to remove the temporal variation of the earth’s main field. This was achieved by subtracting the time-synchronised signal, recorded at a stationary base magnetometer, from the survey data. This procedure relies on the assumption that the temporal variation of the main field is the same at the base station and in the survey area. Best results are obtained if the base station is close to the survey area, the diurnal variation is small and smooth and electromagnetic induction effects are minimal (Lilley, 1982: Milligan, 1995).

On the other hand, the terrain correction was not applied to the magnetic data, since the surveyed area is characterized by its smooth terrain and insignificant elevation differences between survey stations. The survey data were transferred from the field magnetometer to a desktop computer for further processing. The geophysical data set for the study area was co-registered to Universal Transverse Mercator Coordinate System, zone 30 of Northern hemisphere. The geomagnetic correction was calculated at the central point of the study area, where the International Geomagnetic Reference Field (IGRF) reaches approximately 31958.3 nT, the inclination angle attained is -17.01^{o}, and the declination of -5.00^{o} for Nkwanta and inclination of -16.89^{o} and

declination of -5.01^{o} at Asuogya. In 10th May, 2010. The IGRF value was subtracted from the readings of the whole survey stations.

The ArcGIS was used to generate a map for the study area. The ground geophysical datasets namely magnetic and FDEM were obtained from the Geology Department, University of Ghana (Accra) on September, 2013. The methodology applied involved the acquisition of two different Geophysical data sets (magnetic and electromagnetic), building of databases (projects), data processing and interpretation.

3.2.2 Gridding

Gridding interpolates the data from the measurement locations to nodes of a regular mesh, creating a new and fundamentally different construction of the data (Foss, 2011). The dataset was gridded using a cell size of 30 m for both the EM and the magnetics using the minimum curvature technique described by Briggs, (1974). The minimum curvature technique gridding was applied to both the magnetic and EM data. The minimum curvature technique takes the randomly distributed survey data and interpolates it onto a regular grid. The images were produced in the Geosoft® software package, and exported in the GeoTIF format, including associated files that contain spatial reference information.

3.2.3 Enhancement of ground geophysical Dataset

Ground magnetic dataset can be enhanced by a range of linear and non-linear filtering algorithms. A range of imaging routines can be specified to visually enhance the effects of selected geologic sources using mathematical enhancement techniques (Milligan and Gunn, 1997). The following discussion describes some enhancement techniques used and their results.

The MagMap extension in Geosoft®, which offers a number of utilities for processing of magnetic data, was used on the magnetic-anomaly grid (total field intensity minus the Definitive International Geomagnetic Reference Field) for the processing and applying filters. The necessary filters were applied and it was displayed as an image using the GRID AND IMAGE tool. Two-Dimensional Fast Fourier Transformation (2D-FFT) filters were applied to enhance the quality of the data. In order to prepare the data for interpretation, the Total Magnetic Intensity (TMI) was further enhanced using filtering techniques such as Reduction to the Pole, reduction to equator, first horizontal and Vertical, Upward and Downward Continuation, and Analytic Signal. Mathematically, the Fourier transform of a space domain function f(x,y) is defined as:

$$\dot{f}(\mu,\nu) = \iint_{-\infty-\infty}^{\infty\infty} f(x,y)\cdot e^{-i(\mu x+\nu y)}\,dxdy$$

The reciprocal relationship is:

$$f(x,y) = \frac{1}{4\pi^2}\iint_{-\infty-\infty}^{\infty\infty} \dot{f}(\mu,\nu)\cdot e^{i(\mu x+\nu y)}d\mu d\nu$$

where μ and ν are wavenumbers in the x and y directions, respectively, measured in radians per metre if x and y are in given metres. These are related to spatial "frequencies" *fx* and *fy*, in cycles per metre

3.2.4 First Vertical and Horizontal Derivatives

First vertical derivative emphasizes near surface features Second vertical derivative emphasizes the location of boundaries of target zones (specially intra-basement anomaly sources). The vertical derivative grid helped enhance linear features in the area. The first horizontal gradient or derivative (1HD) applied to the total magnetic intensity (TMI) grid is critical when trying to map linear features such as fault and/or

dikes from the magnetic data. The filter provides higher resolution and better accuracy at wider spacing. The horizontal derivative aided in identifying geologic boundaries of formations in the study area. The first and second horizontal derivatives images produced interesting results but several distortions were noted to occur in the images due to the increase in the noise level introduced in the data by this process. These images of the horizontal derivatives were therefore not used in the interpretation. However the images of the first vertical derivative were used in the interpretation. While horizontal derivatives enhance edges, vertical derivative narrows the width of anomalies and so locate the source bodies more accurately (Cooper and Cowan, 2004). It is also essential to note that both horizontal and vertical derivatives enhance the high frequency anomalies relative to low frequencies. Equation for the horizontal derivative or derivative in the X direction is:

$$L(\mu) = (\mu i)^n$$

n = Order of differentiation.

u =The X component of the wave number

$$i = \sqrt{-1}$$

Equation for the vertical derivative is:

$$L(r) = r^n$$

n = Order of differentiation.

r = Wave number (radians/unit). Note: $r = 2\pi k$, where k is cycles/unit.

3.2.5 Upward and Downward Continuation (UC and DC).

Upward continuation

Upward continuation enhances the effects of deeper anomalies relative to shallower ones. Upward continuation is considered a "clean" filter because it produces almost no side effects that may require application of other filters or processes to correct. Because of this, this filter is often used to remove or minimize the effects of shallow sources and noise in grids. The appropriation of the magnetic intensities from deeper structures, led to applying the UC filter to suppress the effects of shallow anomalies. The TMI grid was continued to 50, 100 and 200 m to see deeper signature coming from the subsurface. This helped high frequency anomalies relative to low frequency anomalies to be smoothed out. The equation for the upward continuation is:

$$\mathrm{L}(r) = e^{-hr}$$

h = The distance, in ground units, to continue up relative to the plane of observation.

r = Wavenumber (radians/ground unit). Note: $r = 2\pi k$, where k is cycles/ground unit. The survey ground units used in the grid are in (e.g., metre, foot, etc.).

For upward continuation (where z is positive downward) (Telford, 1990):

$$\mathrm{F(x, y, -h)} = \frac{h}{2\pi} \iint \frac{F(x, y, 0)\, dx\, dy}{\{(x - x')^2 + (y - y')^2 + h^2\}^{\frac{1}{2}}}$$

Where

F (x', y',-h) = Total field at the point P(x', y',-h) above the surface on which F(x, y,0) is known.

h = elevation above the surface

Downward continuation

The downward continuation filters enhance responses from shallow depth sources by effectively bringing the plane of measurement closer to the source. On the contrary the data contain short wavelength noises that appear as signals coming from very shallow sources in the continuation (Milligan and Gunn, 1997). A caveat of dealing with downward continuation is that it also enhances high-frequency noise, so it is inadvisable to continue the field very far from the actual measuring height. Since short-wavelength signal can appear to be from shallow sources, it has to be removed to prevent high magnitude and short wavelength noise in the processed data. To do this, a Butterworth filter (a low-pass filter) must be applied to remove the short wavelength noise before applying the downward continuation filter. The downward continuation was applied but it introduced short wavelength noise into the data and for that reason it was not used in the interpretation. Equation for the downward continuation is:

$$L(r) = e^{hr}$$

h = The distance, in ground units, to continue down relative to the plane of observation.

r = Wavenumber (radians/ground nit). Note: $r = 2\pi k$, where k is cycles/ground unit

3.2.6 Reduction to the Pole (RTP)

Reduction to pole (RTP) filter, for low geomagnetic latitudes was applied to the magnetic anomaly data. The reduction-to-pole recalculates the observed magnetic field to what it would look like at a magnetic pole, where the inclination of the inducing magnetic field is vertical. This can be done assuming that the target in the region of interest contain no remnant magnetization. The approach utilizes an

azimuthal filter in the frequency domain to minimize the directional noise caused by the low geomagnetic latitude (Philips, 1997). The calculation of inclination and declination were made using the central coordinates of the area. This is a processing technique performed on the gridded data that removes the asymmetry in residual magnetic intensity (RMI) data that is caused by the non-vertical inclination of the Earth‘s magnetic field. This simplifies the images so that induced magnetic anomalies from vertical sources are located over the geological body responsible, rather than being skewed and offset to one side (Grant and Dodds, 1972).The images of the RTP filter could not produce any meaningful result as the data was taken close to the equator and therefore was avoided. Equation for Reducing to the Magnetic Pole is:

$$L(\theta) = \frac{[\sin(I) - i \cdot \cos(I) \cdot \cos(D-\theta)]^2}{[\sin^2(Ia) + \cos^2(\mathrm{Ia}) \cdot \cos^2(D-\theta)] \cdot [\sin^2(I) + \cos^2(I) \cdot \cos^2(D-\theta)]},$$

If ($|Ia| < |I|$), then Ia = I

Where

l = Geomagnetic inclination

Ia = Inclination for magnitude correction (never less than I)

D = Geomagnetic declination

Ia = Inclination to be used for the magnitude correction. The default is ±20 degrees. If $|I\mathrm{a}|$ is specified to be less than $|I|$, it is set to I.

The magnitude component is (the sin(I) term) and a phase component is (the $i$cos(I) cos(D-θ) term).

3.2.7 Analytical Signal Amplitude

Analytic signal is the square root of the sum of squares of the derivatives in the x, y, and z directions: The analytical signal amplitude was calculated from the residual magnetic field and applied to visualize the distribution of the magnetic signature irrespective of the direction of the magnetization. The analytical signal amplitude is independent of the direction of the magnetization of the source, and is related to amplitude of magnetization. The analytic signal is useful in locating the edges of magnetic source bodies, particularly where remanence and/or low magnetic latitude complicate interpretation. The most significant concentrations of mineral deposits in this area are correlated with high analytical signal amplitudes. This is supported by Silva et al (2003).

Equation for analytical signal is:

$$|A(x,y)| = \sqrt{\left(\frac{dT}{dx}\right)^2 + \left(\frac{dT}{dy}\right)^2 + \left(\frac{dT}{dz}\right)^2}$$

where

A(x,y) is the amplitude of the analytic signal at (x,y), and

T is the observed magnetic field at (x,y).

3.2.8 Directional cosine filter

The directional cosine filter is very good for removing directional features from a grid. The cosine function makes the filter smooth, so directional ringing effects are usually not a problem. The rejection (or pass) notch can be narrowed or widened by setting the degree of the cosine function, so that highly directional features can be isolated. Equation for directional cosine is:

$L(\theta) = \left|cos^n\left(\alpha - \theta + \frac{\pi}{2}\right)\right|$, to reject direction α

$L(\theta) = 1 - \left|cos^n\left(\alpha - \theta + \frac{\pi}{2}\right)\right|$, to pass direction α

α = Direction of the filter in degrees (0-360 relative to North).

n = The degree of the cosine function. By default, a degree of 2 is used to give a cosine squared function.

0/1 = If 1, apply the filter to pass the specified direction; if 0, apply the filter to reject the specified direction. By default, the direction is rejected.

3.2.9 Reduction to the equator

The total magnetic intensity grid was reduced to the equator in order to center the anomaly directly on the target but this gives a negative anomaly and for that matter the output was subjected to inversion to give a positive anomaly. Reduction to the equator is used in low magnetic latitudes to centre the peaks of magnetic anomalies over their sources. This can make the data easier to interpret while not losing any geophysical meaning. The data was reduced to equator using the appropriate inclination and declination for Nkwanta and Asuogya. Reducing the data to the pole (RTP) does much the same thing, but at low latitudes a separate magnitude correction is usually required to prevent North-South signal in the data from dominating the results and also the reduced to pole at low latitude is affected by the magnetic inclination and declination. As a result, reduced to the pole data may present a less "honest" view of the data.

Equation for reducing to equator

$$L(\theta) = \frac{[\sin(I) - i \cdot \cos(I) \cdot \cos(D - \theta)]^2 \times (-\cos^2(D - \theta))}{[\sin^2(Ia) + \cos^2(Ia) \cdot \cos^2(D - \theta)] \times [\sin^2(I) + \cos^2(I) \cdot \cos^2(D - \theta)]},$$

If ($|Ia| < |I|$), then Ia = I

Where

I = Geomagnetic inclination

D = Geomagnetic declination

$L(\theta)$ = Direction of the wavenumber vector in degrees of azimuth

3.2.10 Creating a 3D view from the analytical signal grid.

From the analytical grid of both Nkwanta and Asuogya a 3D view of the magnetic data was created, displaying the top view using the 3D tool menu. This was done to show the width, depth. Size, trend and the intensity of the anomalies and to compare were possible which of the two areas has a better prospect.

CHAPTER FOUR

RESULTS AND DISCUSSION

The ground magnetic and electromagnetic data generated high resolution images that show major lithologies and structural features that may be present in the study area. Because of the erratic and complex character of magnetic maps, interpretation is often only qualitative. Indeed, interpretation is something of a fine art (Telford et al., 1990). For this reason interpretation of these images was carried out qualitatively virtually to identify the individual lithologies and delineate mineralisation zones. High and low electromagnetic pattern, anomalous high zones magnetic and electromagnetic areas suspected to have resulted from underlining rock were delineated to show the mineralization trend. A qualitative interpretation of the trend and intensity of mineralization from the available geophysical datasets in the study area was performed, the intensity of magnetization of a rock is largely dependent upon the amount, size, shape, and distribution of its content of ferromagnetic minerals that usually represent only a small proportion of its mineral composition. Much qualitative information may be derived from magnetic contour maps. Such qualitative interpretation may be greatly facilitated by the use of digital image-processing techniques, similar to those used in the display of remotely sensed data. The corrected ground magnetic data were subjected to various techniques of analysis in order to aid interpretation.

F1002100R F1002100Q

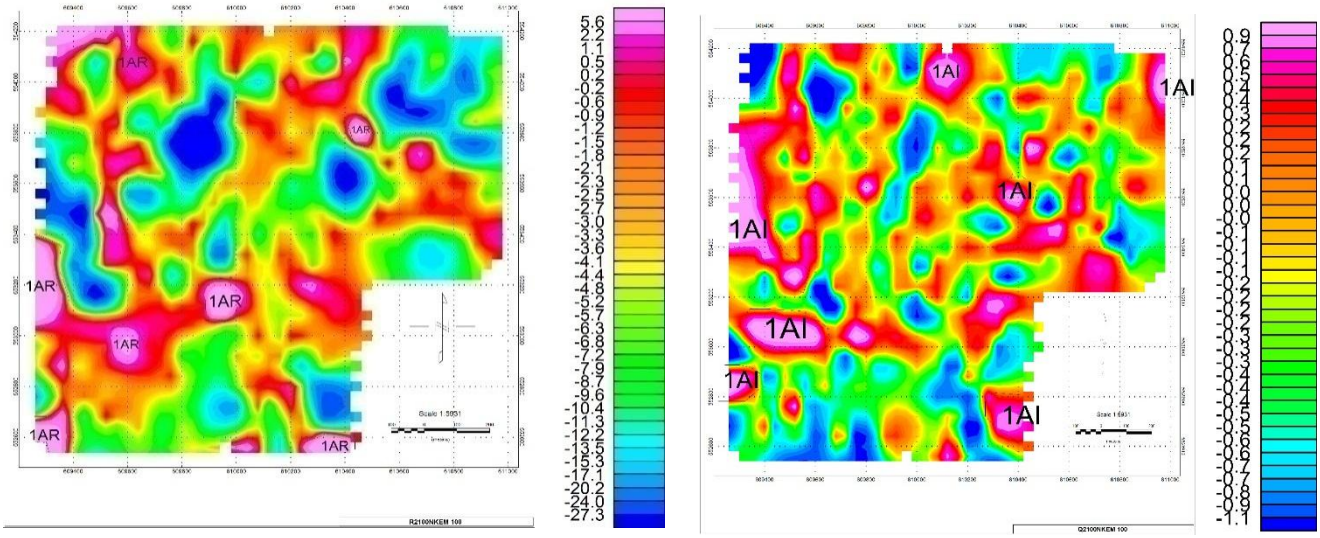

Figure 4.1: In-phase and out-phase components at a frequency of 222 Hz

F10035100R F10035100Q

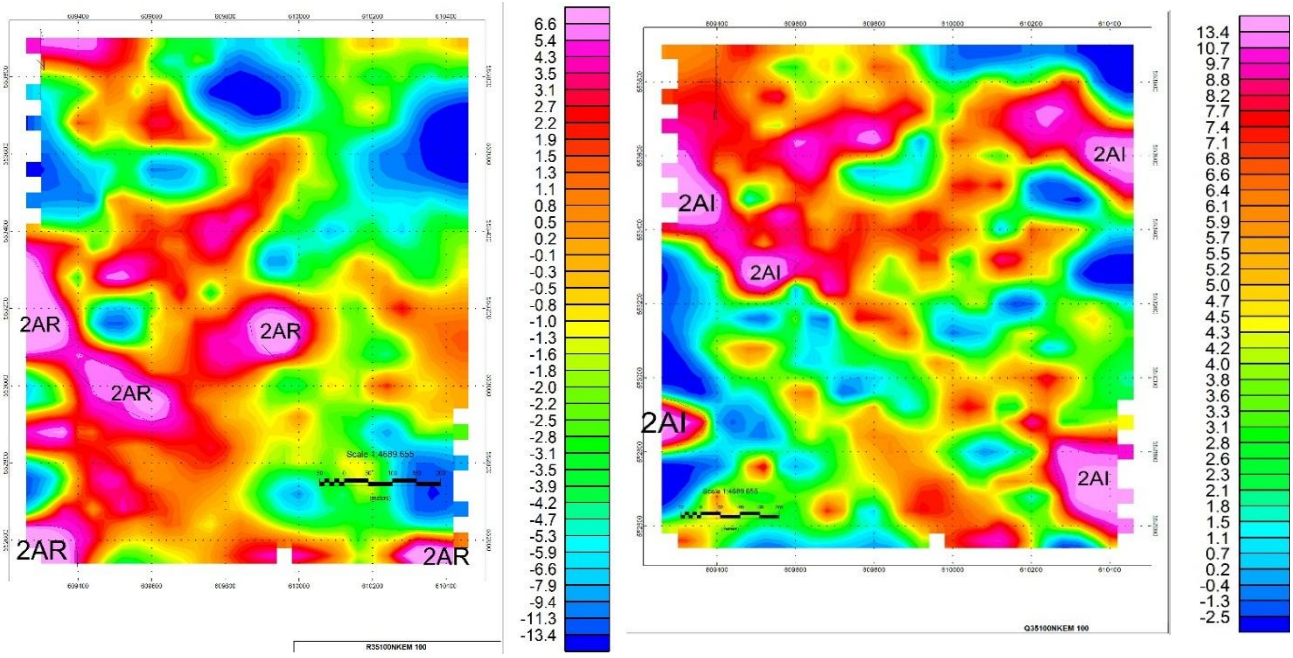

Figure 4.2: In-phase and out-phase components at a frequency of 3555 Hz

F1008100R F1008100Q

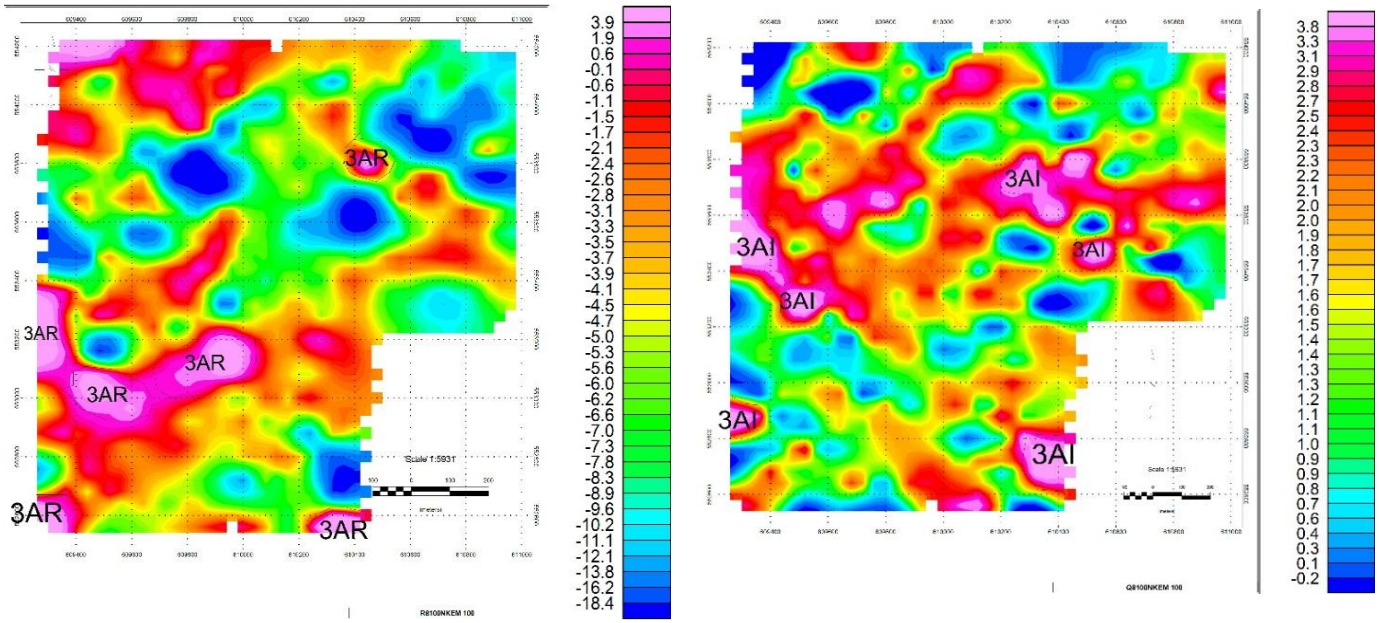

Figure 4.3: In-phase and out-phase components at a frequency of 888 Hz

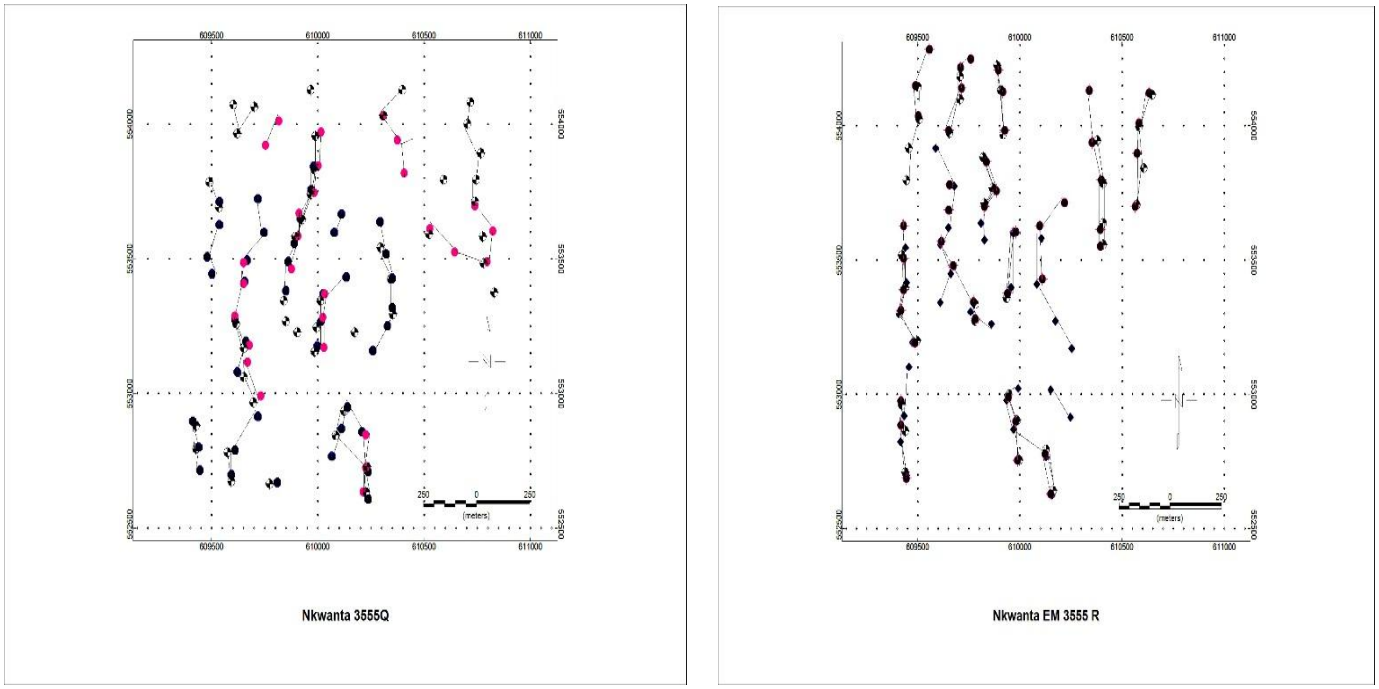

Figure 4.4: Combination of the above in-phase and out-phase component

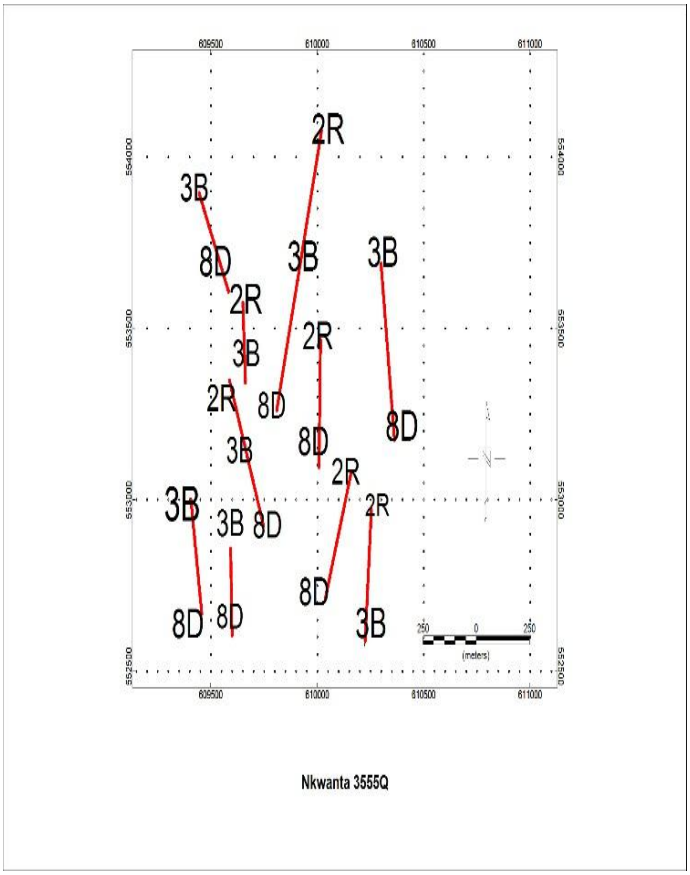

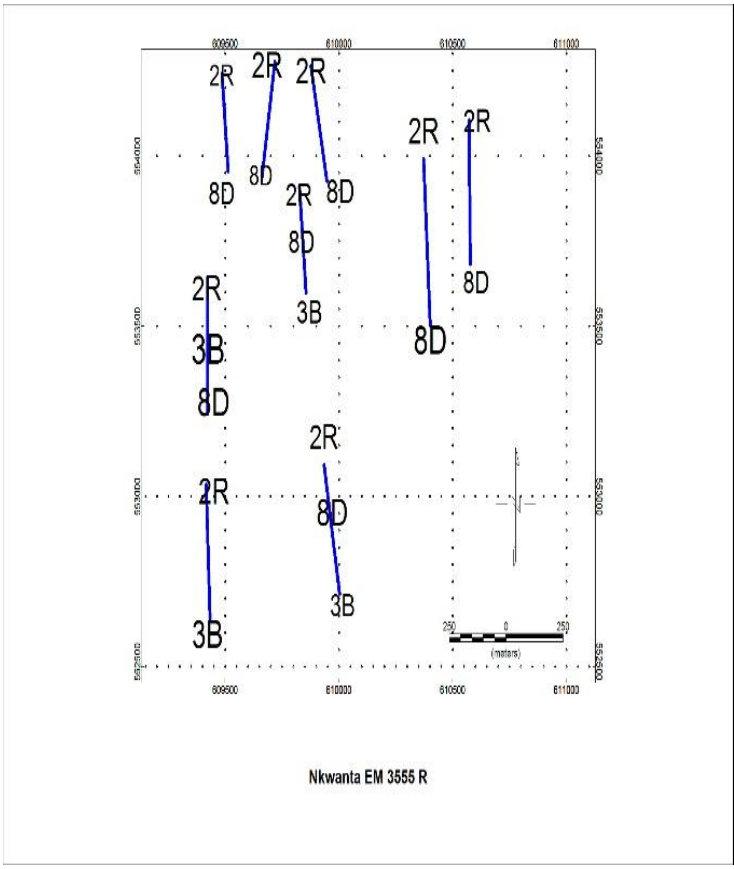

Figure 4.5 A linear trace for both in-phase and out-phase combinations.

The above three coloured pairs of grids (ie. Figure 4.1, 4.2, 4.3) and two pairs of stack profiles (ie. Figure 4.4 and 4.5) depict Nkwanata EM with the in-phase on the left and out phase on the right taken with a transmitter receiver spacing of 100. The Maxmin 11 instrument shows anomalous zones as low with respect to the legend. The high intensity zones of the three frequencies (222 Hz, 888 Hz and 3555 Hz) of both the in-phase and out-phase were labelled. This was done just to distinguish zones in terms of intensity. For frequency domain EM survey using the vertical complainer loop, the anomalies are seen as low with respect to the legend. This fact is illustrated in Figure 2.14 (page 70). The labelled anomalies have not much significance since they are meant to distinguish conductivity zones. Based on the conductivity ratio which states that the ratio of the in-phase to the out phase is high when it is more than one and low when it is less than one or moderate when it is 1:1, the conductivity of the three frequencies could be visually analysed. Looking at the above Nkwanta EM images, it

can be deduced that the conductivity is high for all the frequencies. This is based on the fact that the intensities of all the EM anomalies (showing in blue colour) are higher for the in-phase than the out-phase. The Figure 4.4 shows a separate combination of the stack profiles for both the in-phase and out-phase components. The reason for this is to find the number of anomalies that overlap which gives an indication of whether the particular feature continues with the sounding frequencies that is from the highest frequency (shallow depth) to the lowest frequency (deeper depth). This is clearly shown in the skeletal view of the stack profiles. Figure 4.5 shows the linear trace of the stack profiles. This was instrumental in showing whether the depth of a particular feature terminates or persist with all the three frequencies, besides this, the trend of the particular feature producing the conductive anomaly was deduced. The trend of the continuous feature for both the in-phase and out-phase combinations lies in the N-S and others in the N-W and a few in the N-E of the in-phase. The numbers and letters on the linear trace have their own meaning with the first abbreviated number denoting the frequency and the second letter denoting the colour assigned to a specified profile. For example 3B indicates the frequency 3555 Hz and it is assign colour blue, 8D representing frequency 888 Hz and its colour is dark and 2R the frequency 222 Hz and its colour is red. Also the number of these frequencies on the linear trace shows how many frequencies overlap and hence the continuation of the subsurface anomalous feature. The linear trace shows three of three overlapping anomalies and six of two overlapping anomalies for the in–phase. This is also the case for the out-phase. It can be deduced that if the middle frequency (888 Hz) overlaps with the lowest frequency (222 Hz), then the overburden is not conductive and if the highest frequency (3555 Hz) overlaps the lowest then it could be that the feature in between the two sounding frequencies is transparent to the EM

waves and if the highest and the second frequency overlap, the idea behind is that conductivity terminates only with the first two frequencies. Finally if none of the frequencies overlap then one can say that the subsurface is not conductive up to the lowest frequency.

F100222R F100222Q

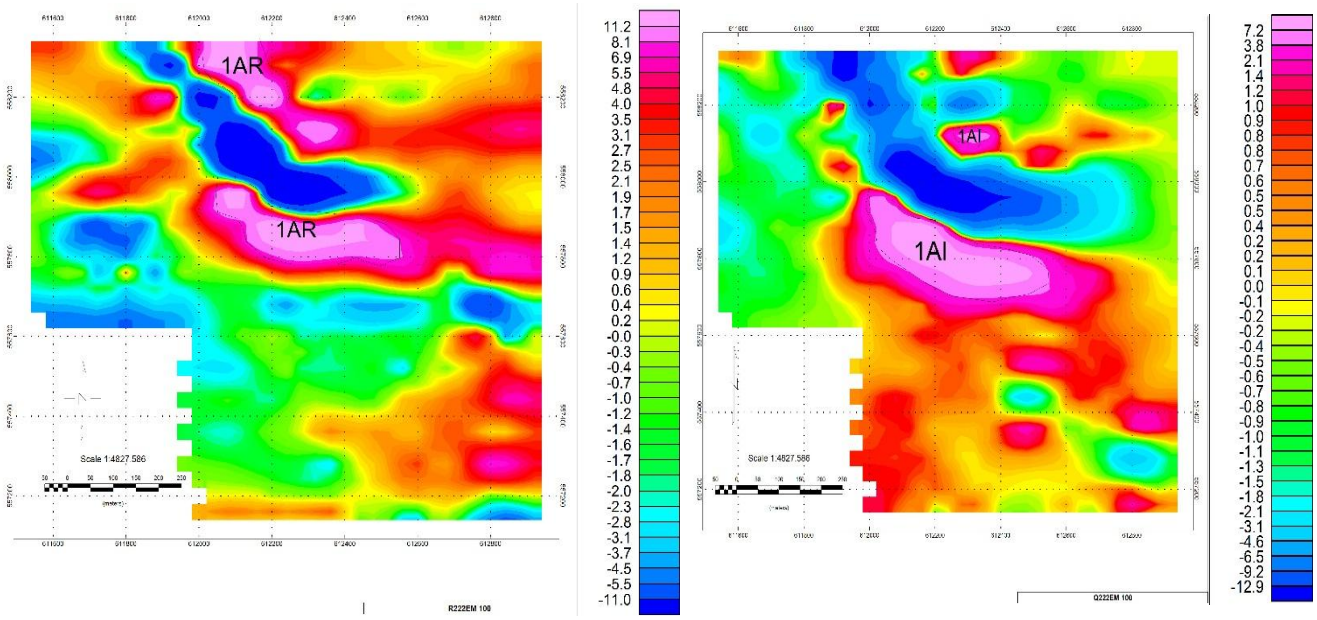

Figure 4.6: In-phase and out-phase components at a frequency of 222 Hz

F1003555R F1003555Q

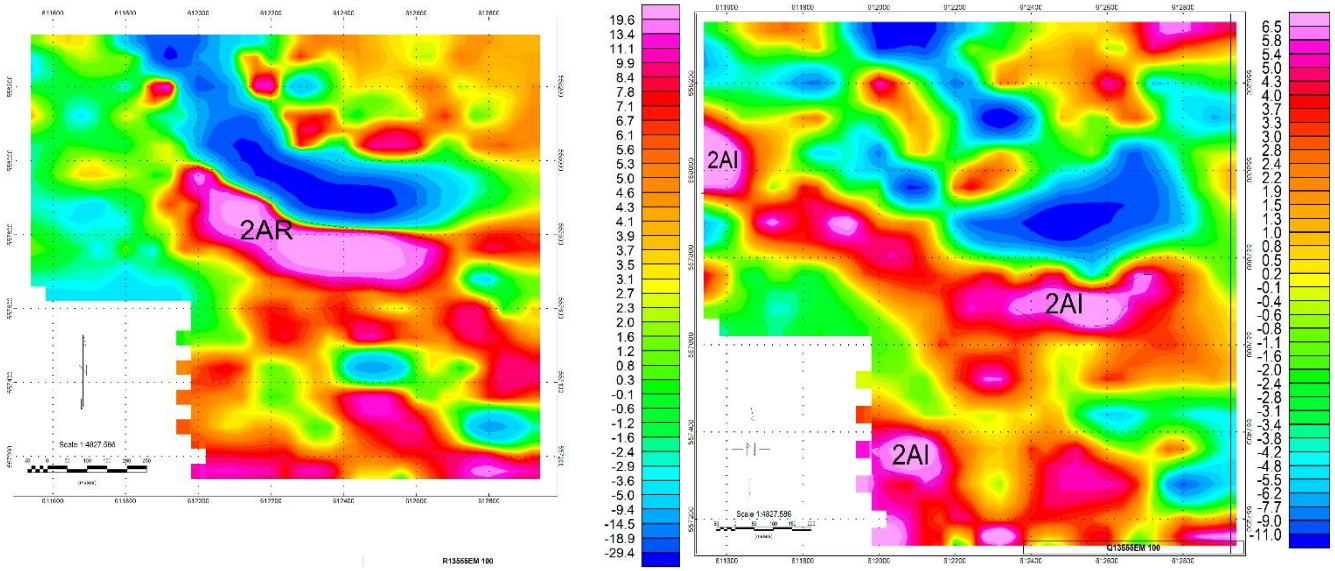

Figure 4.7: In-phase and out-phase components at a frequency of 3555 Hz

F100888R F100888Q

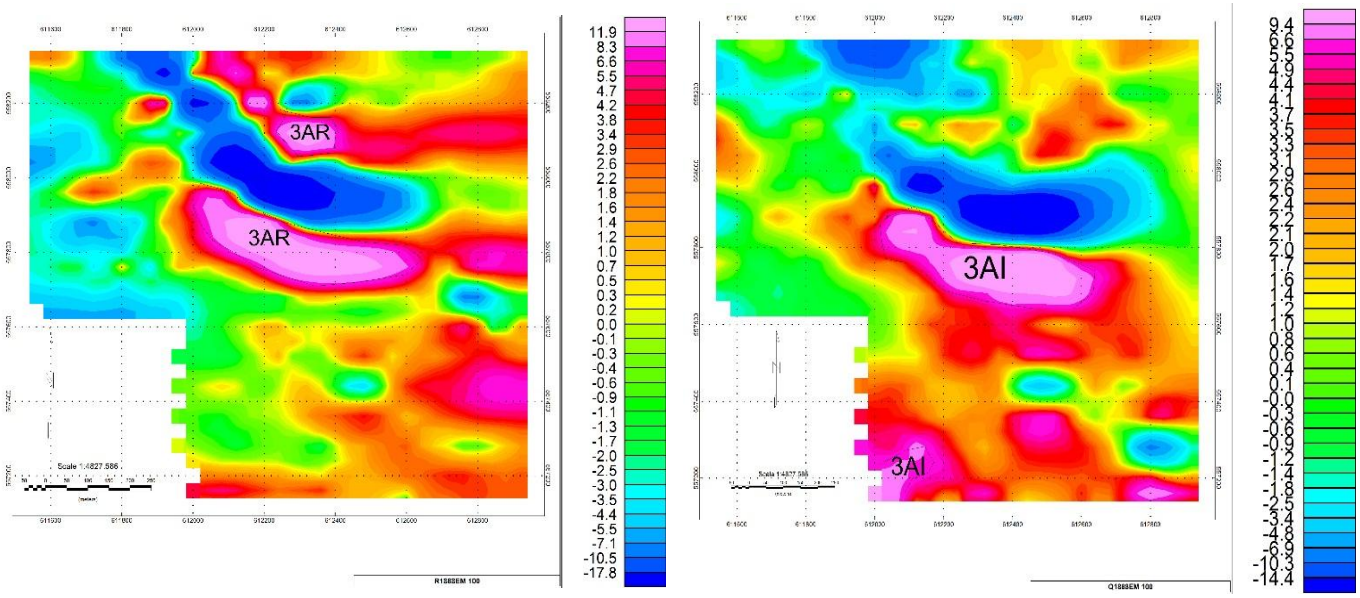

Figure 4.8: In-phase and out-phase components at a frequency of 888 Hz

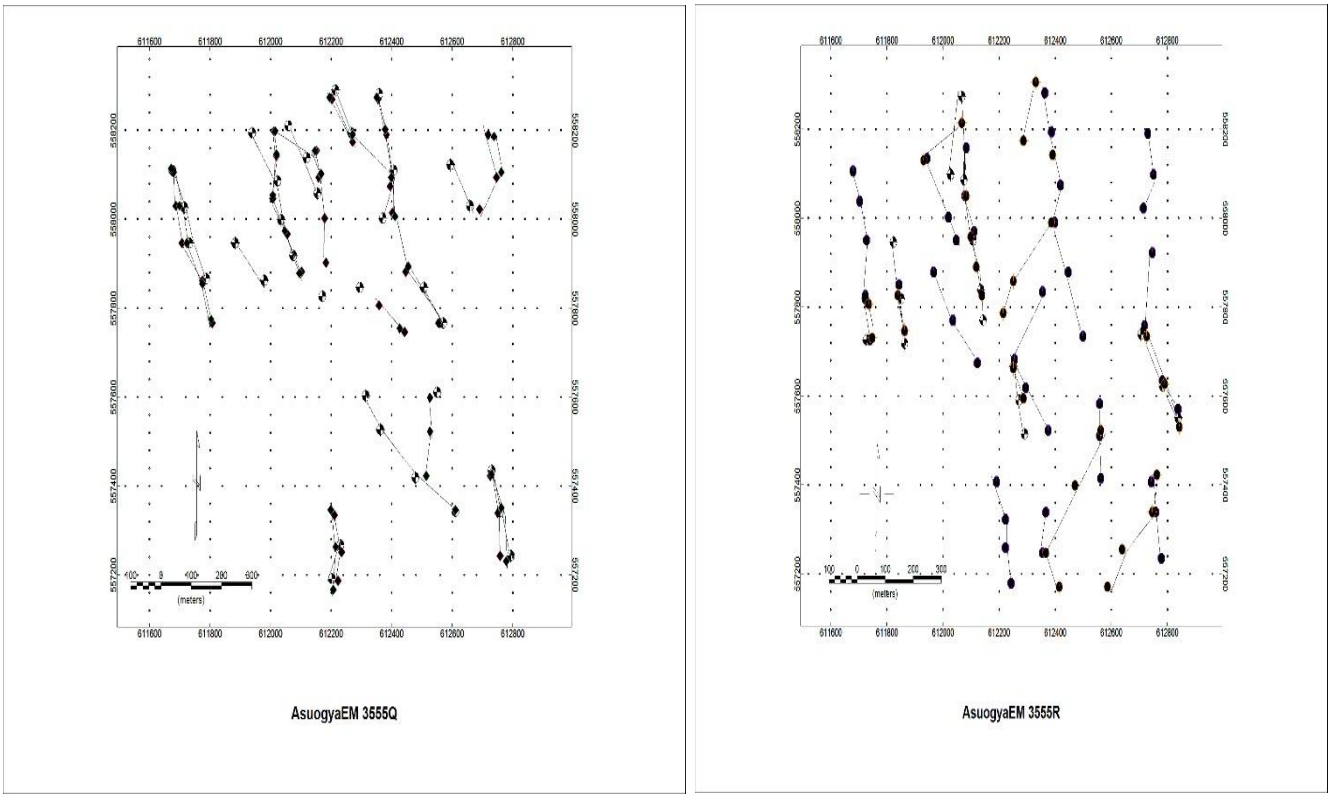

Figure 4.9: Combination of the above in-phase and out-phase components

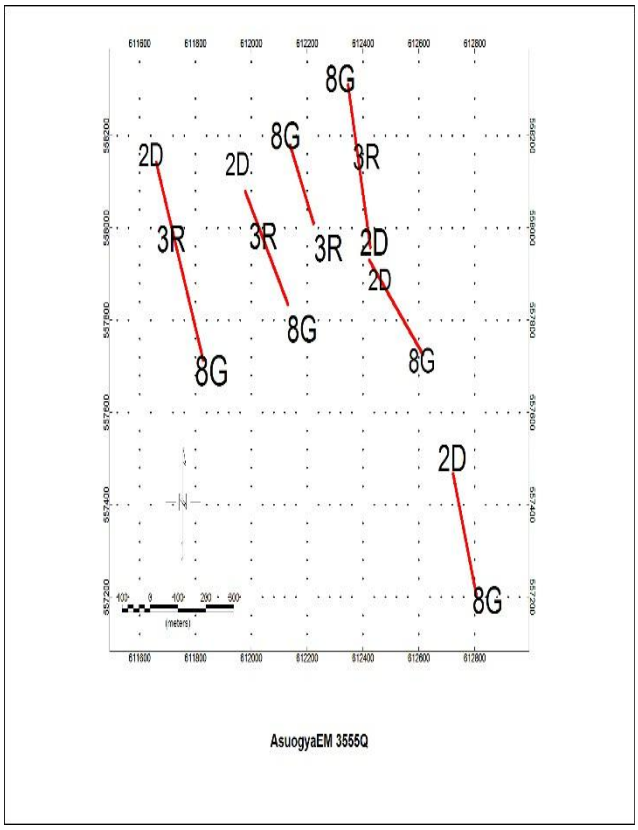

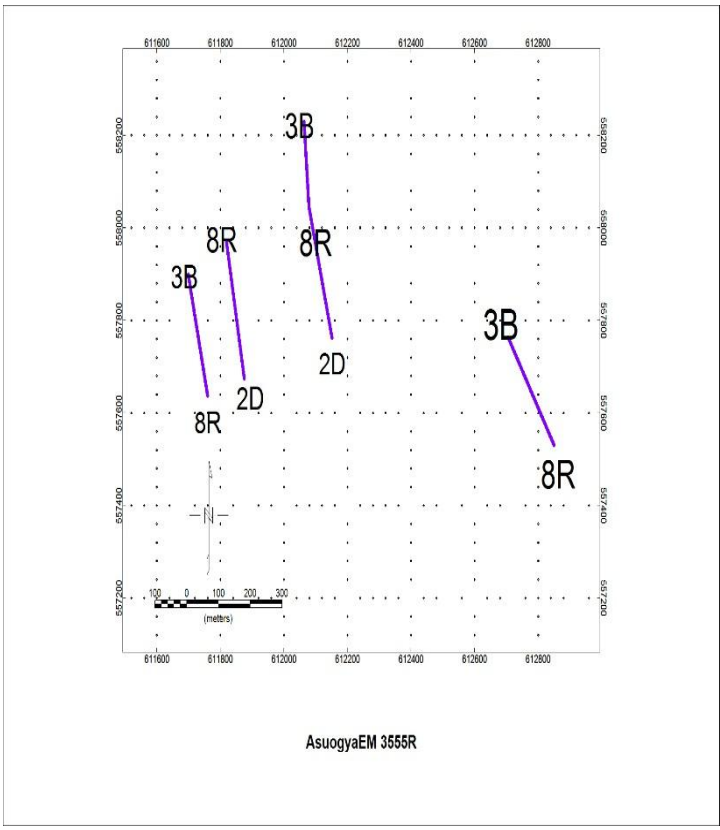

Figure 4.10: A skeleton combination of the above in-phase and out-phase components

Figure 4.6 to figure 4.10 images stand for Asuogya with a transmitter receiver spacing of 100 and with the same trend of frequencies, 222 Hz 3555 Hz and 888 Hz. For reasons already explained, the images above give a moderate conductivity for all the three frequencies. The stack profiles and their respective traces give the number of overlapping anomalies and the structural orientation within the subsurface. Figure 4.10 shows three of three overlapping frequencies and three of two overlapping frequencies for the in-phase. The trend of orientation of the in-phase is in the N-W and S-E. The out-phase has three of two frequencies overlapping and one of three frequencies overlapping. The trend of orientation of the out-phase trace is similar to that of the in-phase.

F150222R F150222Q

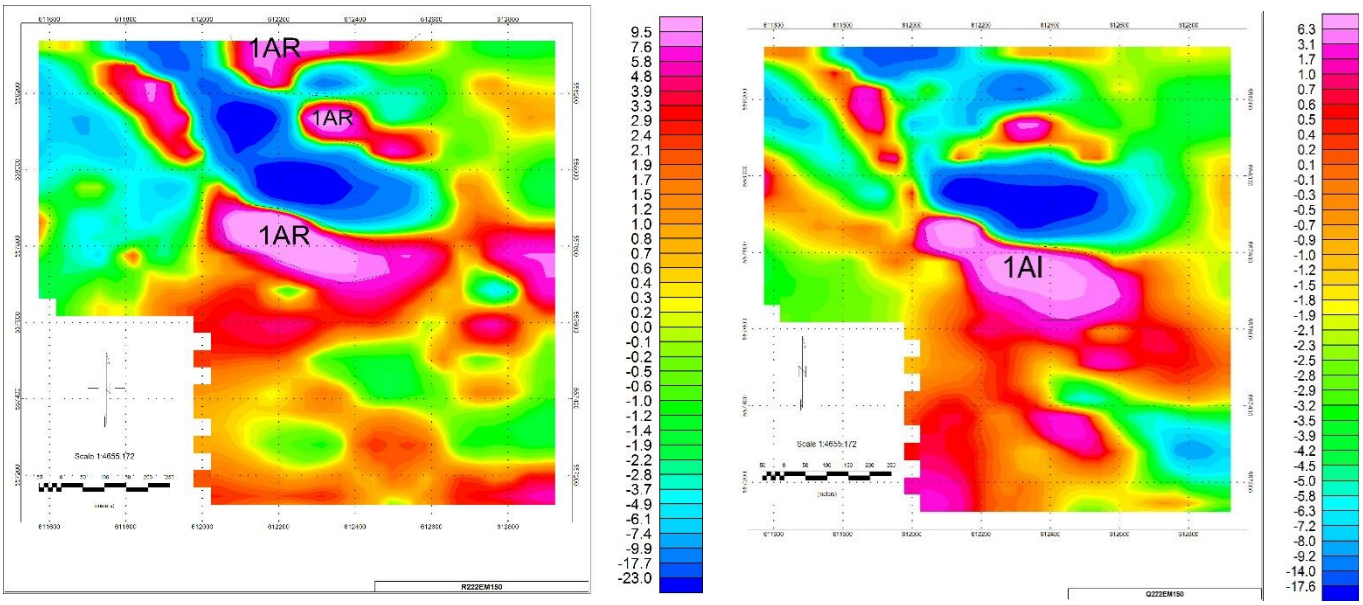

Figure 4.11: In-phase and out-phase components with a frequency of 222 Hz

F1503555R F1503555Q

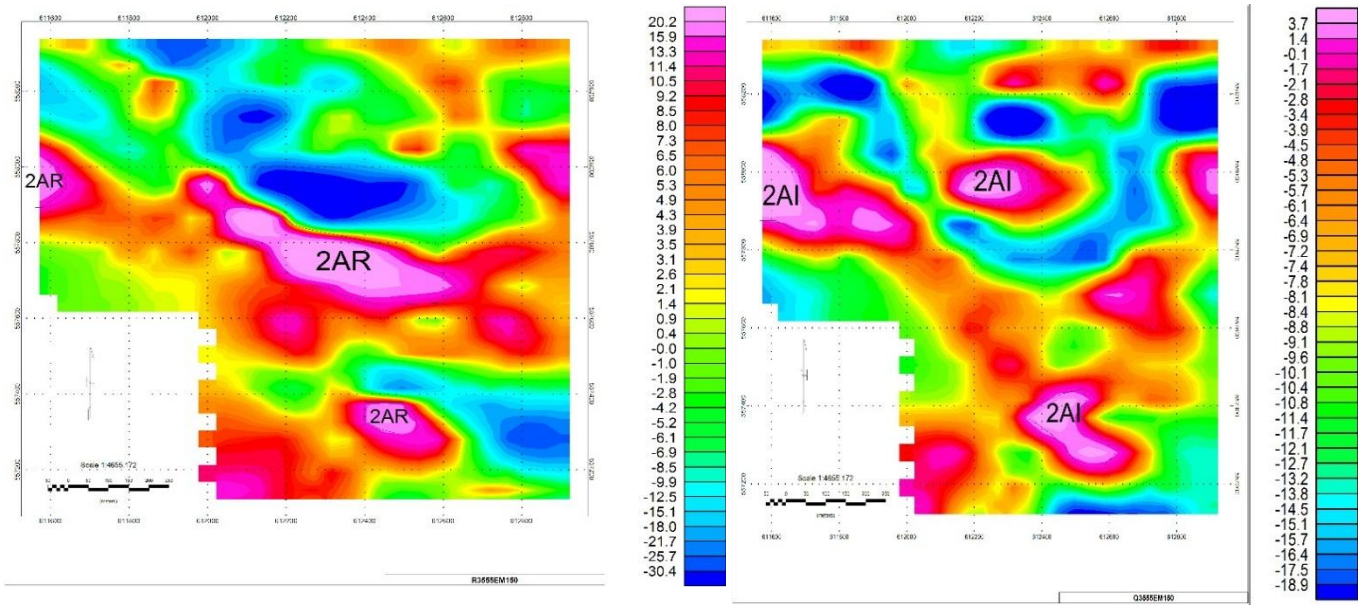

Figure 4.12: In-phase and out-phase components with a frequency of 3555 Hz

F150888R F150888Q

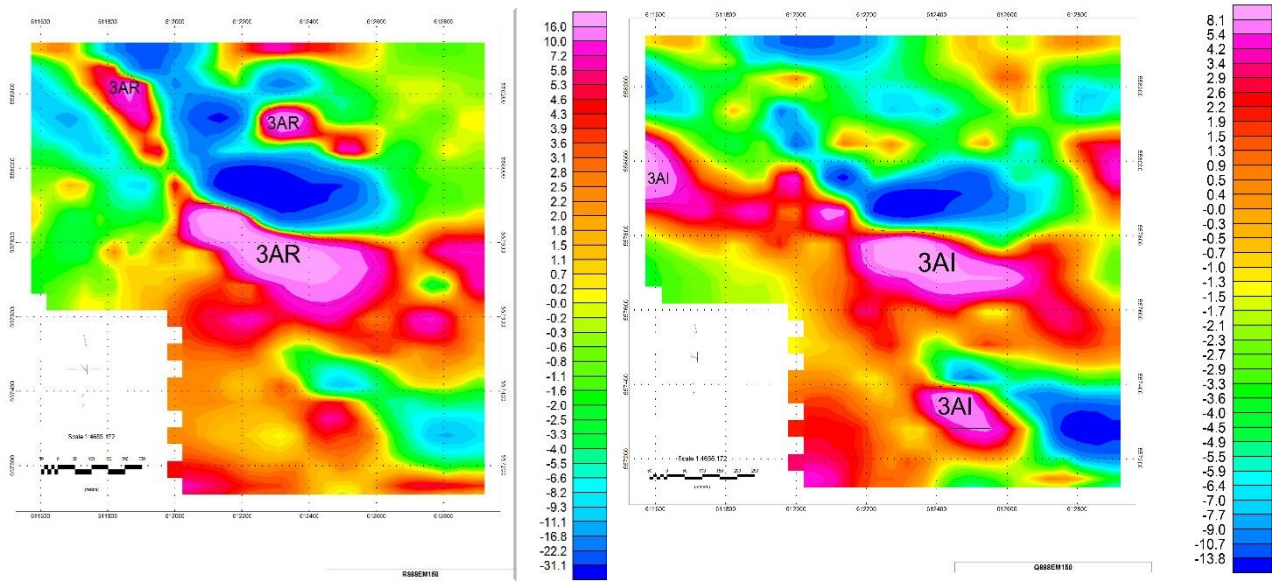

Figure4.13: In-phase and out-phase components with a frequency of 888 Hz

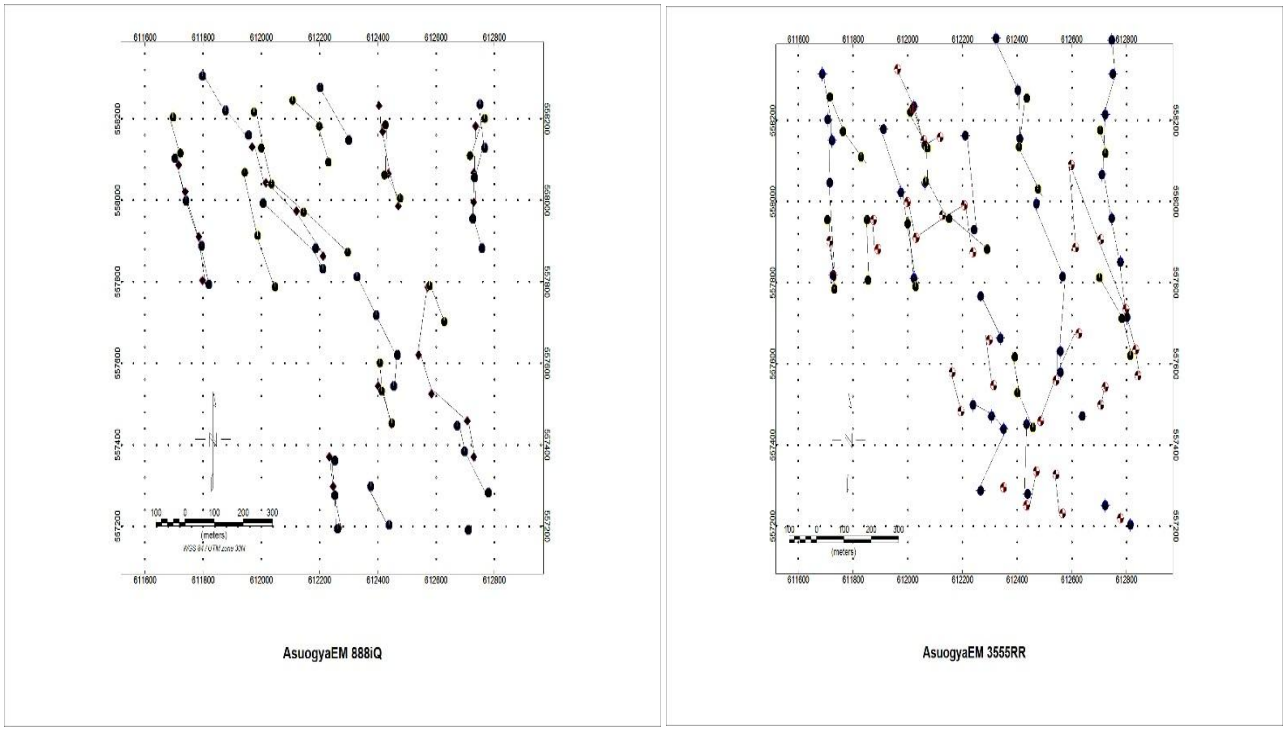

Figure 4.14: A stacked profile combination of the above in-phase and out-phase components.

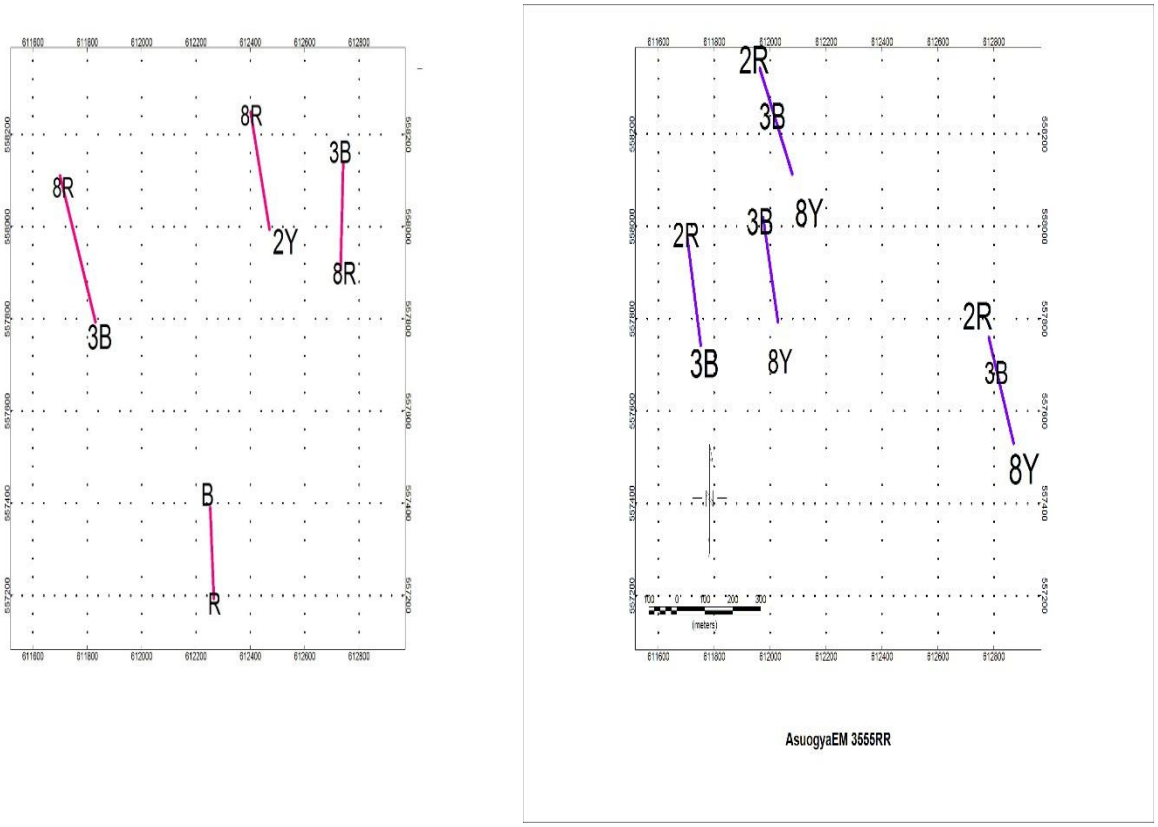

Figure 4.15: Combination of the above inp-hase and out-phase components

Figure 4.11 to 4.15 show Asuogya EM grids with transmitter receiver sepration of 150 and having the same trend of frequencies (222,3555 and 888) as indicated in the Figures. For previous reasons given above, the images have a higher conductivity for the three frquencies, The combined profiles and their traces give a number of overlapping anomalies and their trend. The linear trace shows four of two overlapping frequencies for the in-phase. The out-phase shows two of three overlapping frequencies and two of two overlapping frequencies. A NW-SE trend for both in-phase and out-phase of the anomalies was recognized.

RTE RTEIV

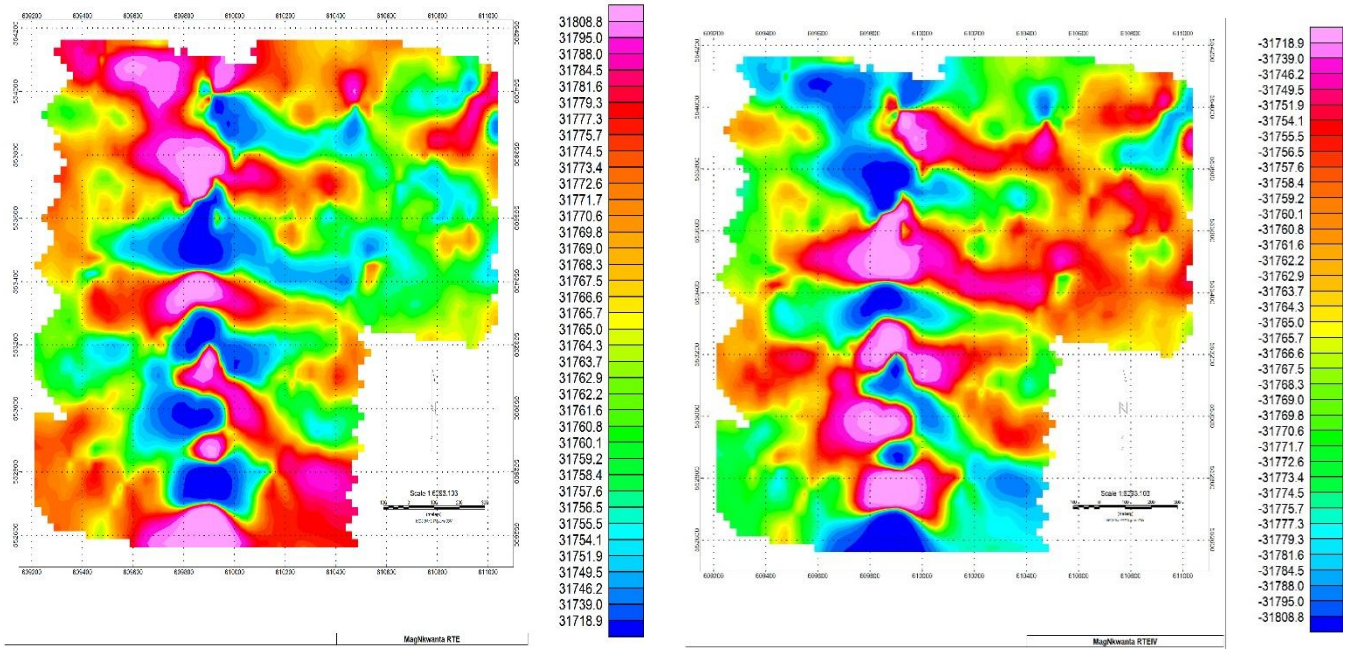

Figure 4.16: Reduced to equator and its inversion

Figure 4.16 shows on the left a reduced to equator and on the right an inversion of the reduced to equator grids from the total magnetic grid of Nkwanta with a travers lines separation of 100. The abbreviation RTE means reduced to equator and RTEIV represent an inverse of reduce to equator. The reduction to equator at lower latitude gives a negative anomaly hence the need for the inversion. The reason for this application is to center the anomaly on the source or target which is the same reason for the reduced to pole but the reduced to equator is preferable to the reduced to pole at low latitude since at this latitude the reduced to pole is affected by the magnetic field inclination and declination and hence does not present proper view.

ANA VD

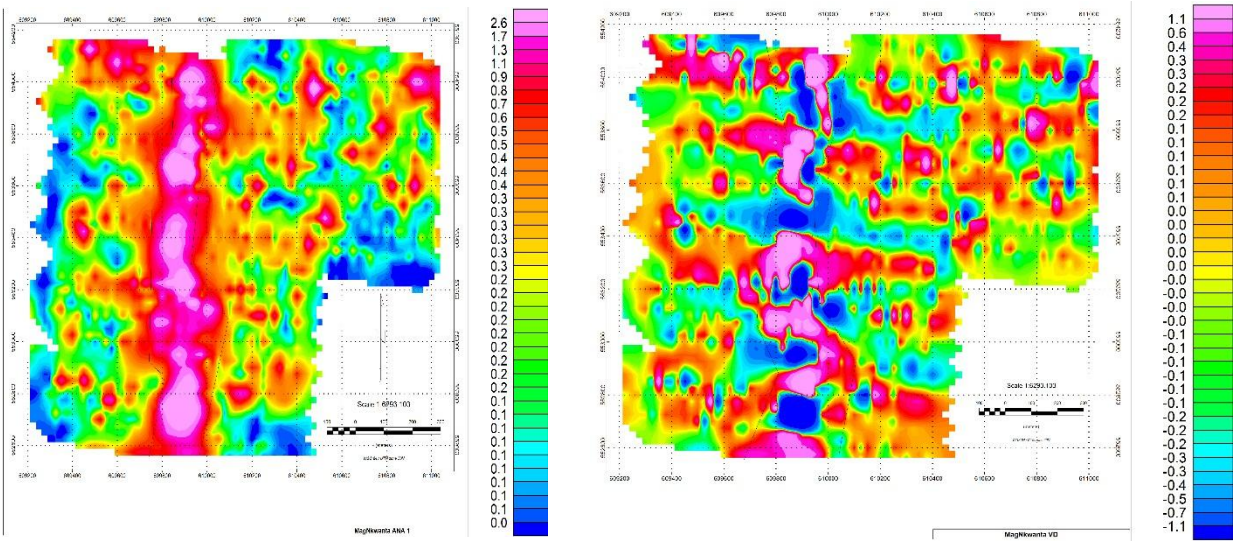

Figure 4.17: Analytical signal and vertical derivative images

ANA & VD ANA & VD L

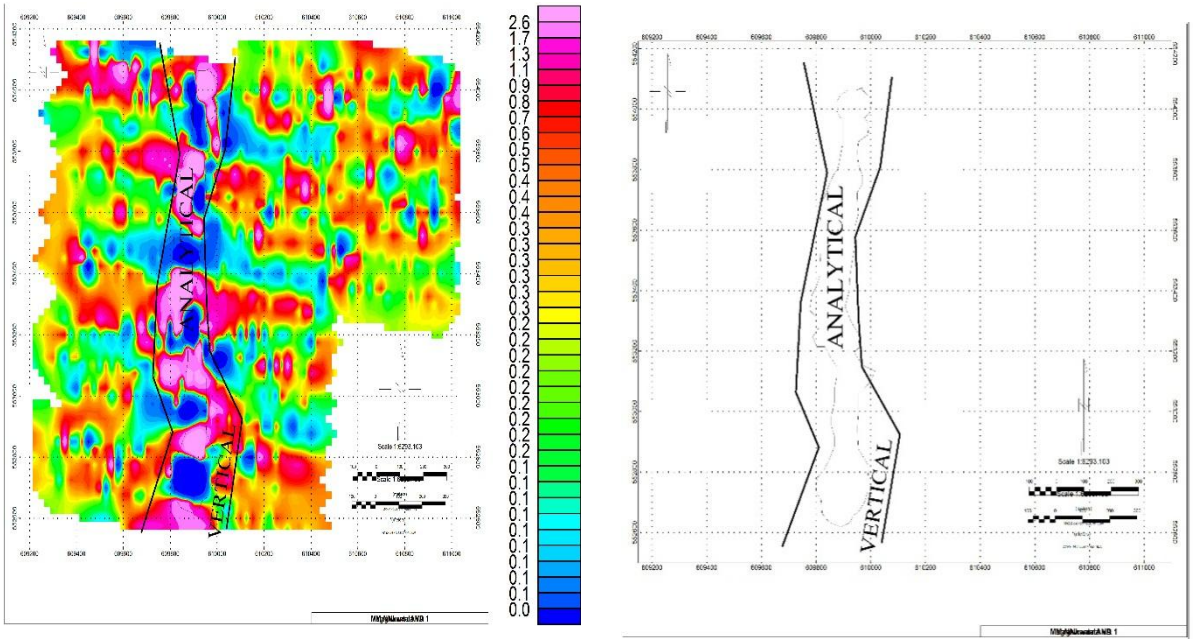

Figure 4.18: An image and a skeleton combination of the analytical and vertical derivatives

Figure 4.17 shows on the left an analytical signal and on the right the first vertical derivative grids of the total magnetic grid of Nkwanta. Figure 4.18 shows on the left the superposition of the analytical signal and the vertical derivative and on the right a skeletal grid of the superimposed image.

The abbreviation ANA means analytical signal, VD means vertical derivative and MAG means magnetics. Both the analytical and the vertical derivative reveal a north-south trending anomaly. To substantiate this, a line was traced along the boundaries of both anomalies and then both images were superimposed to see whether they will overlap. The result proved positive in that the trace of the analytical signal falls exactly within that of vertical derivative. These maps of Figure 4.17 to 4.18 emphasize the trend of the anomalies which are clearly demonstrated in the skeletal grid. The essence of the analytical signal is to position the anomaly on top of the source or target as in RTP but at lower latitudes the reduced to pole is affected by the inclination of the earth magnetic field which introduces noise in the data. For this reason the analytical signal was used since this function is independent of strike, magnetic inclination and remanent magnetism.

RTE RTEIV

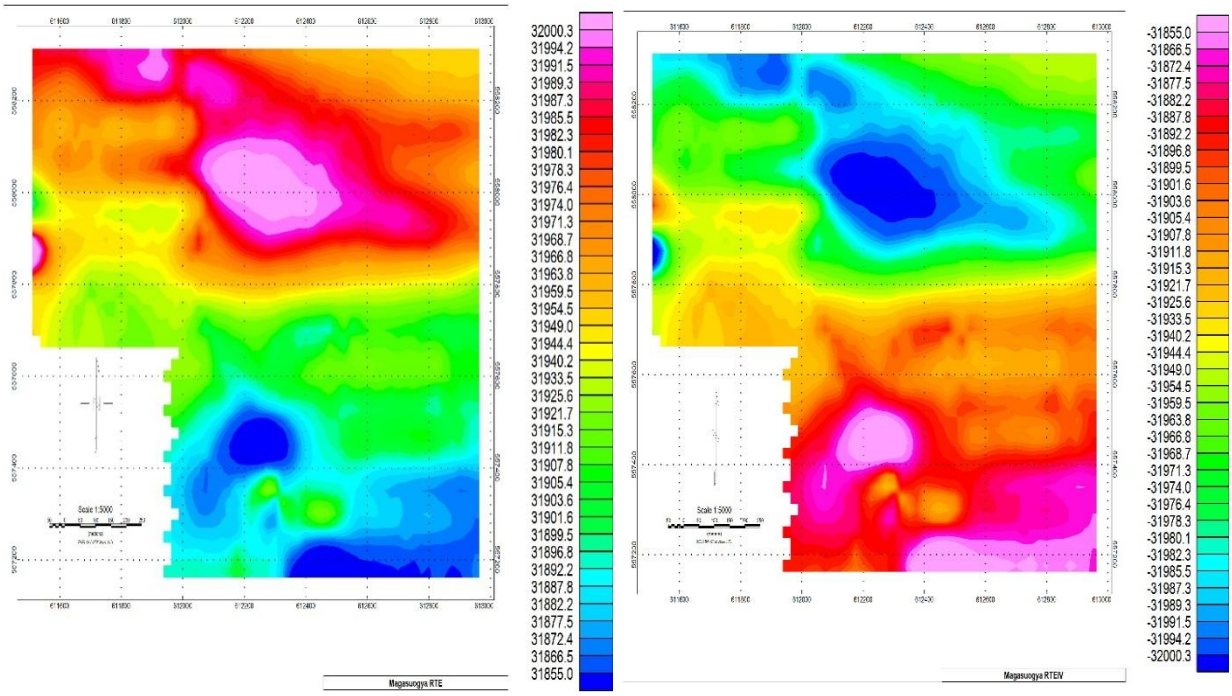

Figure 4.19: A reduced to equator (RTE) and its inversion (RTEINV).

Figure 4.19: Show on the left a reduced to equator of the total magnetic grid and on the right an inversion of the reduce to equator with a travers line spacing of 100m.

The Total Magnetic Intensity (TMI) data of the above was reduced to equator by applying the inclination and declination of the specified areas. The anomaly was better placed on the source by the RTE and its inversion and with the anomaly striking NW-SE to the traverse direction. This trend is confirmed by the EM grid of Asuogya. The inversion was necessary since the TMI data collected near or at the magnetic equator gives a smaller or a negative value for magnetic sources and a high or positive sources to non-magnetic targets hence the need for the inversion to transform the low or negative magnetic source anomalies into high and positive anomalies and the non-magnetic sources into low or negative anomalies.

ANA VD

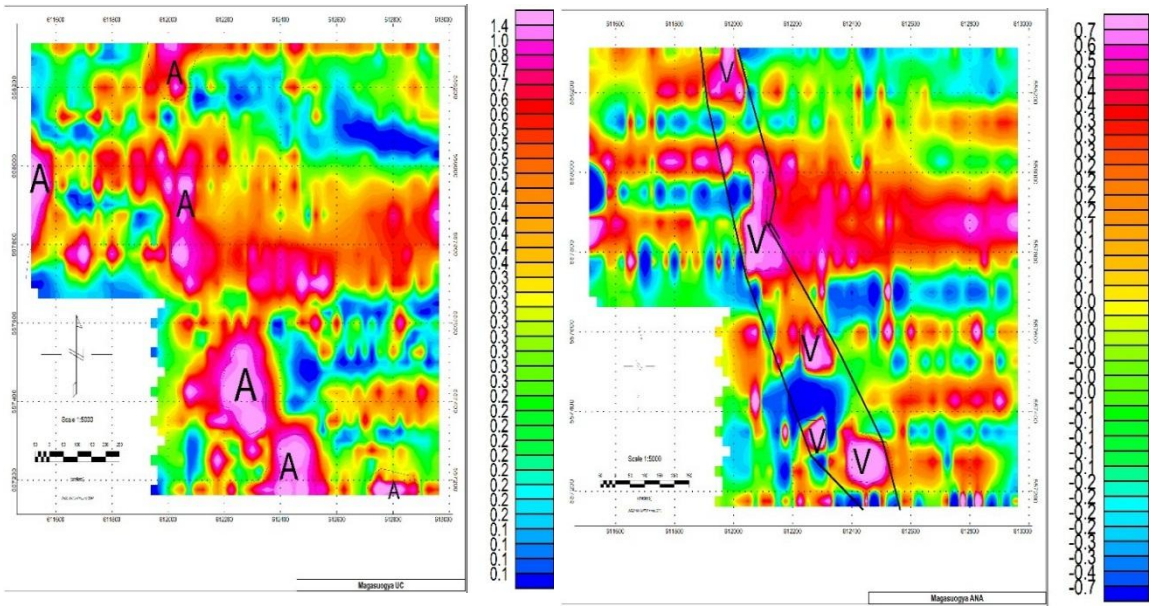

Figure 4.20: Analytical signal (ANA) and vertical derivative (VD)

ANA & VD ANA & VD L

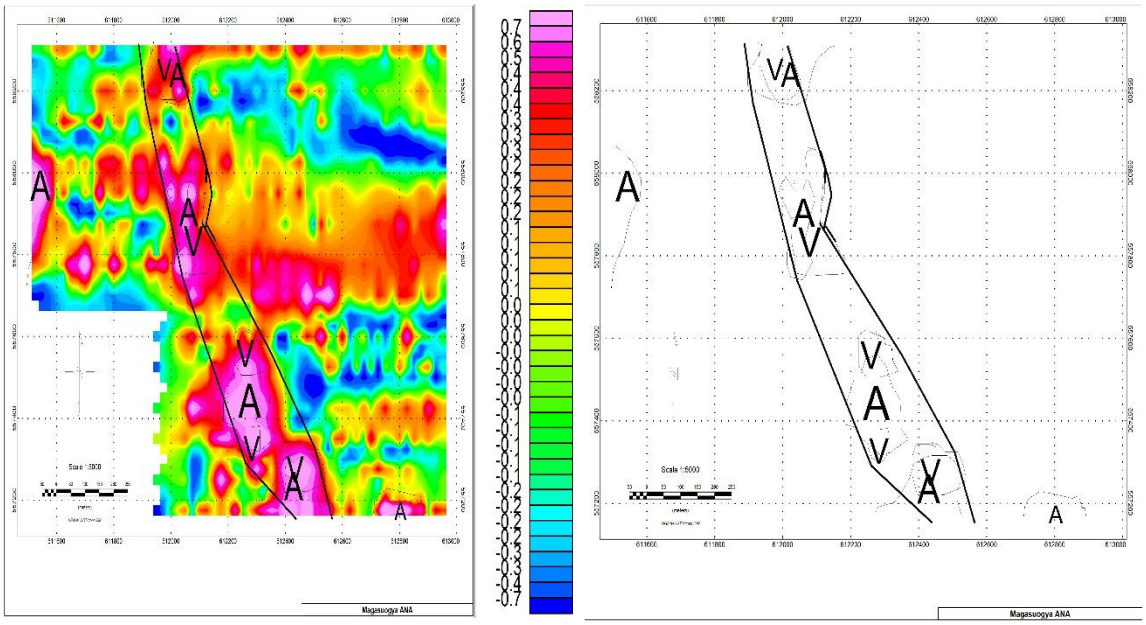

Figure 4.21: An image and a skeleton combination of the analytical and vertical derivative.

Figure 4.20 shows on the left the analytical signal grid and on the right the vertical derivative grids of the Asuogya total magnetic grid and Figure 4.21 shows the image combination of both analytical signal and the vertical derivative on the left and on the right the skeleton view of the same images after the colours were removed. This time, to see the trend of the major anomalies, the various anomalies within both the analytical and the vertical derivative were labelled with the letter A indicating analytical signal and V vertical derivative. A line was drawn along the boundary of only the vertical derivative and both anomalies were combined. This was done to see whether the labelled anomaly of the analytical signal will overlap the labelled anomalies of the vertical derivative and also falls within the boundary line of the vertical derivative. The expected result was achieved showing a NW-SE trend of major feature which confirms the trend of the feature of the Asuogya grid.

UC-50 UC-100

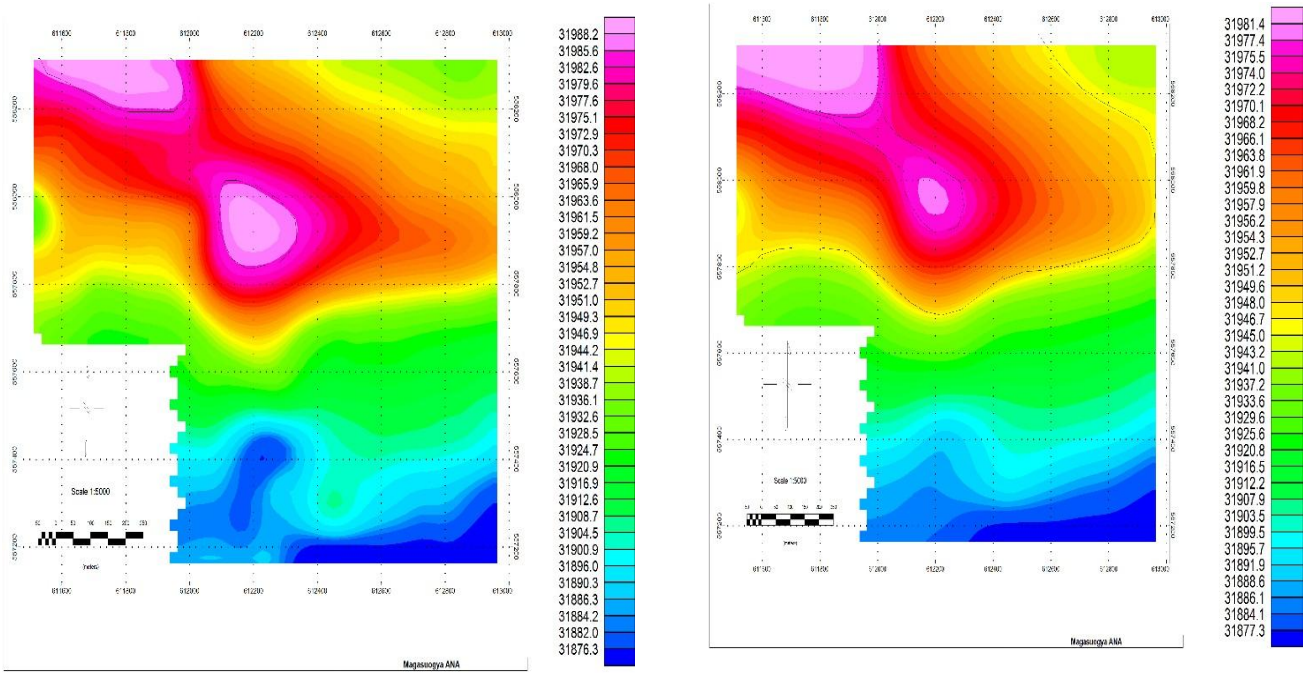

Figure 4.22: Upward continuation of 50 and 100

Figure 4.22 shows Asuogya's total magnetic intensity grid on the left which is upward continued to 50 m and on the right upward continued to 100 m. Upward continuation enhances the effects of deeper anomalies relative to shallower ones (Milligan and Gunn, 1997). The above grid shows a deeper source for the map on the right than of the left. It can be seen, as in the deep blue colour, that the magnetization in Asuogya formation still persist at 50 m and begins to fade out from a depth of 100 m since at 100 m the blue colour begins to spread out indicating the appearance of long wave length. Note, as explained in the RTE, that it is rather the blue colour that indicates magnetic sources.

NKWANTA MAG UC 50 NKWANTAMAG UC IOO

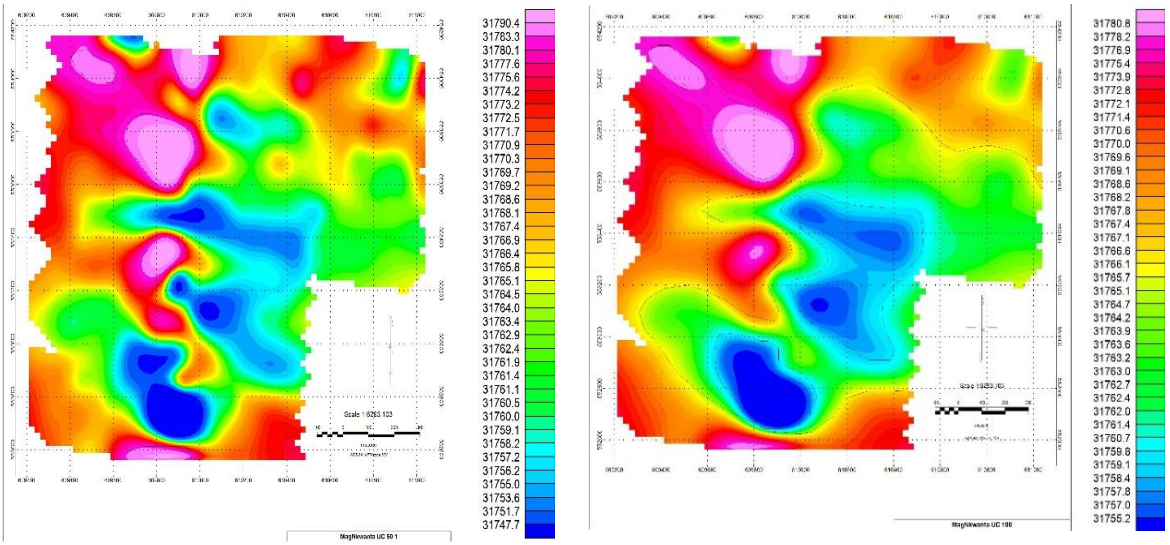

Figure.4.23: Upward continuation of 50 and 100

Figure 4.23 shows total magnetic intensity grid of Nkwanta on the left which is upward continued to 50 m and on the right upward continued to 100 m. Upward continuation is commonly used to interpret the signal from deep-seated or regional scale features and attenuates the signal from small and shallow features (Syberg, 1972b). Figure 4.23 shows a deeper source for the continuation to 100 m on the right than the 50 m on the left. For reasons assign to figure 4.22 it can be seen that the magnetization in Nkwanta persist within 50 and 100 m since the anomalies are still localizes at this depth.

ASUOGYA MAG UC 200 NKWANTA MAG UC 200

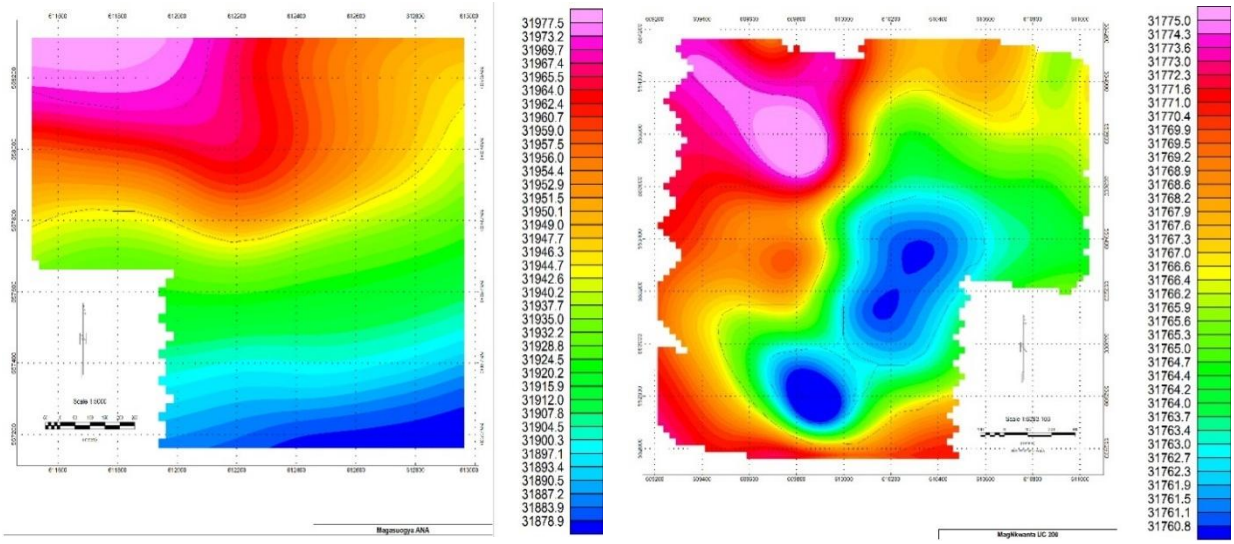

Figure 4.24: Upward continuation of 200 for both Asuogya and Nkwanta

On the left is the total magnetic intensity of Asuogya grid which is upward continued to 200 m and on the right is the total magnetic Nkwanta grid which is continued upward to 200 m. These two grids have been continued upward to 200 m to show the subsurface geology and their depth of extent of mineralization. The Asuogya grid on the left highlights long wavelength which indicates a fade out of magnetization at 200 m. Contrary to Asuogya, the Nkwanta grid is still showing intensity of magnetization at a depth of 200 m.

NKWANTA-MAG

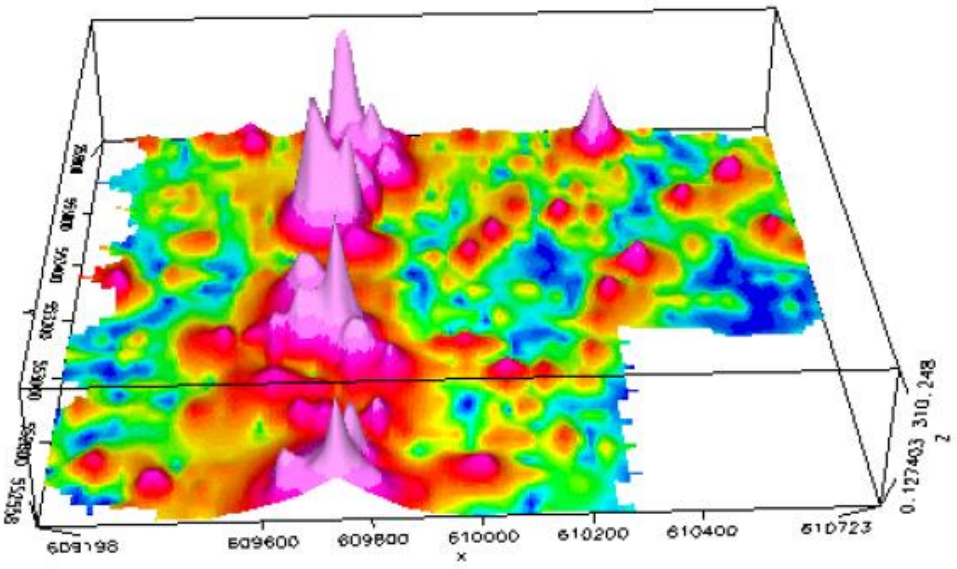

Figure 4.25: A three dimensional display of the analytical signal of Nkwanta.

Figure 4.25 shows the analytical signal of the magnetic data from Nkwanta which has been displayed in three dimensions showing the top view. The initials 3D means a three dimension. The legend for the Nkwanta analytical signal and its initial processing values also stands for its three dimensional displays. This anomaly reveals high magnetic intensity which indicates a high level of mineralization which trends approximately N-S of the traverse direction. The sudden rise and fall of this anomaly is an indication of a dike. The 3D display enables one to see the depth, size and the extent of mineralization.

ASUOGYA-MAG

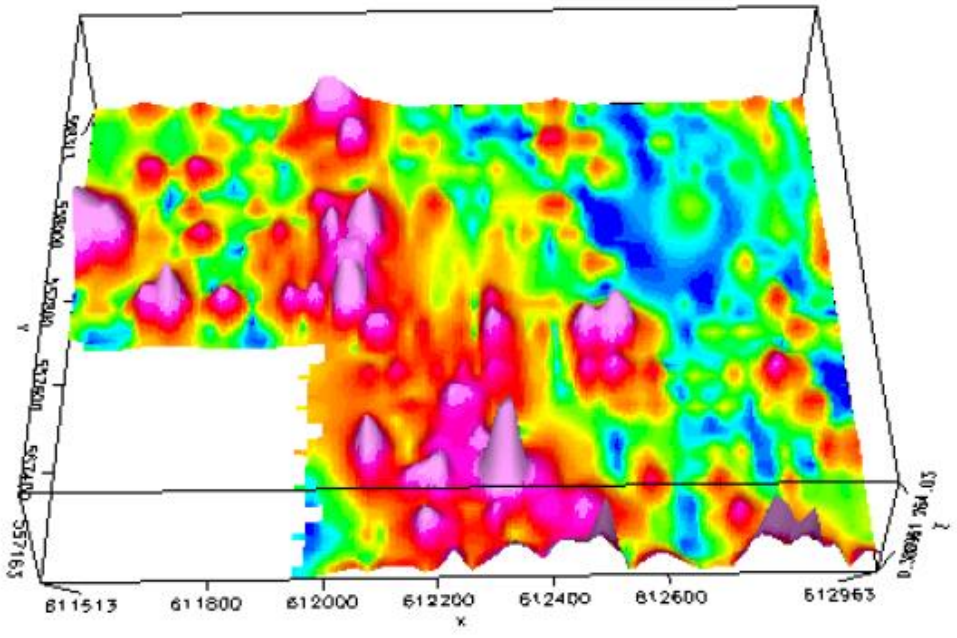

Figure 4.26: A three dimensional display of the analytical signal of Asuogya.

Figure 4.26 indicates a three dimensional display of the analytical signal grid from Asuogya showing the top view. The legend for the Asuogya analytical signal grid and its initial processing values also stands for its three dimensional display. This display shows a moderate intensity and mineralization anomaly with respect to Nkwanta and striking SE-NW in the traverse direction. The spread of the anomaly gives an indication that the feature at the subsurface could either be a dike, a shear zone or a fault in the Tarkwaian in the Ashanti belt.

CHAPTER FIVE

CONCLUSION AND RECOMMENDATON

5.1 CONCLUSION

In order to map mineralization zones and geological structures of the study areas, ground electromagnetics and magnetic datasets collected over the area were processed and enhanced. The EM images for both Asuogya and Nkwanta were able to locate or map conductivity zones and also show the trend of the subsurface feature producing the anomaly. The average conductivity for Nkwanta with intercoil spacing of 100 m and Asuogya with intercoil spacing of 150 m was seen to be high but that of Asuogya with intercoil spacing of 100 m was seen to be moderate. This gives an indication of a higher conductive zones of the survey area. The EM profiles gave the trend and depth estimate of the structure in the subsurface which produces the anomaly. The magnetic images were also instrumental in indicating zones and trend of mineralization. The analytical signal, the reduced to equator and the vertical derivative of Asuogya all showing a NW-SE trend of mineralization which also indicate the trend of the structure controlling the mineralization. On the other hand the analytical signal, the reduced to equator and the vertical derivative images of Nkwanta show a N-S trend of mineralization which is also an indication of the structural trend. The upward continuation images for Asuogya shows a shallow extent of mineralization which is less than 200 m and that of Nkwanta shows a deeper extent of mineralization which is more than 200 m. The three dimensional display of both the Nkwanta and Asuogya grid provided a good view of the width, size, trend and length of the anomalies.

5.2 RECOMMENDATION

Based on this study, the following recommendations are made:

Ground invasion (drilling) is highly recommended to actually confirm the delineated structure and lithology. From the trend of mineralization exhibited by both Asuogya and Nkwanta formation, ground geophysical and geological drilling surveys at the study areas are recommended where possible to validate whether the Asuogya or the Nkwanta delineated structures are faults or dikes for better understanding of the subsurface geology.

REFERENCES

Adadey, K., Clarke, B., Théveniaut, H., Urien, P., Delor, C., Roig, J.Y., Feybesse, J.L., (2009). Geological map explanation—Map sheet 0503 B (1:100 000), CGS/BRGM/Geoman. Geological Survey Department of Ghana (GSD). No MSSP/2005/GSD/5a.

Ako, J.A., Wellmann, P. (1985). The margin of the West African craton: the Voltaian Basin. Journal of the Geological Society London 142, pp 625–632.

Allen, P.A., Homewood, P., Williams, G.D. (1986). Foreland basins: an introduction. In: Allen, P.A., Homewood, P. (Eds.), Foreland Basins. Special Publication No. 8 of the International Association of Sedimentologists, Analysis of aeromagnetic data: Looking at geophysical data pp. 3–12.

Annan-Yorke, R., (1971). Geology of the Voltaian Basin (summary of current ideas). In: Cudjoe, J.E. (Ed.), Special Bulletin for Oil Exploration. Geological Survey Department, Accra, Ghana, pp 29.

Attoh, K., Dallmeyer, R.D., Affaton, P., (1997). Chronology of nappe assembly in the Pan-African Dahomeyide orogen, West Africa: evidence from Ar/Ar mineral ages. Precambrian Research 82, pp153–171.

Barringer, A R. (1962). A new approach to exploration- the INPUT airborne-electrical pulse prospecting system .Min. Cong. Jour. 48, pp.49-52.

Bessoles, B. (1977). Geologie de!'Afrique vol. I, Craton de!'OuestAfricain. Bur. Rech. Geol. Min. Mem.pp 88:402.

Betts, P., Williams, H., Stewart, J. and Ailleres, L., (2007). Kinematic between arbitrary surfaces. Geophysics, 49(6): pp787-795.

Birch, F. S. (1984). Bedrock Depth Estimates from Ground Magnetometer Profiles. Groundwater, 22(4), pp 427-432.

Blakely, R.J. (1995). Potential theory in gravity and magnetic applications. New York, Cambridge University Press :pp 441.

Blakely, R.J. and Simpson, R.W., (1986). Approximating edges of sourcebodies from magnetic or gravity anomalies. Geophysics, 51(7): pp 149.

Breakey, A. & Breakey, E. (1977). The geology of 1/4° field sheets of 0603/ A3 (117) Goaso SW and 0603/ A4 (118) Goaso SE. Ghana Geol. Surv. Dept., Accra, pp 95.

Briggs, I. (1974). Machine contouring using minimum curvature. Geophysics, 39(1), pp 39-48.

Clark, D. A. (1997): Magnetic petrophysics and magnetic petrology: aids to geological interpretation of magnetic surveys, AGSO J. Aust. Geol. Geophys., **17(2)**, pp 83–103.

Cooper, G. R. J., & Cowan, D. R. (2004). Filtering using variable order vertical derivatives. Computers and Geosciences, 30, pp 455-459.

Cooper, W. G .G. (1934). The geology of the Prestea goldfield. Gold Coast Geological Survey, Memoir 3, pp 20.

Dalan, R.A., J.M. Musser, Jr., and J. K. Stein (1992). Geophysical Exploration of the Shell Midden. In Deciphering a Shell Midden,ed. By J.K. Stein, pp. 41-59.

Dallmeyer, R.D., Le´corche´, J.P., (1989). 40Ar/39/ar polyorogenic mine´ral record within the central Mauritanides orogen, West Africa. Geological Society America Bulletin 101, pp 55–70.

Davis, D.W., Hirdes, W., Schaltegger, U., Nunoo, E.A., (1994). U–Pb age constraints on deposition and provenance of Birimian and gold-bearing Tarkwaian sediments in Ghana, West Africa. Precambrian Research 67, pp 89–107.

Deynoux, M., Affaton, A., Trompette, R., Villeneuve, M., (2006). Pan-African tectonic evolution and glacial events registered in Neoproterozoic to Cambrian cratonic and foreland basins of West Africa. Journal of African Earth Sciences 46, pp 397–426.

Dobrin, M.B., and Savit, C.H., (1988), Introduction to geophysical prospecting 4th edition: McGraw-Hill, Inc., New York. pp 630.

Dolan, W. M. (1970). Geophysical detection of deeply buried sulfide bodies in weathered regions. In Mining and GroundwaterG~physics, Econ. Geol. Report 16,L. W. Morley, ed. Geol. Surv. Canada, pp. 336-44.

Eisenlohr, N. & Hirdes, W. (1992). The structural development of the early Proterozoic Birimian and Tarkwaian rocks of southwest Ghana, West Africa. Journal African Earth Sciences 14, 3 pp 13-325.

Eisenlohr, N. (1992). Conflicting evidence on the timing of mesothermal and paleoplacer gold mineralization in early Proterozoic rocks from southwest Ghana, West Africa. MineraliumDeposita 27, pp 23-29.

Feybesse, J.-L., Billa, M., Guerrot, C., Duguey, E., Lescuyer, J.-L., Milési, J.-P., Bouchot, V., (2006). The Palaeoproterozoic Ghanaian province: geodynamic model and ore controls, including stress modeling. Precambrian Research 149, pp 149–196.

Foss, C. (2011). Magnetic data Enhancement and Depth Estimation. (H. Gupta, Ed.) Encyclopedia of Earth Sciences Series, pp 736-746.

Gerald W. H. & Stanley, H. W. (2010). Geology and Geophysics Department University of Utah, Salt Lake City, UT 84112 pp 3

Gibson, R. I. and Millegan, P. S. (1998): Geology applications of gravity and magnetic: Case histories. Society of Exploration Geophysicist, 170. pp 162.

Godio, A., Chiara, P. Gaill, C. C. and Naldi, M. (1998). A Combined Geophysical Survey for Hydrogeological Purposes in North-Eastern Italy. Proceedings of IV Meeting Environmentl and Engineering Geophysial Society, pp. 209-212.

Grant, F.S. & Dodds, J. (1972). 'MAG MAP FFT processing system development notes', Paterson Grant and Watson Limited.

Grant, F.S., and G.F. West (1965). Interpretation Theory in Applied Geophysics. McGraw-Hill, New York.

Gunn, P.J., Maidment, D. & Milligan, P.R., (1997). Interpreting magnetic data in areas of limited outcrop. AGSO Journal of Geology and Geophysics pp.175-185.

Gupta, V. K. & Fitzpatrickt, M. M., (1971). Evaluation of terrain effects in ground magnetic surveys. Geophysics, 5: pp 582-589.

Hansen, R.O. and Miyazaki, Y., (1984). Continuation of potential fields between arbitrary surfaces. Geophysics, 49(6): pp 787-795.

Hassen R. O. & Pawlowski R. S. (1989): Reduction to pole at low latitudes by Weiner filtering.Geophysics, 54, pp 1607–1613.

Hastings, D.A. (1982). On the tectonics and the metallogenesis of West Africa: A model incorporating new geophysical data. Geoexploration 20:pp 295-327.

Hastings, D.A., (1983). On the tectonics and metallogenesis of Ghana: a model based on a new synthesis of geological and geophysical data. United States Geol. Surv. (unpublished draft).

Hirdes, W., Davies, D.W., Lu¨ dtke, G., Konan, G., (1996). Two generations of Birimian (Paleoproterozoic) volcanic belts in northeastern Coˆ te d'Ivoire (West Africa): consequences for the 'Birimian controversy. Precambr. Res. 80, pp 173–191.

Hirdes, W., Davis, D. W. and Eisenlohr, B. N. (1992). Interpretation using 3D analytical signal. Geophysics, 57, pp116

Hirdes, W., Nunoo, B., (1994). The proterozoicpaleoplacers at Tarkwa Gold Mine, SW Ghana: sedimentology, mineralogy, and precise age dating of the main reef and west reef, and bearing of the investigations on source area aspects. GeologischesJahrbuch D 100, pp 247–311.

Hirdes, W., Senger, R., Adjei, J., Efa, E., Loh, G. and Tettey, A. (1993). Explanatory notes for the geological map of southwest Ghana. 1:100,000: sheets Wiawso (0603D), Asafo (0603C), Kukuom (0603B), Goaso (0603A), Sunyani (0703D) and Berekum (0703C). Geologisches Jahrbuch B83. Schweizerbart'sche Vertagsbuchhandlung, Stuttgart. pp 139

Hoover, D.B., Heran, W.D., & Hill, P.L., eds., (1992). The geophysical expression of selected mineral depositmodels: U.S. Geological Survey Open-file Report 92-557, pp.129.

Hottin, G. & Quedraogo, O.F., (1975). Notice explicative de Ia carte geologique a 1 000 000 de IaRepublique de Haute Volta. Dir. Geol. Min. Rep., Haute Volta, Ouagadougou, pp 58.

Hünken, U., Klemd, R., Olesch, M., (1994). Fluid inclusions in quartz-pebbles of proterozoictarkwaian conglomerates in Ghana. GeologischesJahrbuch D 100, pp 313–341.

Jacobsen, B.H., (1987). Case for upward continuation as a standard separation filter for potential field maps. Geophysics, 52(8): pp 1138-1148.

John, T., Klemd, R., Hirdes, W., Loh, G., (1999). The metamorphic evolution of the Paleoproterozoic (Birimian) volcanic Ashanti belt (Ghana, West Africa). Precambrian Research 98, pp11–30.

Junner, N. R. (1932). Geology of the Obuasi goldfield. Gold Coast Geological Survey, Memoir 2, pp 71

Junner, N. R. (1940). Geology of the Gold Coast and western Togoland. Gold Coast GeologicalSurvey, Bulletin 10. pp 40.

Junner, N.R. (1935). Gold in the Gold Coast. Gold Coast Geol. Surv. Mem. 4: pp 67.

Kearey, P., Brooks, M. and Hill, I. (2002). An Introduction to Geophysical Exploration (Third Edition), Blackwell Science, Oxford, pp.163-164

Kesse, G.O., (1985). The Mineral and Rock Resources of Ghana. A.A. Balkema Publishers, pp 610.

Kitson, A.E. (1928). Provisional geological map of the Gold Coast and Western Togoland, with brief descriptive notes thereon. Gold Coast Geological Survey, Accra, Ghana.

Klein, D.P., & Bankey, V., (1992). Geophysical model of Creede, Comstock, Sado, Goldfield and related epithermal precious metal deposits, in Hoover, D.B., Heran, W.D., and Hill, P.L., Editors, The geophysical expression of selected mineral deposit models: U.S. Geological Survey Open-File Report 92-557, pp. 98-106.

Kleinschrot, D., Klemd, R., Brocker, M., Okrusch, M., Franz, L., Schmidt, K., (1994). Protores and country rocks of the Nsuta manganese deposit. Neues Jahrbuch Mineral 168, pp 67–108.

Klemd, R., Hirdes, W., Olesch, M., Oberthür, T., (1993). Fluid inclusions in quartzpebbles of the gold-bearing Tarkwaian conglomerates of Ghana as guides to their provenance area. MineraliumDeposita 28, pp 334–343

Lane, R., (2000). Conductive unit parameters: summarising complex conductivity distributions. 70th Meeting, Society of Exploration Geophysicists (SEG), Calgary, Expanded Abstracts 1, Section EM4.2, pp. 328-331.

Layton, W., (1958). The geology of 1/4 o field sheet 32. Ghana Geol. Surv., Bull, 24, pp 66.

Leube, A., & Hirdes, W., (1986), The Birimian Supergroup of Ghana: Depositional environment, structural development, and conceptual model of an Early Proterozoic suite: Hanover, Bundesanstaltfür Geowissenschaften und Rohstoffe, 99 529, pp 260.

Leube, A., Hirdes, W, Mauer, R., Kesse, G.O. (1990).The early Proterozoic BirimianSupergroup of Ghana and some aspects of its associated gold mineralization. Precambrian Res. 46: pp 139-165.

Lilley, F.E.M., (1982). Geomagnetic field fluctuations over Australia in relation to magnetic surveys. Bulletin of the Australian Society of Exploration Geophysics 13: pp 68-78.

Lowrie, W. (1990). Identification of ferromagnetic minerals in a rock by coercivity and unblocking temperature properties. Geophysics. Res. Lett., 17, pp 159–162.

Lowrie, W. (2007). Fundamentals of GeophysicsSwiss Federal Institute of Technology, Zürich, 2nd ed pp 271-272

Lowrie, W. and Alvarez, W. (1981). One hundred million years of geomagnetic polarity history. Geology, 9, pp 392–397.

Macleod, I.N., Vierra, S. and Chaves, A.C. (1993), 'Analytic signal and reduction-to-the-pole in the interpretation of total magnetic field data at low magnetic latitudes'. Proceedings of the third international congress of the Brazilian Society of Geophysicists.

McNeill, J.D. (1980a). Electromagnetic Terrain Conductivity Measurement at Low Induction Numbers. Geonics Limited, Technical Note TN-5. Mississauga, Ontario, Canada.

McNeill, J.D. (1980b). Electrical Conductivity of Soils and Rocks. Geonics Limited, Technical Note TN-6. Mississauga, Ontario, Canada.

McNeill, J.D., (1980). Electromagnetic terrain conductivity measurement at low induction numbers. Geonics Technical Note TN-6: pp 15.

McNeill, J.D., (1990). Use of electromagnetic methods for groundwater studies: Geotech-nical and Environmental Geophysics, v. 1, pp 191-217.

Meehan, G.M., (1980), Geologic factors affecting the mining of the upper Freeport coal seam in west central Preston County, West Virginia: Pittsburgh, PA, MS Thesis, University of Pittsburgh.

Mekonnen, T. K. (2004). Interpretation and Geodatabase of Dukes using Aeromagnetic data of Zimbabwe and Mozambique. M. Sc. Thesis, International Institute for Geoinformation science and Earth Observation, Enschede, the Netherlands. Retrieved from http://www.slideserve.com/phila/partners

Mendonça, C. A. and Silva, B. C. (1993): A stable truncated series approximation of the reduction-topole operator, Geophysics, 58, pp 1084–1090.

Milesi, J.P., Ledru, P., Feybesse, J.L., Dommanget, A., Marcoux, E., (1992). Early Proterozoic ore deposits and tectonics of the Birimian orogenic belt, West Africa. Precambr. Res. 58, pp 305–344.

Milesi, J. P.,Ledru, P., Ankrah P., Johan, V., Marcoux E., and C. Vinchon, (1991). The metallogenic relationship between Birimian and Tarkwaian gold deposits in Ghana. Min.Deposita v 26, pp. 228 – 238.

Milesi, J.P., Feybesse, J.L., Ledru, P., Dommanget, A., Ouedraogo, M.F., Marcoux, E., Prost, A., Vinchon, C., Sylvain, J.P., Johan, V., Tegyey, M., Calvez, J.Y., Lagny, Ph. (1989) West Africa gold deposits in their Lower Proterozoic lithostructural setting. Chron. Rech. Min. 497: pp 3-98

Milligan, P., & Gunn, P. (1997). Enhancement and presentation of airborne geophysical data. AGSO Journal of Australian Geology & Geophysics, 17(2), pp 63-75.

Milligan, P.R.M., (1995). Short-period geomagnetic variations recorded concurrently with an aeromagnetic survey across the Bendigo area, Victoria. Exploration Geophysics 26: pp 527-534.

Milsom, J. (2003). Field Geophysics. (Third, Ed.) London: Wiley.pp.156

Mørk, M. B. E., Mc Enroe, S. A. and Olesen, O. (2002): Magnetic susceptibility of Mesozoic and Cenozoic sediments off Mid Norway and the role of siderite: Implications for interpretation of high resolution aeromagnetic anomalies, Mar. Petrol. Geol., **19**, pp 1115–1126.

Murray, R. J. (1960). The geology of the Zuanengu 1/2 ° field sheet. Ghana Geol. Surv. BulL pp 25.

Nabighian, M.N. (1972), The analytic signal of two-dimensional magnetic bodies with polygonal cross-section: Its properties and use for automated anomaly interpretation, Geophysics 37.

Nabighian, M.N. (1974), 'Additional comments on the analytic signal of two-dimensional magnetic bodies with polygonal cross-section', Geophysics 39, pp 85-92

Nabighian, M.N. (1984), 'Toward a three-dimensional automatic interpretation of potential field data via generalised Hilbert transforms: Fundamental relations', Geophysics 49, pp 780-786.

Nicolas O.Mariita, (2009). Exploratiom for Geothermal Resources, pp.5

Oberthür, T., Vetter, U., Davis, D.W., Amanor, J.A., (1998). Age constraints on gold mineralization and Paleoproterozoic crustal evolution in the Ashanti belt of southern Ghana. Precambrian Research 89, pp 129–143.

Oberthür, T., Vetter, U., Schmidt Mumm, A., Weiser, T., Amanor, J.A., Gyapong, W.A., Kumi, R., Blenkinsop, T.G., (1994). The Ashanti Gold Mine at Obuasi, Ghana: mineralogical, geochemical, stable isotope and fluid inclusion studies on the metallogenesis of the deposit. Geologisches Jahrbuch D 100, pp31–129.

Palacky, G. J., Ritsema, I. L., and De Jong, S. L. (1981). "Electromagnetic Prospecting for Groundwater in Precambrian Terrains in the Republic of Upper Volta," Geophysical Prospecting, Vol 29, pp 932-955.

Palacky, G.J., and F.L. Jagodits (1975). Computer Data Processing and Quantitative Interpretation of Airborne Resistivity Surveys. Geophysics 40: pp 818-830.

Papon, A., (1973). GeologieetMineralisations du Sud-Ouest de Ia Cote d'lvoire. Mem. Bur. Rech. Geol. Min. Fr., pp 80:

Perrouty, S., Aillères, L., Jessell, M. W., Baratoux, L., Bourassa, Y., & Crawford, B. (2012). Revised Eburnean geodynamic evolution of the gold-rich southern Ashanti Belt, Ghana, with new field and geophysical evidence of pre-Tarkwaian deformations. Precambrian Research, 204-205, doi:10.1016/j.precamres.2012.01.003 pp 12–39

Petters, S. W., (1991). Regional Geology of Africa. Springer-Verlag (Publ.), Berlin, pp 722.

Philips, J. (1997). Potential-Field Geophysical Software for the PC, U.S.G.S. Open-File Report pp 97-725.

Phillips, J. D., and Grauch, V. J. S., (2001). Some current research on the processing and interpretation of potential-field data at the U.S. Geological Survey, *in* Workshop on future directions in the analysis of potential-field data, August 18, 2001, Perth, Australia, pp 4.

Pigois, J.P., Groves, D.I., Fletcher, I.R., McNaughton, N.J., Snee, L.W., (2003). Agepotential fields. Geophysical Prospecting, 20: pp 47-75.

Rain van Enk,Drydeni (1984) Doran Resources CorporationWcEDWards Lake Property :Detailed Geophysical Survey pp 2.

Reeves, C. V., (2005). Aeromagnetic interpretation. Prnciple,practice & interpretation pp 2-10.

Reeves, C., Reford, S., & Millingan, P. (1997). Airborne geophysics:old methods, new images. In A. Gubins (Ed.), Proceedings of the Fourth Decennial International Conference on Mineral Exploration, Australia pp. 13-30.

Rein, V. E. (1984).detailed geophysical survey – Max-Min/VLF-EM/MAG. Morgan resource Co., pp 1-7.

Reynolds, D. L. (1951). The geology of Slieve Gullion, Foughill and Carrickarnan. Transactions of the Royal Society of Edinburgh, 62, pp 85–145.

Reynolds, J.M. (1997). An introduction to Applied and Environmental Geophysics, pp.171

Reynolds, J.M. (1997). An introduction to Applied and Environmental Geophysics, pp.556-585.

Roberts, R. L., Hinze, W. J., & Leap, D. I. (1990). Data enhancement Procedure on magnetic Data from LandfillInvestigations. pp 261-267.

Roset, W.E., Verhoef,J., and Pilkington, M. (1992). Magnetic interpretation using 3D analytical signal Geophys., 57, pp 116-125.

Sandberg, S.K. (1993) "Examples of Resolution Improvement in Geoelectrical Soundings Applied to Groundwater Investigations." Geophysical Prospecting.Vol. 41, pp. 207–22.

Schmidt Mumm, A., Oberthür, T., Vetter, U., Blenkinsop, T.G., (1997). High CO2 content of fluid inclusions in gold mineralisations in the Ashanti Belt, Ghana: a new category of ore forming fluids? Mineralium Deposita 32,pp 107–118.

Sestini, G., (1973). Sedimentology of a Paleoplacer: the gold-bearing Tarkwaian of Ghana. Ores in Sediments, International Union of Geological Sciences, Series A 3,pp 275–305.

Sharma, P. V., (1997). Environmental and Engineering Geophysics: Cambridge University Press, New York. pp 475.

Sharma, P. V., (1997). Environmental and Engineering Geophysics: Cambridge University Press, New York. pp 475.

Sidorov, V. A., and V. V. Tickshaev, (1969), Electrical prospecting with transient field in near zone: Saratov University Press.

Silva AM, Pires AC, McCafferty A, Moraes R, Xia H (2003). Application of airborne geophysical data to mineral exploration in the uneven exposed terrains of the Rio Das Velhas greenstone belt. RevistaBrasileira de Geociências, 33(2): pp17-28.

Spies, B., (1989), Depth of investigation in electromagnetic sounding methods, Geophysics, 54, pp 872-888.

Statham, L. (1936). Electric earth transients in geophysical prospecting. Geophysics 1. pp 271-277.

Stewart, M.T., (1981). Evaluation of electromagnetic terrain conductivity measurements for detection and mapping of salt water interfaces in coastal aquifers: Florida water resources research centersurfaces. Geophysical Prospecting, 20(2): pp 267-282.

Strogen, P. (1988). The structure and sedimentology of the Survey Memoir 2, pp 43.

Syberg, F.J.R., (1972a). A Fourier method for the regional-residual problem of potential fields. Geophysical Prospecting, 20: pp 47-75.

Syberg, F.J.R., (1972b). Potential field continuation between general surfaces. Geophysical Prospecting, 20(2): pp. 267-282.

Taylor, P.N., Moorbath, S., Leube, A. and Hirdes, W., (1988). Geochronology and crustal evolution of Early Proterozoicgranite-greenstone terrains in Ghana/West Africa, Abstr., International Conference on the Geology of Ghana with Special Emphasis on Gold Comm. 75th Anniversaryof Ghana Geol. Surv. Dept., Accra, pp. 43-45.

Taylor, P.N., Moorbath, S., Leube, A., Hirdes, W., (1992). Early Proterozoic crustal evolution in the Birimian of Ghana: constraints from geochronology and isotope geochemistry. Precambrian Research 56, pp 97–111.

Telford, W., Gelbert, I., & Sheritt, R. (1990). Applied Geophysics (Second ed.). London: Cambridge University Press.

Telford, W.M., Geldart, L.P., Sheriff, R.E. and Keys, D.A.(1990) Applied Geophysics(Second Edition), Cambridge University Press, Cambridge, 770 pp. Wiley, Chichester, pp.56

Telford,W.M., Geldart, L.P., Sheriff, R.E. and Keys, D.A., (1976), Applied Geophysics: Cambridge University Press.

Tunks, A.J., Selley, D., Rogers, J.R., Brabham, G., (2004). Vein mineralization at theUniversity Press, New York. pp 475.

Walsh, D. C. (1989). Surface geophysical exploration for buried drums in urban environments applications in New York City in Proc of the Third Nat Outdoor Action Conf. on Aquifer Restoration, Groundwater Monitoring and Geophysical Methods, Orlando pp 935-949.

Whitelaw, O.A.L., (1929). The Geological and Mining Features of the Tarkwa-Abosso Workshop on the Geology of Ghana with Special EmphasisYork, Cambridge University Press: pp 441.

Wright, J. B., Hastings, D. A., and W. B. Jones, (1985). Geology and Mineral Resources of West Africa. G. Allen and Unwin, pp 187.

Zhdanov,M. S., and G.Keller, (1994), The geoelectrical methods in geophysical exploration: Elsevier.

APPENDIX

A screen shot of Magnetic and EM data displayed in Geosoft

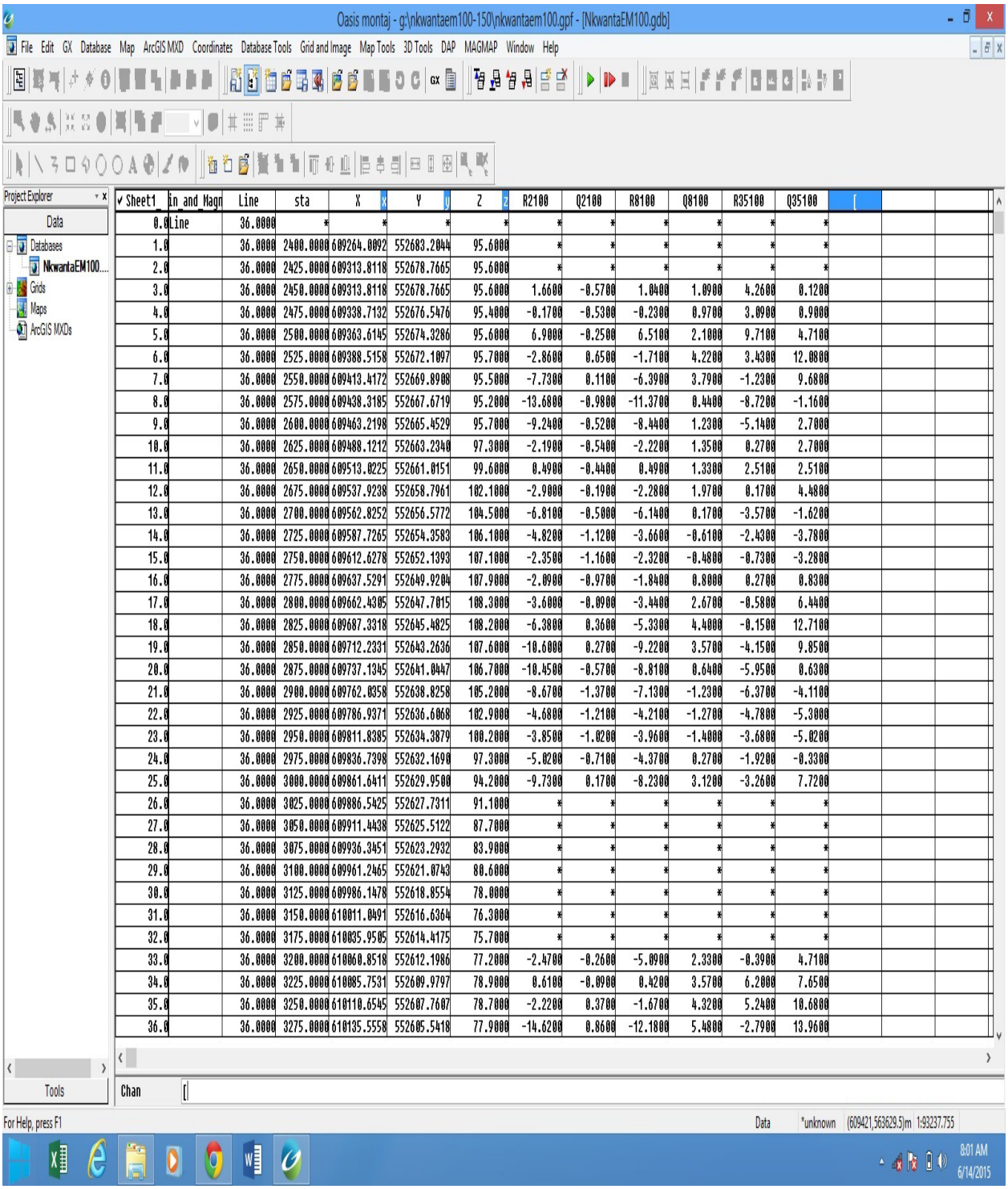

Sheet1	in_and_Magn	Line	sta	X	Y	Z	R2100	Q2100	R8100	Q8100	R35100	Q35100	[
0.0	Line	36.0000	*	*	*	*	*	*	*	*	*	*	
1.0		36.0000	2400.0000	609264.8092	552683.2044	95.6000	*	*	*	*	*	*	
2.0		36.0000	2425.0000	609313.8118	552678.7665	95.6000	*	*	*	*	*	*	
3.0		36.0000	2450.0000	609313.8118	552678.7665	95.6000	1.6600	-0.5700	1.0400	1.0900	4.2600	0.1200	
4.0		36.0000	2475.0000	609338.7132	552676.5476	95.4000	-0.1700	-0.5300	-0.2300	0.9700	3.0900	0.9000	
5.0		36.0000	2500.0000	609363.6145	552674.3286	95.6000	6.9000	-0.2500	6.5100	2.1000	9.7100	4.7100	
6.0		36.0000	2525.0000	609388.5158	552672.1097	95.7000	-2.8600	0.6500	-1.7100	4.2200	3.4300	12.0800	
7.0		36.0000	2550.0000	609413.4172	552669.8908	95.5000	-7.7300	0.1100	-6.3900	3.7900	-1.2300	9.6800	
8.0		36.0000	2575.0000	609438.3185	552667.6719	95.2000	-13.6800	-0.9800	-11.3700	0.4400	-8.7200	-1.1600	
9.0		36.0000	2600.0000	609463.2198	552665.4529	95.7000	-9.2400	-0.5200	-8.4400	1.2300	-5.1400	2.7000	
10.0		36.0000	2625.0000	609488.1212	552663.2340	97.3000	-2.1900	-0.5400	-2.2200	1.3500	0.2700	2.7000	
11.0		36.0000	2650.0000	609513.0225	552661.0151	99.6000	0.4900	-0.4400	0.4900	1.3300	2.5100	2.5100	
12.0		36.0000	2675.0000	609537.9238	552658.7961	102.1000	-2.9000	-0.1900	-2.2800	1.9700	0.1700	4.4800	
13.0		36.0000	2700.0000	609562.8252	552656.5772	104.5000	-6.8100	-0.5000	-6.1400	0.1700	-3.5700	-1.6200	
14.0		36.0000	2725.0000	609587.7265	552654.3583	106.1000	-4.8200	-1.1200	-3.6600	-0.6100	-2.4300	-3.7800	
15.0		36.0000	2750.0000	609612.6278	552652.1393	107.1000	-2.3500	-1.1600	-2.3200	-0.4800	-0.7300	-3.2800	
16.0		36.0000	2775.0000	609637.5291	552649.9204	107.9000	-2.0900	-0.9700	-1.8400	0.8000	0.2700	0.8300	
17.0		36.0000	2800.0000	609662.4305	552647.7015	108.3000	-3.6000	-0.8900	-3.4400	2.6700	-0.5800	6.4400	
18.0		36.0000	2825.0000	609687.3318	552645.4825	108.2000	-6.3800	0.3600	-5.3300	4.4000	-0.1500	12.7100	
19.0		36.0000	2850.0000	609712.2331	552643.2636	107.6000	-10.6000	0.2700	-9.2200	3.5700	-4.1500	9.8500	
20.0		36.0000	2875.0000	609737.1345	552641.0447	106.7000	-10.4500	-0.5700	-8.8100	0.6400	-5.9500	0.6300	
21.0		36.0000	2900.0000	609762.0358	552638.8258	105.2000	-8.6700	-1.3700	-7.1300	-1.2300	-6.3700	-4.1100	
22.0		36.0000	2925.0000	609786.9371	552636.6068	102.9000	-4.6800	-1.2100	-4.2100	-1.2700	-4.7800	-5.3000	
23.0		36.0000	2950.0000	609811.8385	552634.3879	100.2000	-3.8500	-1.0200	-3.9600	-1.4000	-3.6800	-5.0200	
24.0		36.0000	2975.0000	609836.7398	552632.1690	97.3000	-5.0200	-0.7100	-4.3700	0.2700	-1.9200	-0.3300	
25.0		36.0000	3000.0000	609861.6411	552629.9500	94.2000	-9.7300	0.1700	-8.2300	3.1200	-3.2600	7.7200	
26.0		36.0000	3025.0000	609886.5425	552627.7311	91.1000	*	*	*	*	*	*	
27.0		36.0000	3050.0000	609911.4438	552625.5122	87.7000	*	*	*	*	*	*	
28.0		36.0000	3075.0000	609936.3451	552623.2932	83.9000	*	*	*	*	*	*	
29.0		36.0000	3100.0000	609961.2465	552621.0743	80.6000	*	*	*	*	*	*	
30.0		36.0000	3125.0000	609986.1478	552618.8554	78.0000	*	*	*	*	*	*	
31.0		36.0000	3150.0000	610011.0491	552616.6364	76.3000	*	*	*	*	*	*	
32.0		36.0000	3175.0000	610035.9505	552614.4175	75.7000	*	*	*	*	*	*	
33.0		36.0000	3200.0000	610060.8518	552612.1986	77.2000	-2.4700	-0.2600	-5.0900	2.3300	-0.3900	4.7100	
34.0		36.0000	3225.0000	610085.7531	552609.9797	78.9000	0.6100	-0.0900	0.4200	3.5700	6.2000	7.6500	
35.0		36.0000	3250.0000	610110.6545	552607.7607	78.7000	-2.2200	0.3700	-1.6700	4.3200	5.2400	10.6800	
36.0		36.0000	3275.0000	610135.5558	552605.5418	77.9000	-14.6200	0.8600	-12.1800	5.4800	-2.7900	13.9600	